Diagnosis of Damages in Beam Structures using Vibration Parameters and Artificial Intelligence Techniques

Deepak Kumar Agarwalla

Diagnosis of Damages in Beam Structures using Vibration Parameters and Artificial Intelligence Techniques

Thesis Submitted to the

Department of Mechanical Engineering
National Institute of Technology, Rourkela

for award of the degree

of

Master of Technology
by
Deepak Kumar Agarwalla

under the guidance of

Prof. Dayal R. Parhi

Department of Mechanical Engineering
National Institute of Technology Rourkela
Orissa (India)-769008
May 2013

Certificate

This is to certify that the thesis entitled, ***"Diagnosis of Damages in Beam Structures using Vibration Parameters and Artificial Intelligence Techniques",*** *being submitted by Mr. Deepak Kumar Agarwalla to the Department of Mechanical Engineering, National Institute of Technology, Rourkela, for the partial fulfillment of award of the degree Master of Technology, is a record of bona fide research work carried out by him under my supervision and guidance.*

This thesis in our opinion, is worthy of consideration for award of the degree of Master of Technology in accordance with the regulation of the institute. To the best of my knowledge, the results embodied in this thesis have not been submitted to any other University or Institute for the award of any degree or diploma.

Prof. D.R. Parhi
(Supervisor)

Acknowledgements

In this thesis, I have been supported by many people who motivated me to do deliver the best.

First of all, I would like to thank my supervisor Prof. Dayal R. Parhi for guiding me to do my thesis at N.I.T. Rourkela and for his enormous support to develop this work. His patience, stimulating suggestions and encouragement helped me in all the time of research and writing of this thesis.

I am thankful to Prof. Sunil Kumar Sarangi, Director of National Institute of Technology, Rourkrela for giving me an opportunity to work under the supervision of Prof. Dayal R. Parhi. I am thankful to Prof. K.P. Maiti, Head of the Department, Department of Mechanical Engineering, for his moral support and valuable suggestions regarding the research work.

I would like to thank Mr. P.K. Mohanty, PhD project scholar for his conceptual guidance regarding implementation of fuzzy logic & Mr. Maheshwar Das, Technical assistant, Robotics Lab. for his help in preparing the test specimens.

Finally I would like to thank my Parents, Mrs. Kiran Devi Agarwalla & Mr. Suresh Lal Agarwalla for all their support and encouragement. I would like to mention a special thanks to my brother, Mr. Rakesh Kumar Agarwalla and my sister, Ms. Sushama Agarwalla for their constant support. Also, reservoirs of thanks to the man “Sachin Great Tendulkar” who always keeps me motivated.

Abstract

This thesis diagnoses the damaged vibrating structural members of different materials using the parametric responses of the dynamic system. Almost all engineering structures designed for long life span are influenced by alteration in loading patterns. Changes in the loading patterns, loss of load carrying capacity of structures with time and impact of environment often lead to the structural damage. Therefore, early diagnosis of damage can avert the sudden failure of the structures by rendering the system to sound monitoring of the response generated. Damage diagnostic tool for condition monitoring of the structural systems appealed the scientists and researchers for more analysis. The modal parameters of the vibrating structures play a crucial role in monitoring the damaged structures. In the present analysis, special attention has been focused for detecting the damages present in Al, composite and steel beam structures by comparing the characteristics of damaged and undamaged state of the structures. In the current research, damage detection of damaged cantilever and fixed-fixed beam is carried out using numerical, finite element analysis (FEA), fuzzy logic and neural network techniques. Numerical analysis has been performed on the cantilever beam & fixed-fixed beam with damage in the transverse direction to obtain the vibration parameters of the beam members utilizing the expression of strain energy release rate and stress intensity factor. The presence of damage in a structural member introduces local stiffness that affects its dynamic characteristics. The local stiffness matrices have been determined using the inverse of local dimensionless compliance matrix for finding out the deviations in the vibrating signatures of the damaged beam structures from that of the intact beams. Finite Element Analysis has been carried out to derive the vibration indices of the damaged structures using the overall stiffness matrix, total stiffness matrix, stiffness matrix of the intact beams. It is concluded from the conducted research that the performance of the damage diagnosis techniques depends on several factors for example, the material type, the number of sensors used for acquiring the dynamic response, position and severity of damages. Different artificial intelligent model based on fuzzy logic, neural network have been designed using the estimated vibration signatures for damage diagnosis in beam structures with higher precision and remarkably low calculating time.

Table of Contents

List of Tables

List of Figures

Nomenclature

a_1 = depth of damage

A = cross-sectional area of the beam

$A_{i\ (i = 1to\ 18)}$ = unknown coefficients of matrix A

B = width of the beam

C_{11} = Axial compliance

$C_{12}= C_{21}$ = Coupled axial and bending compliance

C_{22} = Bending compliance

$\bar{C}_{11}$ = Dimensionless form of C11

$\bar{C}_{12}= \bar{C}_{21}$ = Dimensionless form of C12= C21

$\bar{C}_{22}$ = Dimensionless form of C22

C'_{12} = Axial compliance for damage position

$C'_{12} = C'_{21}$ = Coupled axial and bending compliance for damage position

C'_{22} = Bending compliance for damage position

E = young's modulus of elasticity of the beam material

$F_{i\ (i = 1, 2)}$ = experimentally determined function

i, j = variables

J = strain-energy release rate

$K_{1, i\ (i = 1, 2)}$ = stress intensity factors for P_i loads

K_{ij} = local flexibility matrix elements

K' = Stiffness matrix for damage position

L = length of the beam

L_1 = location (length) of the damage from fixed end

Le = Length of the damage from one end of the beam

Lc = Length of damaged element

$M_{i\ (i=1,4)}$ = compliance constant

$P_{i\ (i=1,2)}$ = axial force (i=1), bending moment (i=2)

Q = stiffness matrix for free vibration.

$u_{i\ (i=1,2)}$ = normal functions (longitudinal) $u_i(x)$

x = co-ordinate of the beam

y = co-ordinate of the beam

$y_{i\ (i=1,2)}$ = normal functions (transverse) $y_i(x)$

W = depth of the beam

ω = natural circular frequency

β_1 = relative damage location (L_1/L)

ρ = mass-density of the beam

Λ = aggregate (union)

Λ = minimum (min) operation

$\forall$ = for every

Chapter 1
INTRODUCTION

In recent times, damage diagnosis in the vibrating beam structures challenges the scientists and researchers due to the usage of varieties of materials. The existence of damage or fault like crack, fracture, surface irregularities etc. in a beam structure for prolonged time enhances the chances the system failure which lead to causalities and loss of properties. In various engineering systems, vibration response of the structural members can be utilized as an effective tool for damage arbitration. The current chapter presents the various damage diagnosis methods that are being used over the time. The background and motivation in the field of analysis of dynamically vibrating damaged structures has been depicted in the first section. The second part of this chapter describes the aims and objective of the research. The last part of the current chapter gives a brief description of each chapter of the thesis for the current research.

1.1 Motivation for Damage Diagnosis

Engineering structures play a pivotal role in many areas like the bridges, construction sites, industries, towers etc. Long life span is the most important parameters required for these structures. The failure or irregular behavior of engineering structures may cause devastation in transportation system leading to loss of lives and property. Hence, structural integrity of the structural member is to be maintained by installing a efficient and reliable monitoring, so that proper remedial measures can be taken.

Many techniques have been implemented in the past for damage diagnosis. Some of these methods are based on visual detection using some dye and other use sensors involving acoustic emission, magnetic field, eddy current, radiographs and thermal fields to identify local damage. The drawbacks of these methods are their inability to test the structure without going in to minute structural analysis which is very time consuming. Moreover, if damage is rooted away from the surface and deep within the structure, it may not be detectable by these localized methods. The changes in the modal parameters of the structural beam member are used by the researchers to characterize the damage using various reverse engineering

techniques like Artificial Intelligence (AI) based techniques for quicker and precise estimation.

Motivated by the above reasons, this thesis aims at exploring the use of AI techniques such as fuzzy and neural network for damage diagnosis in engineering structures at an early stage by perceiving the vibration responses.

1.2 Objectives of the thesis

Various engineering fields like mechanical, civil, aerospace etc. by some way or other associated with the services of structural members. So to ensure the safe operation, damage of any kind is to be diagnosed properly so that any sudden failure of the system can be halted to introduce required measures. Therefore, early identification of damage is very much required to avoid the complete abortion of any system in a functioning mode.

Different types of beam elements constitute the structures which are main supports of almost every engineering system. Therefore, it is obvious that the structures are subjected to fluctuation of loading i.e. static loading & dynamic loading. So the load carrying capacity of the structures gradually diminishes which results in the formation of damage in the member. Moreover, the environmental conditions are also having a huge impact on the structures. Hence life span of the structural element is drastically reduced. An analytical model can be developed utilizing the presence of damage which helps in the investigation of effect of the damage on the vibration characteristics of the system. An additional stiffness is introduced in the structural beam member due to the presence of damage, which can be utilized along with the existing boundary conditions to express the vibration chacteristics of the beam in terms of mathematical equation. The modal parameters such as the natural frequency, mode shape and damage characteristics such as the damage depth and damage position can be extracted from the characteristics equation. The present investigation aims to develop an intelligent diagnosis system of structures consisting of different materials like aluminium, steel and glass fiber reinforced composite beam using the deviation in modal parameters of the structural members due to the presence of damage.

For this prospect, cantilever beams & fixed-fixe beams of Al, steel and composite materials with uniform cross section have been examined, which act as a structural member in various engineering applications. The dynamic responses of the structural beam members have been evaluated in the undamaged state, which act as the basis for standardization. Thereafter, damages of various severities at different positions have been introduced and thus alterations in modal parameters have been identified for each state of damage. Consequently, a correlation has been established between the dynamic behavior and the existence of damage in the structures which helps in the development of different AI technique based model to conduct the structural health monitoring, varying the damage characteristics for different materials. The objective is to compare the results obtained from different methods for damage diagnosis.

In the present analysis, extensive literature survey has been carried out related to the domain of damage diagnosis in engineering applications. From the previous analysis, it is observed that the results obtained by the researchers have not been effectively used to design tools for real applications such as damage diagnosis of different materials. In the current investigation, an attempt has been made to design and develop a tool using the dynamic behavior of damaged and undamaged beam structure using theoretical analysis, finite element analysis, experimental analysis and artificial intelligence techniques.

The different stages for the present analysis are listed below:

1. Theoretical analysis for the cantilever and fixed-fixed beam structures with damage have been performed to evaluate the modal parameters.
2. Finite Element Analysis (FEA) has been carried out to measure the vibration responses of the damaged and undamaged cantilever beam and fixed-fixed beam with different damage characteristics.
3. First three relative natural frequencies and average relative mode shape differences of the damaged structural beams are estimated by the observations obtained from the experimental set up.
4. The vibration responses such as natural frequencies and mode shapes obtained from theoretical, finite element and experimental methodologies have been used to design the

models based on artificial intelligence techniques. The developed AI based models have made use of the first three relative natural frequencies and first three average relative mode shape differences as the input parameters and relative crack positions and relative damage depths as the outputs.

The theoretical study has been materialized for a structural beam element with a damage to obtain the vibration characteristics by utilizing the expressions of strain energy release rate and stress intensity factors. The presence of damages produces the local stiffness at the localized damage position and lowers the stiffness of the structure. The stiffness matrix has been formulated to explore the impact of relative damage position on the dimensionless compliances of the structure varying the boundary conditions. The arbitrated vibration signatures from theoretical, finite element and experimental analysis of the beam member have been used to conceptualize and train the AI model (fuzzy, neural network). Conclusively, relative damage positions and relative damage depths are the outputs from the model.

The results obtained from the various methodologies such as theoretical, finite element, experimental, fuzzy, neural network conceived in the current investigation have been compared and a close agreement has been found. Concrete conclusions have been drawn from the results of respective sections. The results are approved by experimentations performed for the various techniques mentioned above.

1.3 Organization of the thesis

The content of the thesis is organized as follows:

The investigations carried out in the present research for damage identification in faulty structures are presented in following chapters.

Chapter 1 depicts the effect of damage on the functionality execution of different engineering applications and also outlines the methodologies being adopted by the researchers to diagnose damages in different industrial applications involving the structural beam elements. The motivation to carry out the research along with the focus of the current analysis is also explained in this chapter.

Chapter 2 is the literature survey section representing the published work from the domain of damage identification using vibration signatures and AI techniques. This chapter also expresses the classification of techniques in the field of damage diagnosis and justifies the need of current analysis.

Chapter 3 presents the theoretical model to estimate the vibration characteristics (natural frequencies, mode shapes) by using stress intensity factor, strain energy release rate and employing different boundary conditions. The presence of damage in the structure introduces flexibility at the localized damage position which in turn, brings down the natural frequencies and the change in the mode shapes. This concept has been applied in the numerical interpretation to detect the existence of damages in the structure beam members and also to estimate the damage positions and their intensities.

Chapter 4 of this work develops the finite element model of the damaged structural beams to arbitrate the vibration responses, which in turn can be utilized to determine the presence of damage and damage characteristics. The responses from finite element analysis are arranged in contrast to the responses obtained from experimental method and numerical analysis for validation.

Chapter 5 introduces the implementation of fuzzy inference system for damage identification in structural beams. In this section, the paths for developing the fuzzy models are illustrated. The triangular, Gaussian and trapezoidal membership functions based intelligent model with their detail architecture are briefly discussed. The comparison of fuzzy based results and experimental results is also presented.

Chapter 6 presents a reverse engineering based artificial neural network technique for effective diagnosis of damage in a structure. The multi layer perceptron with the input and output parameters are depicted and narrated thoroughly. The results from artificial neural network are presented and discussed to demonstrate the implementation of the AI model.

Chapter 7 presents the experimental procedure along with the instruments used for validating the results from methodologies being adopted in the present investigation for damage

identification. The test specimen fabrication steps are outlined. The results from the developed experimental set-up have been obtained and presented for discussion.

Chapter 8 provides a comprehensive review of the results obtained from all the techniques adopted in the current research.

Chapter 9 discusses the conclusions drawn from the research carried out on the current topic and gives the recommendations for scope of future work in the same domain.

Chapter 2
LITERATURE REVIEW

This chapter presents a contemporary study of the vibration based damage identification in structural systems. The main objective is to study the developments made by researchers during the last few decades. Different issues like implementation of damage diagnosis methods, general methods of classification, and a review of a selected group of methods are discussed. Finally, the applications of artificial intelligence techniques for damage diagnosis are discussed from the early developments.

2.1 Introduction

The literature review section presents the analysis of the published work confined to the areas of structural health monitoring, damage detection algorithm, damage diagnostic methodologies and modal testing. The review begins with the description of different vibration analysis methods used for damage identification. Besides, vibration of damaged structures, fault identification methodologies to develop damage diagnostic tool using Finite Element Analysis (FEA) and wavelet technique are discussed. Then, the artificial intelligence techniques (fuzzy logic, neural network) based models for damage identification can be designed. The aim of the present investigation is to develop an artificial intelligent technique, which can be capable to predict the presence of damage irrespective of the material and dimension used for vibrating structures. The possible directions for research can be obtained from the analysis of the literature cited in this section.

From the authentic works, wide variations are observed in damage identification of various systems. In spite of the fact that, there is a wide variation in development of fault diagnostic methodology, the upcoming section demonstrates the review of the literature relevant to damage detection and identification.

2.2 Methodologies for damage detection

Researchers have zeroed in on many techniques for identification of fault in various stages of engineering structures applications. Dynamics based methods are found to be effectively used for health monitoring in irregular systems. The recent methods seasoned for fault diagnosis are presented below.

Douka et al. [1] have presented a method for determining the location and crack depth in double cracked beam. For diagnosing the crack, variation in natural frequency and anti-resonance properties are used by them. Huh et al. [2] have used a methodology in which the rate of vibration energy determined from the accelerations of the beam structures to detect a local damage. This method is approved by using a uniform beam with an open crack both by Numerical and experiment method. Nahvi et al. [3] have used natural frequencies and mode shapes of the beam structure as input parameters for analytical and finite element method to identify the crack in cantilever beam. Darpe et al. [4] have analyzed the cracked rotor with a crack present at the center imposed with axial forces for it's unbalanced response with the help of electro-dynamic exciter to differentiate between rotating and non rotating conditions. Hein et al. [5] have presented a new method for identification of delamination in homogeneous and composite beams. They have used Haar wavelets and neural networks to establish the mapping relationship between frequencies, Haar series expansion of fundamental mode shapes of vibrating beam and delamination status. They have revealed that the simulations show the proposed complex method can detect the location of delaminations and identify the delamination extent with high precision. Curry et al. [6] have suggested a fault detection and isolation methodology based on fixed threshold using a closed loop system with the help of sensors. They have noticed the fault and distinguished the failure for each sensor. Hoffman et al. [7] have employed a diagnostic technique based on neural network. As described in the paper, it is impossible to determine the degree of imbalance in a bearing system using single vibration feature and to overcome this problem they have used the neural network technique for processing of multiple features. For the purpose of fault detection of different bearing conditions they have employed different neural network technique and compared their performances. They have found that the developed algorithm can be suitably used for identifying the presence of defects. Salam et al. [8] have analyzed the lateral vibration of an Euler-Bernoulli beam accompanied with a single edge open crack to compare the mode shapes of damaged and undamaged beam by a interpreted formula for the stress correction factor in terms of the damage characteristics. Sanza et al. [9] have developed a new method for health monitoring of rotating machinery by utilizing the capabilities of wavelet transform and auto associative neural network for

arbitrating the vibration responses. Numerical and experimental dynamic analysis is performed to test the effectiveness of the results obtained. Murigendrappa et al. [10] have diagnosed damaged pipes of aluminium & mild steel with water as fluid medium at different pressure utilizing the variations in natural frequencies.

2.3 Analysis of different methodologies for damage detection

In this section, the various techniques applied for damage detection in vibrating structures have been outlined. The different methods that have been proposed by various experimenters for damage identification are categorized into four sections such as:

1. Classical method
2. Finite Element Method
3. AI method
4. Miscellaneous methods.

2.3.1 Damage detection using classical methods

This section presents the review of energy based method, analytical methods, algorithms based on dynamic responses etc. used for arbitrating the damage location and its intensity in dynamically vibrating damaged structures. The works of various researchers connected to the above methodologies are discussed below.

Chinchalkar [11] has extracted the first three natural frequencies of the cracked beam to identify the crack using a finite element by considering the different boundary conditions and crack depth. Loutridis et al. [12] have interpreted the dynamic behavior of the cracked structure theoretically and experimentally by a new technique based on instantaneous frequency and empirical mode decomposition. A compliance matrix is formulated by Tada et al. [13] in damaged structure for determining the crack location and crack depth. A modal analysis is conducted by Ravi et al. [14] on an aluminium sheet having micro cracks generated by compression loading and the deformation is tracked using the acoustic emission technique. Owolabi et al. [15] have investigated the position and severity of crack for Al fixed-fixed and simply supported beams by fixing the first three natural frequencies and mode shapes. Dado [16] has worked out a mathematical model to observe the crack position and

severity for beams with various end conditions such as pinned-pinned, clamped free, clamped-pin and clamped-clamped considering the beam to be Euler-Bernoulli beam and concluded that the results obtained are useful input parameters to codify the crack though the assumptions don't have the convergence with the real time applications. Babu et al. [17] have proposed a technique using the amplitude deviation curve, which is a modification of the operational deflection shape for crack identification in rotors. Gounaris et al. [18] have established a functional relationship between the crack parameters and modal responses assuming development of an open crack and the results are approved by the Eigen mode comparison of damaged and undamaged beam. Patil et al. [19] have assumed the cracks as rotational spring for developing an algorithm for damage properties evaluation in a slender Euler-Bernoulli beam using variation in natural frequencies and transfer matrix method. Prasad et al. [20] have analyzed crack growth rate at different frequencies using the experimental setup to determine the effect of location in a vibrating cantilever beam. Al-said [21] has implemented the crack diagnostic method using the alteration in natural frequencies for a stepped cantilever beam carrying concentrated masses and subsequent results obtained are validated by finite element method. Wang et al. [22] have investigated the crack position and severity of a composite cantilever having a surface crack by establishing a dependency between frequencies of the vibrating cantilever beam and material properties.

The finite element methods and wave propagation technique have been used for estimating the size and severity of damages and those are being discussed in the next section.

2.3.2 **Damage *detection using finite element method***

Apart from the classical methods, the finite element methods are also implemented by various experimenters for damage detection in affected structures, those have been reviewed in this section.

Ostachowicz et al. [23] have proposed a method assuming an open and closed crack with triangular disk finite elements. He has analyzed the forced vibrations of the beam, the effects of the crack locations and sizes on the vibration behavior and discussed a basis for crack identification. Krawczuk et al. [24] have proposed a finite spectral element method & wave

propagation analysis to determine the modal parameters of a cracked Timoshenko beam. Saavedra et al. [25] have developed a finite element stiffness matrix for the vibration analysis of the multi-beam structure with different boundary conditions. Kisa [26] has investigated to trace the cracks and nature of cracks in a composite structure made of graphite fiber reinforced polyamide cantilever. He has modeled the problem using finite element and the component mode synthesis methods. He has used fracture mechanics theory to derive stiffness matrix as the increase of the compliance matrix calculated with proper stress intensity factor and strain energy release rate expressions. He has studied the effects of location and depth of crack and the volume fraction and orientation of fiber on the natural frequencies and mode shapes of the beam with transverse no propagating open crack. Chandros et.al [27] have analyzed the dynamic characteristic of a breathing crack and have compared the effect of breathing crack and open crack on natural frequency of the damaged beam. They have considered the non-linearity associated with the breathing crack using one dimensional crack beam theory. They have observed that a fatigue crack behaves as breathing crack in absence of preload and will result in smaller drop in natural frequency. Qian et al. [28] have employed stress intensity factor to realize a finite element model for crack detection in a damaged beam and the results obtained are validated by the experimentation performed on complex structures. Panigrahi [29] have performed a three dimensional non-linear finite element analysis to evaluate the normal and shear stress along the overlap zone in a fiber reinforced composite material. Shekhar et al. [30] has determined the dynamic responses utilizing a model based on finite element analysis.

Besides the classical methods, wave propagtaion and finite element methods, Artificial Intelligence Techniques are also being fitted by researchers for damage identification.

2.3.3 Damage detection using AI technique

In this section different types of Artificial Intelligence Techniques are discussed in the field of damage detection in damaged structures. The AI techniques again are categorized in two sub group.

a) Fuzzy Inference method

b) Neural Network method

2.3.3.1 Fuzzy inference method

In this section, or damage identification technique supplemented with different fuzzy inference models are outlined.

Chandrashekhar et al. [31] have proposed that, for the damage diagnosis the geometric and measurement uncertainty are the issues to be taken care of. They have addressed the uncertainty associated with the fuzzy logic system for structural damage detection utilizing the results obtained from Monte Carlo simulation involving the study of changes in the damage indicator due to uncertainty in the geometric properties of the beam. Boutros et al. [32] have identified the transient and gradual abnormalities using fuzzy logic approach with the help of four condition monitoring indicators. They have compared the fuzzy based technique in two different applications with satisfactory validation. Miguel et al. [33] have developed a decision making segment based on fuzzy logic the damage diagnosis applications. The input and output parameters of an isolation system are successfully utilized in laboratory equipments to maintain the uncertainty level with in the acceptable range. Parhi [34] has developed a fuzzy inference based guiding mechanism for multiple robots working in obstacles hindered environment. They have been designed to navigate in an environment without hitting any obstacles along with other robots. Fox [35] has analyzed the role of fuzzy logic in medical diagnosis and reveals the presence of various concerns regarding the information-processing techniques in the development of medical computing. Dash & Parhi [36] have used the fuzzy logic based techniques to detect the cracks in a cantilever beam of uniform cross section. They have utilized the dynamic characteristics such as change in natural frequencies and mode shapes as input to the fuzzy model to predict the crack position and severity, which is subsequently validated by finite element and experimental methods. Angelov et al. [37] have used the developed fuzzy system for image classification in on line mode utilizing the approaches cited for improving the realization of on line fuzzy classifier. Zimmermann [38] has obtained the comparatively effective solution for linear vector

maximum problem through fuzzy linear programming approach for solving linear vector maximum problem. Sugumaran et al. [39] have proposed a decision tree of a fuzzy classifier for selecting best few feature that will differentiate the fault condition of the bearing from given trained samples. The vibration signal from a piezoelectric transducer is captured for different types of fault condition of bearing and is used to build the fuzzy rules. The results obtained from the fuzzy classifier are encouraging when compared with that of the experimental analysis. Kim et al. [40] have come up with a computer based damage diagnosis system for concrete structures using Fuzzy set theory. They have applied the enhanced technique to diagnose the damage using the damage attributes as building blocks to model the fuzzy inference system and the results obtained are very encouraging when compared with the standard ones. Mohanta et al. [41] have done the justice to the maintenance scheduling of a captive power plant with the help of a fuzzy Markov model, taking the various parameters affecting the failure repair cycle in to account. Parhi [42] has developed a fuzzy inference based navigational control system for multiple robots working in a clumsy environment. They have been designed to navigate in an environment without hitting any obstacles along with other robots.

2.3.3.2 Neural network method

In this section, the important role played by Artificial Neural Networks (ANN) for damage characterization has been described.

Eski et al. [43] have proposed damage detection technique for an experimental industrial welding robot via neural network modeling, for which measurement parameters are extracted from the Joint accelerations of robot. They have analyzed the welding robot having six degree of freedom to note the related values and accelerations. The results confirm the robot stability of RBNN to interpret the acceleration of manipulator joints in a prescribed trajectory. Parhi & Dash [44] have analyzed the cantilever beam with multiple crack for it's vibrational characteristics, which in turn is being utilized to train the neural network controller complemented with back propagation technique. Paviglianiti et al. [45] have developed a method for detecting and isolating sensor faults in industrial robot manipulators. They have adopted a procedure to separate the disturbance effect from the effect of the fault generated in

the system. The dynamics of the proposed methodology has been refined by using radial basis functions neural network. Mehrjoo et al. [46] have presented a damage identification inverse algorithm to investigate the damage severities of joints in truss bridge structure using back propagation neural network method. Saravanan et al. [47] have implemented the fault diagnosis in bevel gear box with the effcetiveness of an artificial neural network, wave let and proximal support vector machine. Wu et al. [48] have proposed a damage diagnosis technique for internal combustion engine using discrete wavelet transform (DWT) and neural network. The DWT technique has been amalgamated with the selective feature of energy spectrum for the development of the purposed fault detection algorithm. Oberholster et al. [49] have come up with a technique for online structure health monitoring of blades with axial flow utilizing neural network. The vibration responses are extracted from the experimental test structures for the modeling of neural network by the implementation of frequency response function and finite element models. They are assured regarding the online damage classification using sensor for the test structures by their proposed technique. Agosto et al. [50] have coupled the neural network method with a combination of vibration and thermal damage detection signatures to develop a damage defection tool, which they have implemented on sandwich composite for the purpose of damage detection. Ghate et al. [51] have developed a multi layer perceptron neural network based classifier for damage detection in induction motors which is inexpensive, reliable by engaging the available information such as stator current. They have used simple statistical parameters as input feature and principal component analysis has been used for reduction of input dimensionality. They have also certified their methodology to noise based technique. Das & Parhi [52] have presented an artificial neural network (ANN) technique to predict crack location and crack depth in a cracked cantilever beam. They have used first three relative natural frequencies and relative mode shapes as input parameters to the ANN and obtained relative crack location and crack depth as output parameters. They have obtained local stiffness using strain energy release rate at the location of the crack. Parhi & Chaudhury [53] have presented a paper using the concept of fuzzy logic and artificial neural network (ANN) for damage diagnosis of the cracked cantilever beam. They have used the local flexibility introduced at the crack location as parameter to detect the presence of crack with its location and size. The analysis is based on using hybrid membership functions (triangular, trapezoidal, Gaussian) as input to fuzzy controller and trapezoidal membership functions as output.

2.3.4 *Miscellaneous techniques used for Damage detection*

Besides all techniques reviewed above, some miscellaneous methods and tools are also very important in identifying the damage with refined accuracy and some of them are briefly discussed in this section.

Gentil and Messina [54] have investigated the usefulness of continuous wavelet transform (CWT) technique to detect the crack in beam structure by minimizing measurement data and baseline information of the structure. They have used the intrinsic capability of the wavelet for translating the data into the CWT and the redundancy of the data of the CWT in the functional space is able to locate the cracks even in the presence of noisy data. Rao et al. [55] have presented a method for crack identification in a cracked cantilever beam by the vibration signatures using continuous wavelet transform technique. The results obtained from this method on comparison with the analytical and experimental methods give satisfactory remarks. Kim et al. [56] have proposed a methodology for condition-based maintenance scheme in industrial machines by correctly measuring the remaining life of the machine component utilizing the support vector machine tool. The results obtained have been very satisfying and can be used as an important tool for prediction of remaining life of machineries. Zheng et al. [57] have presented a tool for dynamic stability analysis of damaged hollow beams. According to him each damage is attached with a local flexibility coefficient which is a function of intensity of damage. He has used least squared method to formulate the shallow cracks and deep cracks. In this work, he has adapted Hamilton's principle to formulate the governing equation by employing the flexibility coefficient of the cracks which serves as that of the rotational spring. Quek et al. [58] have analyzed the sensitivity of wavelet technique in the identification of cracks in beam structures considering the effects of different crack properties, boundary conditions, and wavelet functions. From the analysis, they have concluded that the wavelet transform is a useful tool in identification of cracks in beam structures. Cao et al. [59] have developed a genuine Laplacian technique to form an enhanced damage identification algorithm. They have noted the modal curvature to develop the diagnostic technique. The results from the proposed Laplacian scheme have been compared with experimental results to only have encouraging remarks. Karagac et al. [60] have investigated the effect of crack ratios and crack location on the fundamental frequency of a cantilever slender beam with an edge crack subjected to

free vibration and lateral buckling. They have established that the presence of cracks reduce the fundamental frequency and buckling load. Rus et al. [61] have developed a methodology based on hyper singular shape sensitivity boundary integral equation for solution of the inverse problem for crack identification. The accuracy and convergence of the sensitivity for the proposed method has been verified with the simulation and experimentation. Friswell [62] has described the use of inverse method in the detection of damage location and size by using vibration responses and identified the abnormal parameters associated with the model. Moreover, he has pointed out a number of concerns involved in this method for health monitoring, including modeling error, environmental efforts, damage localization and regularization. Fagerholt et al. [63] have analyzed the fracture behavior of a cast aluminium alloy by making use of classical flow theory for modeling the fracture. They have also taken care of Digital Image Correlation (DIC) to obtain information of the displacement and strain field in the test specimen. The results from the numerical analysis are found to be in very good agreement with the experimental data. An & Sohn [64] have proposed a damage identification technique utilizing the impedance and guided wave signals obtained from piezoelectric transducers mounted on surface. The proposed technique is very effective on high temperature condition. Fledman [65] has presented the application of Hilbert transform to non-stationary and nonlinear vibration system by conceptualizing the actual mechanical signals and utilizes the Hilbert transform for diagnosis of mechanical systems.

2.4 Concluding remarks from literature review

The concluding remarks drawn from the above literature review are actually showing the direction for the concerned research conducted. Though, analytical methods and artificial intelligence (AI) techniques are already in use by various researchers, but the concentration is focused on same material without varying the damage characteristics. Therefore, analyzing the dynamic characteristics of different materials with variations in damage characteristics in the same platform is really interesting, which is explored in this research work.

In the current research, a systematic effort has been made to develop AI based intelligent system for structural health monitoring of beam model using fuzzy inference, neural network

techniques. The dynamic parameters required to design and train the AI model have been obtained by using the theoretical, finite element and experimental analysis of the beam structure.

Chapter 3

ASSESSMENT OF MODAL PARAMETERS OF BEAM STRUCTURE WITH DAMAGE IN TRANSEVERSE DIRECTION

Presence of damage hinders the optimum performance of structural beam assembly or constituents of machinery. Presently, most of the failures encountered by various mechanical structures are due to material fatigue which leads to the development of different forms of damage like crack, fracture or any other irregularities. Therefore damage detection and localization is the main topic of discussion for various researchers across the globe. The dynamic characteristics such as natural frequencies and mode shapes due to vibration of whole structure are affected due to the presence of a crack as the stiffness of that structural element is altered i.e. there is a reduction in natural frequencies, an increase in modal damping.

3.1 Introduction

In the recent times, the modal parameters of damaged structure have been investigated thoroughly by different experimenters. The responses of vibrating members are found to alter due to presence of damage in the structure and the extent of variation is a function of damage intensity and it's position. Engineers and scientists have pronounced the effect of damage on the natural frequencies and mode shapes of dynamically vibrating structure, utilizing which in turn can be efficiently utilized for developing crack identification algorithms can be actualized. This chapter puts forth a systematic approach to evolve a theoretical model to estimate the effect of damage on the dynamic characteristics of the cantilever beam & fixed-fixed beam structure. The dimensionless compliance matrices and subsequently the local stiffness matrices can be developed by making use of the Stress intensity factor and strain energy release rate from linear fracture mechanics theory. Moreover, the stiffness matrix has been utilized to assess the deviation in the dynamic response of the damaged beams in contrast to that of the undamaged beam. In the theoretical interpretation, different boundary

conditions have been engaged to evaluate the natural frequencies and mode shapes for the cantilever and fixed-fixed beam structure with various damage depths and damage positions. The dynamic responses obtained from the theoretical modeling have been validated by comparing the results with that of the experimental analysis.

3.2 Vibration attributes of damaged beam structures

3.2.1 Theoretical interpretation

In this section, theoretical modeling of cantilever beam and fixed-fixed beam is realized to estimate the vibration characteristics such as natural frequencies and mode shapes of the damaged structures with different relative damage positions and relative damage severities presents the approach adopted to build the theoretical model for measuring the modal and undamaged beam structure. During the interpretation of the theoretical outcomes, significant divergence is noticed for the first three mode shapes in the localized damage position, which can further be certified with the results obtained from the experimental analysis.

3.2.1.1 Evaluation of local flexibility of the damaged beam under axial force and bending

Fig. 3.1(a) and 3.1(b) illustrate cantilever & fixed-fixed beam, subjected to axial load (P_1) and bending moment (P_2), which effectuate combining effect in terms of longitudinal and transverse motion of the beam respectively. The beams contain damage in transverse direction of depth 'a_1' having width 'B' and thickness 'W'. The existence of damage in the beam structure modifies the localized flexibility square matrix of two dimensions.

At the damaged portion, strain energy release rate can be explained as [13];

$$J = \frac{1}{E'}(K_{I1} + K_{I2})^2, \text{ Where } \frac{1}{E'} = \frac{1-v^2}{E} \text{ (for plane strain condition);} \quad (3.1a)$$

$$= \frac{1}{E} \text{(for plane stress condition)} \quad (3.1b)$$

The $K_{I1,}$ K_{I2} are Stress intensity factors for 1st mode of vibration for load P_1 and P_2 respectively. The values of stress intensity factors from the referred article [13] are;

$$\frac{P_1}{WB}\sqrt{\pi a}(F_1(\frac{a}{W}))=K_{I1},\ \frac{6P_2}{W^2B}\sqrt{\pi a}\,(F_2(\frac{a}{W}))=K_{I2} \tag{3.2}$$

The expressions for F_1 and F_2 are as follows

$$\left.\begin{aligned} F_1(\frac{a}{W}) &= (\frac{2W}{\pi a}\tan(\frac{\pi a}{2W}))^{0.5}\left\{\frac{0.752+2.02(a/W)+0.37(1-\sin(a\pi/2W))^3}{\cos(a\pi/2W)}\right\} \\ F_2(\frac{a}{W}) &= (\frac{2W}{\pi a}\tan(\frac{\pi a}{2W}))^{0.5}\left\{\frac{0.923+0.199(1-\sin(a\pi/2W))^4}{\cos(a\pi/2W)}\right\} \end{aligned}\right\} \tag{3.3}$$

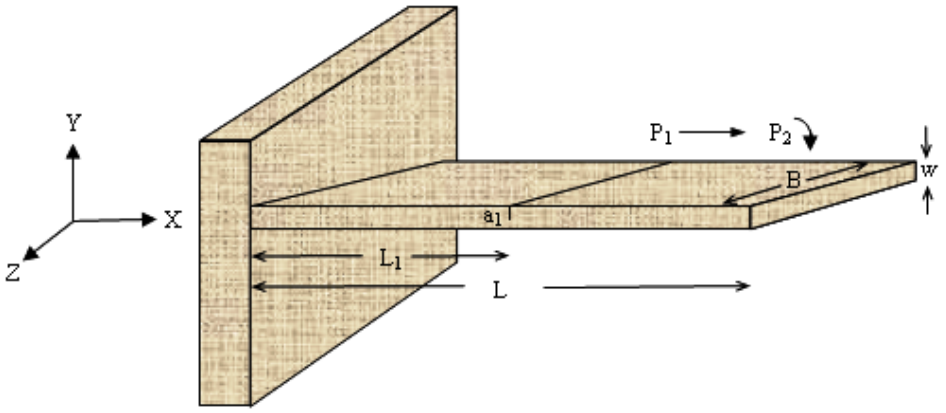

Fig. 3.1 (a) Schematic diagram of cantilever beam

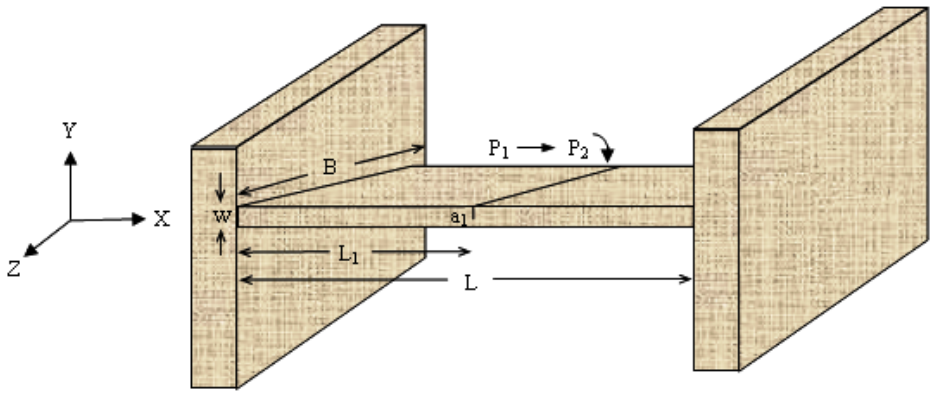

Fig. 3.1 (b) Schematic diagram of fixed-fixed beam

According to Castigliano's theorem (Taking the assumption, strain energy due to the damage as U_t) the extra extension along the force P_i is;

$$\frac{\partial U_t}{\partial P_i} = u_i \tag{3.4}$$

The form of strain energy will have, $U_t = \int_0^{a_1} J\,da = \int_0^{a_1} \frac{\partial U_t}{\partial a}\,da$ (3.5)

Where J= $\frac{\partial U_t}{\partial a}$ the strain energy density function.

Hence, from equations (3.1) and (3.3), we can have

$$\frac{\partial}{\partial P_i}\left[\int_0^{a_1} J(a)\,da\right] = u_i \tag{3.6}$$

C_{ij} the flexibility influence co-efficient by definition is

$$\frac{\partial u_i}{\partial P_j} = \frac{\partial^2}{\partial P_j \partial P_i}\int_0^{a_1} J(a)\,da = C_{ij} \tag{3.7}$$

and can be expressed as, $\frac{WB}{E'}\frac{\partial^2}{\partial P_j \partial P_i}\int_0^{\xi_1} (K_{I2} + K_{I1})^2\,d\xi = C_{ij}$ (3.8)

Using equation (3.8) the compliance C_{11}, C_{22}, C_{12} (=C_{21}) are as follows;

$$C_{11} = \frac{BW}{E'}\int_0^{\xi_1} \frac{\pi a}{B^2 W^2} 2(F_1(\xi))^2\,d\xi$$

$$= \frac{2\pi}{BE'}\int_0^{\xi_1} \xi (F_1(\xi))^2\,d\xi \tag{3.9}$$

$$C_{12} = C_{21} = \frac{12\pi}{E'BW}\int_0^{\xi_1} \xi F_1(\xi) F_2(\xi)\,d\xi \tag{3.10}$$

$$C_{22} = \frac{72\pi}{E'BW^2} \int_0^{\xi_1} \xi F_2(\xi) F_2(\xi)\, d\xi \tag{3.11}$$

The dimensionless form of the influence co-efficient will be;

$$\overline{C_{11}} = C_{11} \frac{BE'}{2\pi} \quad \overline{C_{12}} = C_{12} \frac{E'BW}{12\pi} = \overline{C_{21}} \; ; \; \overline{C_{22}} = C_{22} \frac{E'BW^2}{72\pi} \tag{3.12}$$

The inversion of compliance matrix will lead to the formation of local stiffness matrix and can be written as;

$$K = \begin{bmatrix} C_{11} & C_{12} \\ C_{21} & C_{22} \end{bmatrix}^{-1} = \begin{bmatrix} K_{11} & K_{12} \\ K_{21} & K_{22} \end{bmatrix} \tag{3.13}$$

The stiffness matrix for the damage position can be obtained as follows:

$$K' = \begin{bmatrix} k'_{11} & k'_{12} \\ k'_{21} & k'_{22} \end{bmatrix} = \begin{bmatrix} C'_{11} & C'_{12} \\ C'_{21} & C'_{22} \end{bmatrix}^{-1}$$

3.2.1.2 Vibration analysis of damaged beam structures

A cantilever beam of length 'L' width 'B' and depth 'W', with a damage of severity 'a_1' at a distance 'L_1' from the fixed end is considered. Taking $u_1(x,t)$ and $u_2(x,t)$ as the amplitudes of longitudinal vibration for the sections before and after the damage and $y_1(x,t)$, $y_2(x,t)$ are the amplitudes of bending vibration for the same sections (Fig. 3.2.3).

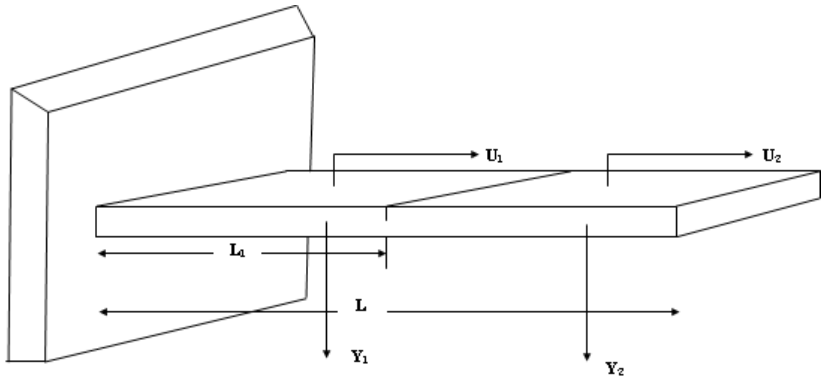

Fig. 3.2 Cantilever beam Model

The normal function for the system can be defined as

$$\bar{u}_1(\bar{x}) = A_1 \cos(\bar{K}_u \bar{x}) + A_2 \sin(\bar{K}_u \bar{x}) \quad (3.2.16a)$$

$$\bar{u}_2(\bar{x}) = A_3 \cos(\bar{K}_u \bar{x}) + A_4 \sin(\bar{K}_u \bar{x}) \quad (3.2.16b)$$

$$\bar{y}_1(\bar{x}) = A_5 \cosh(\bar{K}_y \bar{x}) + A_6 \sinh(\bar{K}_y \bar{x}) + A_7 \cos(\bar{K}_y \bar{x}) + A_8 \sin(\bar{K}_y \bar{x}) \quad (3.2.16c)$$

$$\bar{y}_2(\bar{x}) = A_9 \cosh(\bar{K}_y \bar{x}) + A_{10} \sinh(\bar{K}_y \bar{x}) + A_{11} \cos(\bar{K}_y \bar{x}) + A_{12} \sin(\bar{K}_y \bar{x}) \quad (3.2.16d)$$

Where $\bar{x} = \frac{x}{L}, \bar{u} = \frac{u}{L}, \bar{y} = \frac{y}{L}, \beta = \frac{L_1}{L}$

$$\bar{K}_u = \frac{\omega L}{C_u}, C_u = \left(\frac{E}{\rho}\right)^{1/2}, \bar{K}_y = \left(\frac{\omega L^2}{C_y}\right)^{1/2}, C_y = \left(\frac{EI}{\mu}\right)^{1/2}, \mu = A\rho$$

A_i, (i=1, 12) Constants are to be determined, from boundary conditions. The boundary conditions of the cantilever beam in consideration are:

$\bar{u}_1(0) = 0$; 3.2.17(a) $\bar{y}_1(0) = 0$; 3.2.17(b) $\bar{y}_1'(0) = 0$; 3.2.17(c) $\bar{u}_2'(1) = 0$; 3.2.17(d)

$\bar{y}''_2(1) = 0$; 3.2.17(e) $\bar{y}_2'''(1) = 0$; 3.2.17(f)

At the damaged section:

$\bar{u}'_1(\beta) = \bar{u}'_2(\beta)$; 3.2.18(a) $\bar{y}_1(\beta) = \bar{y}_2(\beta)$; 3.2.18(b) $\bar{y}_1''(\beta) = \bar{y}_2''(\beta)$; 3.2.18(c)

$\bar{y}_1'''(\beta) = \bar{y}_2'''(\beta)$ 3.2.18(d)

Also at the damaged section (due to the discontinuity of axial deformation to the left and right of the damage), we have:

$$AE\frac{du_1(L_1)}{dx}=K_{11}\,(u_2(L_1)-u_1(L_1))+K_{12}\left(\frac{dy_2(L_1)}{dx}-\frac{dy_1(L_1)}{dx}\right) \tag{3.2.19}$$

Multiplying both sides of the above equation by $\frac{AE}{LK_{11}K_{12}}$ we get;

$$M_1M_2\bar{u}'(\beta)=M_2(\bar{u}_2(\beta)-\bar{u}_1(\beta))+M_1(\bar{y}_2'(\beta)-\bar{y}_1'(\beta)) \tag{3.2.20}$$

Similarly at the damaged section (due to the discontinuity of slope to the left and right of the crack)

$$EI\frac{d^2y_1(L_1)}{dx^2}=K_{21}\,(u_2(L_1)-u_1(L_1))+K_{22}\left(\frac{dy_2(L_1)}{dx}-\frac{dy_1(L_1)}{dx}\right) \tag{3.2.21}$$

Multiplying both sides of the above equation by $\frac{EI}{L^2K_{22}K_{21}}$ we get,

$$M_3M_4\bar{y}_1''(\beta)=M_3(\bar{u}_2(\beta)-\bar{u}_1(\beta))+M_4(\bar{y}_2'(\beta)-\bar{y}_1'(\beta)) \tag{3.2.22}$$

Where, $M_1=\frac{AE}{LK_{11}}$, $M_2=\frac{AE}{K_{12}}$, $M_3=\frac{EI}{LK_{22}}$, $M_4=\frac{EI}{L^2K_{21}}$

The normal functions, Eq. {3.2.16} along with the boundary conditions as mentioned above, yield the characteristic equation of the system as:

$$|Q|=0 \tag{3.2.23}$$

Where Q is a 12x12 matrix and is expressed as

$$Q = \begin{bmatrix} 1 & 0 & 1 & 0 & 0 & 0 & 0 & 0 & 0 & 0 & 0 & 0 \\ 0 & 1 & 0 & 1 & 0 & 0 & 0 & 0 & 0 & 0 & 0 & 0 \\ 0 & 0 & 0 & 0 & G_3 & G_4 & -G_7 & -G_8 & 0 & 0 & 0 & 0 \\ 0 & 0 & 0 & 0 & G_4 & G_3 & G_8 & -G_7 & 0 & 0 & 0 & 0 \\ G_1 & G_2 & -G_5 & -G_6 & -G_1 & -G_2 & G_5 & G_6 & 0 & 0 & 0 & 0 \\ G_2 & G_1 & G_6 & -G_5 & -G_2 & -G_1 & -G_6 & G_5 & 0 & 0 & 0 & 0 \\ G_1 & G_2 & G_5 & G_6 & -G_1 & -G_2 & -G_5 & -G_6 & 0 & 0 & 0 & 0 \\ S_1 & S_2 & S_3 & S_4 & -G_2 & -G_1 & G_6 & -G_5 & S_5 & S_6 & S_7 & S_8 \\ 0 & 0 & 0 & 0 & 0 & 0 & 0 & 0 & 0 & 0 & 0 & 0 \\ 0 & 0 & 0 & 0 & 0 & 0 & 0 & 0 & 0 & 0 & -T_8 & T_7 \\ 0 & 0 & 0 & 0 & 0 & 0 & 0 & 0 & -T_6 & T_5 & T_6 & -T_5 \\ S_9 & S_{10} & S_{11} & S_{12} & S_{13} & S_{14} & S_{15} & S_{16} & S_{17} & S_{18} & -T_5 & -T_6 \end{bmatrix} \quad (3.2.24)$$

Where G1= Cosh ($\overline{K_y}\alpha$), G_2=Sinh ($\overline{K_y}\alpha$), G_3= Cosh ($\overline{K_y}$), G_4=Sinh ($\overline{K_y}$), G_5=Cos ($\overline{K_y}\alpha$),

G_6=Sin ($\overline{K_y}\alpha$), G_7=Cosh ($\overline{K_y}$), G_8=Sin ($\overline{K_y}$),

T_5=Cos ($\overline{K_u}\alpha$), T_6=Sin ($\overline{K_u}\alpha$), T_7=Cos ($\overline{K_u}$), T_8=Sin ($\overline{K_u}$)

$M_{12}=\frac{M_1}{M_2}$, $M_{34}=\frac{M_3}{M_4}$

$S_1=G_2 + M_3\overline{K_y}\,G_1$, $S_2= G_1 + M_3\overline{K_y}\,G_2$, $S_3= -G_6 - M_3\overline{K_y}\,G_5$, $S_4= G_5 - M_3\overline{K_y}\,G_6$, $S_5=\frac{M_{34}}{K_y}$,

$S_6= \frac{M_{34}}{K_y}T_6$, $S_7= \frac{-M_{34}}{K_y}T_5$, $S_8= \frac{-M_{34}}{K_y}T_6$, $S_9= M_{12}\overline{K_y}\,G_2$

$S_{10}=M_{12}\overline{K_y}\,G_1$, $S_{11}=-M_{12}\overline{K_y}\,G_6$, $S_{12}= M_{12}\overline{K_y}\,G_5$

$S_{13} = -M_{12}\ \overline{K_y}\ G_2$, $S_{14} = -M_{12}\overline{K_y}\ G_1$,

$S_{15} = M_{12}\overline{K_y}\ G_6$, $S_{16} = -M_{12}\overline{K_y}\ G_5$, $S_{17} = T_5 - M_1\overline{K_u}\ T_6$, $S_{18} = T_6 + M_1\overline{K_u}\ T_5$

This determinant is a function of natural circular frequency (ω_n), the relative position of the damage (L_1/L) and the local stiffness matrix (K) which in turn is a function of the relative damage severity (a_1/W). Similarly, local stiffness matrix for fixed-fixed beam can be derived.

3.2.2 Numerical interpretation

The cantilever and fixed-fixed beams of Al, Steel and Glass fiber reinforced Composite with and without damage have been engaged for numerical analysis, to estimate the relative natural frequencies and relative amplitude of vibration for different damage positions and damage severities. The dimensions of all beams is considered as 1000mm x 50mm x 8mm with different damage severities of 3mm, 4mm and 5mm at different positions i.e. middle of the beam, one fourth and three fourth of the total length of the beam from the fixed end. Mechanical properties (Young's modulus, Poisson's ratio, Density) of Al & steel are considered as 70 Gpa, 0.35, 2700 kg/m^3 and 200 Gpa, 0.26, 7850 kg/m^3 respectively. Young's modulii (along longitudinal and transverse direction) of composite beam are found to be (from tensile & flexural test) 9 Gpa and 4.83 Gpa respectively. Poisson's ratio (along longitudinal 'Major' and transverse direction 'Minor') of composite beam are found to be 0.41 & 0.22 respectively. The density of the composite beam material is found to be 1950 kg/m^3.

3.2.2.1 Results of numerical interpretation

The theoretical analysis has been engaged to obtain the mode shapes for the first three modes of the damaged aluminum, composite and steel cantilever beam & fixed-fixed beam models with different damage positions and damage severities using the equation (3.2.24).

3.3 Analysis of experimental results

The cantilever beam and fixed-fixed beams of Al, glass fiber reinforced composite and steel embedded with and without damage with dimension (1000mm x 50mm x 8mm) have been

considered to conduct the experiments for arbitrating the relative natural frequency and relative amplitude of vibration. A number of experiments have been performed on the test specimens with different values of damage positions and damage severities to determine the first three mode shapes and natural frequencies.

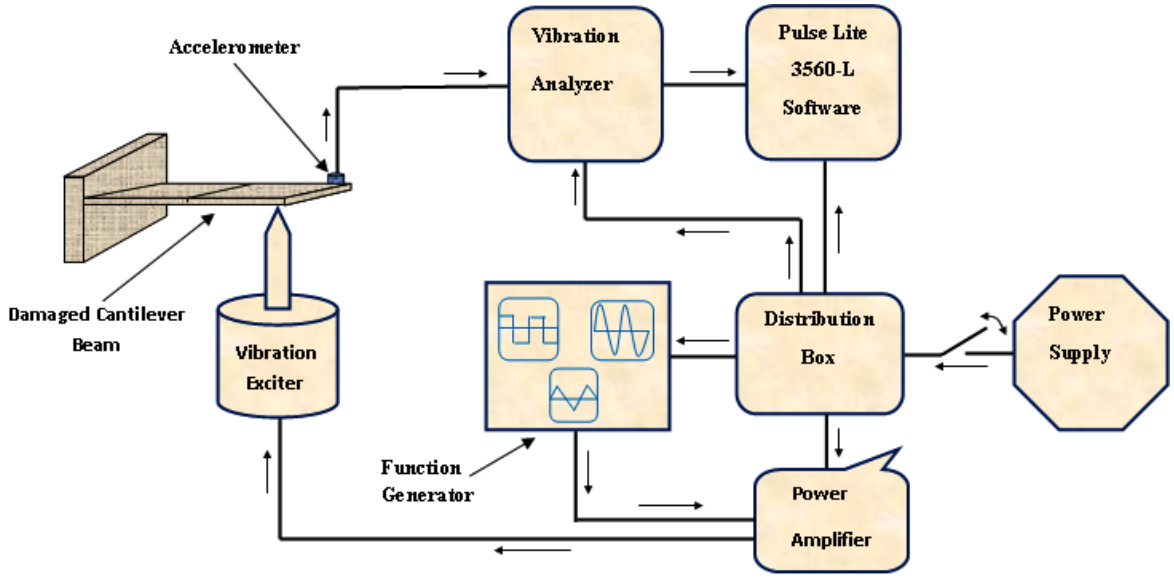

(a)

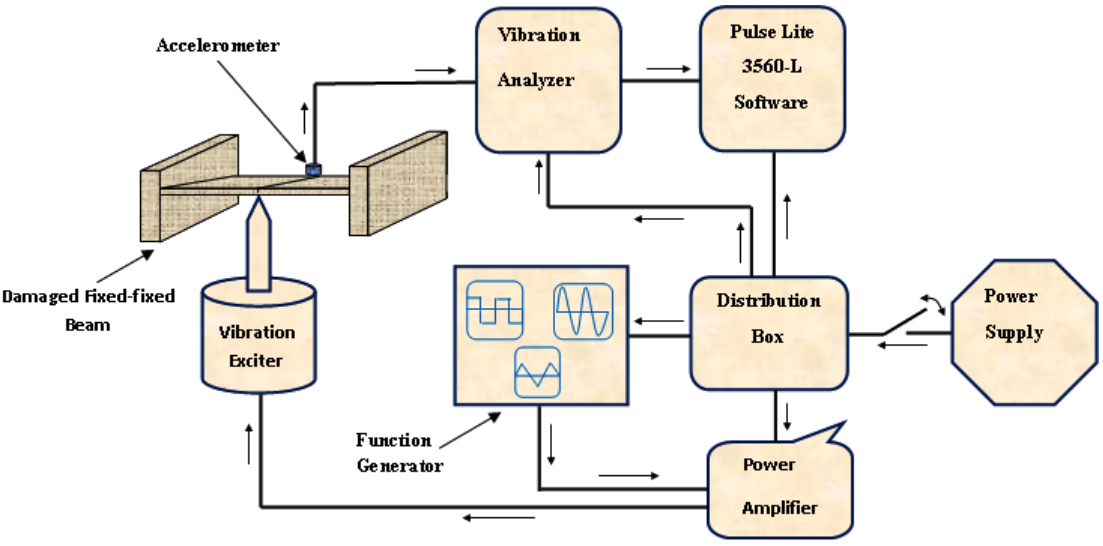

(b)

Fig. 3.3 Schematic block diagram of (a) Cantilever (b) Fixed-fixed beam experimental set ups

3.3.1 Experimental results

The relative natural frequencies & relative mode shape differences obtained from experimentation (Fig. 3.3) for three relative damage positions (0.25, 0.50 and 0.75) and three relative damage severities (0.375, 0.500 and 0.625) have been compared with that of the numerical analysis of both damaged and undamaged beam structures. The comparisons are presented in Table 3.1 to Table 3.6.

3.3.2. Comparison between the results of numerical and experimental analyses

The relative damage positions and relative damage severities of Al, composite & steel cantilever and fixed-fixed beams corresponding to nine sets of first three natural frequencies and first three mode shape differences from numerical and experimental analysis are presented in Table 3.1 to Table 3.6.

The relative natural frequency and relative mode shape difference used in the above analysis can be defined as follows.

$$\text{Relative natural frequency} = \frac{\text{(Natural frequency of cracked beam)}}{\text{(Natural frequency of undamaged beam)}}$$

$$\text{Relative mode shape difference} = \frac{\text{(Modal amplitude of undamaged beam} - \text{Modal amplitude of cracked beam)}}{\text{Modal amplitude of undamaged beam}}$$

Table 3.1 Comparison of modal parameters and damage characteristics of Al cantilever beam obtained from numerical and experimental analysis

FNF	SNF	TNF	FMD	SMD	TMD	Numerical		Experimental	
						RDS	RDP	RDS	RDP
0.9979	0.9986	0.9992	0.0021	0.0075	0.0037	0.373	0.49	0.375	0.50
0.9956	0.9885	0.9986	0.0043	0.0011	0.0036	0.487	0.49	0.500	0.50
0.9910	0.9702	0.9983	0.0083	0.0140	0.0097	0.628	0.48	0.625	0.50
0.9924	0.9964	0.9944	0.0016	0.0301	0.0161	0.376	0.26	0.375	0.25
0.9837	0.9918	0.9880	0.0039	0.0094	0.0373	0.494	0.24	0.500	0.25
0.9661	0.9841	0.9752	0.0089	0.0147	0.0293	0.623	0.26	0.625	0.25
0.9999	0.9999	0.9908	0.0169	0.0682	0.0435	0.369	0.73	0.375	0.75
0.9998	0.9996	0.9805	0.0359	0.0429	0.0711	0.497	0.73	0.500	0.75
0.9995	0.9931	0.9604	0.0724	0.0465	0.0313	0.619	0.74	0.625	0.75

Table 3.2 Comparison of modal parameters and damage characteristics of Al fixed-fixed beam obtained from numerical and experimental analysis

FNF	SNF	TNF	FMD	SMD	TMD	Numerical		Experimental	
						RDS	RDP	RDS	RDP
0.9939	0.9996	0.9916	0.1484	0.0043	0.0039	0.368	0.49	0.375	0.50
0.9868	0.9991	0.9823	0.1727	0.0078	0.0103	0.489	0.51	0.500	0.50
0.9745	0.9987	0.9666	0.2679	0.0156	0.0094	0.627	0.51	0.625	0.50
0.9999	0.9943	0.9936	0.1388	0.0333	0.0257	0.373	0.27	0.375	0.25
0.9998	0.9879	0.9867	0.3955	0.0572	0.0227	0.495	0.26	0.500	0.25
0.9994	0.9757	0.9742	0.4135	0.0667	0.0496	0.620	0.24	0.625	0.25

Table 3.3 Comparison of modal parameters and damage characteristics composite cantilever beam obtained from numerical and experimental analysis

FNF	SNF	TNF	FMD	SMD	TMD	Numerical		Experimental	
						RDS	RDP	RDS	RDP
0.9964	0.9990	0.9999	0.0075	0.0031	0.0015	0.373	0.52	0.375	0.50
0.9957	0.9903	0.9998	0.0017	0.0053	0.0063	0.508	0.48	0.500	0.50
0.9914	0.9726	0.9998	0.0030	0.0074	0.0057	0.619	0.51	0.625	0.50
0.9926	0.9964	0.9946	0.0051	0.0082	0.0137	0.362	0.24	0.375	0.25
0.9843	0.9919	0.9885	0.0076	0.0014	0.0125	0.507	0.25	0.500	0.25
0.9671	0.9841	0.9761	0.0087	0.0024	0.0491	0.621	0.27	0.625	0.25
0.9999	0.9999	0.9911	0.0165	0.0110	0.0312	0.381	0.73	0.375	0.75
0.9997	0.9997	0.9811	0.0350	0.0233	0.0264	0.511	0.73	0.500	0.75
0.9995	0.9947	0.9616	0.0704	0.0561	0.0533	0.617	0.74	0.625	0.75

Table 3.4 Comparison of modal parameters and damage characteristics composite fixed-fixed beam obtained from numerical and experimental analysis

FNF	SNF	TNF	FMD	SMD	TMD	Numerical		Experimental	
						RDS	RDP	RDS	RDP
0.9940	0.9999	0.9918	0.0043	0.0091	0.0066	0.361	0.49	0.375	0.50
0.9872	0.9998	0.9828	0.0080	0.0123	0.0237	0.509	0.52	0.500	0.50
0.9753	0.9997	0.9676	0.0119	0.0087	0.0411	0.631	0.52	0.625	0.50
0.9998	0.9944	0.9937	0.1237	0.0265	0.0761	0.372	0.23	0.375	0.25
0.9997	0.9883	0.9869	0.3741	0.0465	0.0379	0.502	0.21	0.500	0.25
0.9994	0.9768	0.9751	0.3699	0.0823	0.0531	0.634	0.27	0.625	0.25

Table 3.5 Comparison of modal parameters and damage characteristics of Steel cantilever beam obtained from numerical and experimental analysis

FNF	SNF	TNF	FMD	SMD	TMD	Numerical		Experimental	
						RDS	RDP	RDS	RDP
0.9979	0.9969	0.9996	0.0021	0.0069	0.0044	0.374	0.50	0.375	0.50
0.9955	0.9866	0.9992	0.0043	0.0019	0.0045	0.498	0.49	0.500	0.50
0.9908	0.9676	0.9988	0.0081	0.0138	0.0105	0.623	0.49	0.625	0.50
0.9921	0.9963	0.9941	0.0018	0.0288	0.0179	0.374	0.26	0.375	0.25
0.9833	0.9918	0.9875	0.0041	0.0129	0.0341	0.499	0.26	0.500	0.25
0.9653	0.9842	0.9744	0.0094	0.0122	0.0274	0.622	0.24	0.625	0.25
0.9999	0.9999	0.9905	0.0174	0.0607	0.0461	0.376	0.76	0.375	0.75
0.9998	0.9989	0.9798	0.0099	0.0477	0.0693	0.502	0.74	0.500	0.75
0.9994	0.9913	0.9593	0.0743	0.0419	0.0375	0.622	0.74	0.625	0.75

Table 3.6 Comparison of modal parameters and damage characteristics of Steel fixed-fixed beam obtained from numerical and experimental analysis

FNF	SNF	TNF	FMD	SMD	TMD	Numerical		Experimental	
						RDS	RDP	RDS	RDP
0.9936	0.9997	0.9913	0.1444	0.0137	0.0153	0.377	0.49	0.375	0.50
0.9864	0.9992	0.9817	0.1713	0.1265	0.1117	0.499	0.48	0.500	0.50
0.9736	0.9989	0.9656	0.2627	0.2137	0.2106	0.628	0.49	0.625	0.50
0.9999	0.9941	0.9933	0.1354	0.1366	0.1291	0.376	0.26	0.375	0.25
0.9997	0.9875	0.9863	0.3899	0.3528	0.2205	0.502	0.27	0.500	0.25
0.9994	0.9751	0.9736	0.4082	0.3167	0.2496	0.623	0.24	0.625	0.25

The first three columns of the Table 3.1 to Table 3.6 represent first three relative natural frequencies, where as the fourth, fifth and sixth number columns present the average relative mode shape difference for first three modes of vibration. The columns number seven & eight present the relative damage severity and relative damage position respectively obtained from numerical analysis. The columns number nine & ten present the relative damage severity and relative damage position respectively obtained from experimental analysis.

3.4 Summary

The conclusions drawn from the above analysis are described in this section. Due to the presence of damage the modal parameters of the damaged beams such as natural frequencies and mode shapes exhibit a significant divergence near the damage positions as compared to undamaged beam, which can be witnessed in the magnified views of the mode shapes. The vibration characteristics obtained from the numerical analysis have been validated using the results from experimental analysis and are found to be in very good agreement. The deviation in the dynamic response can be used as the basis for fault detection in damaged structural members and the measured vibration parameters can also be used for design and development of reverse engineering methodologies for damage diagnosis. The proposed method can be effectively used to design artificial intelligent techniques based models for online structural health monitoring.

Chapter 4

FINITE ELEMENT BASED DAMAGE IDENTIFICATION

Damage in the transverse mode can lead to the complete failure of structural members subjected to vibration. Vibration based techniques are found wide application in the damage detection of structures as traditional methods like inspection with naked eye and non-destructive techniques such as x-ray, ultrasonic test etc are not useful for periodic inspection. This technique can be effectively used to identify the damage severity and damage position utilizing the modal characteristics of the damaged beam structure. The presence of damage introduces an additional flexibility at the localized damage position of the structure which in turn, alters the natural frequencies and the mode shapes. Therefore, damage can be diagnosed by utilizing the alteration in vibration responses. This chapter introduces finite element based methodology for identification of damage existing in structural systems. The results from the finite element analysis have been compared with that of the numerical analysis and experimental analysis. The comparison results are very encouraging.

4.1 Introduction

Damage identification in the structural members in many engineering applications is inevitable, considering the fact that almost all engineering system are subjected to various fluctuating loading conditions. The vibration parameters of the damaged structures can be effectively utilized for evaluating the damage characteristics present in the beam members. The realization of FEA technique is found to be very satisfying when compared with that of the theoretical analysis.

In this present analysis for damage identification in structural beam members, finite element based model is adopted to characterize the damage with respect to it's severity and position. The dynamic behavior of the structure is altered with the presence of damage. The results obtained from finite element analysis of the damaged and undamaged structural beam members of Aluminium, composite and steel are validated with the theoretical and experimental results.

4.2 Finite element analysis

Finite element analysis (FEA) is a numerical method for solving a differential or integral equation. It has been applied to a number of physical problems, where the governing differential equations are available. The method essentially consists of assuming the piecewise continuous function for the solution and obtaining the parameters of the functions in a manner that reduces the error in the solution. Due to the systematic and useful modeling of the complex shapes, FEA finds wide applications in many technical applications. Different vibrating structures can be analyzed by employing the suitable boundary conditions. Commercial finite element packages are available to take care of the various problems occurred in many engineering applications. FEA is realized, first by dividing the structure into a number of small parts which are known as finite elements and the procedure adopted to attain these small elements is known as discretization. Each element of the structure is generally associated with an equation of motion and that can be easily approximated. The each element has nodes as end points. The nodes are connecting point between the elements. The finite elements and nodes as together are known as finite element mesh or finite element grid. Subsequently, the equation of motion for each finite element is formulated and solved. The solution for each finite element brought together to attain the global mass and stiffness matrix describing the dynamic response of the whole structure. The displacement associated with the solution explores the motion of the nodes of the finite element mesh. This global mass and stiffness matrix represent the lumped parameter approximation of the structure and can be analyzed to obtain natural frequencies and mode shapes of damaged vibrating structures.

4.2.1 Analysis of damaged beam structures using finite element analysis (FEA)

In the current section, FEA is used for vibration analysis of a cantilever damaged beam (Fig. 4.1). The relationship between the displacement and the forces can be expressed as;

$$\begin{Bmatrix} u_j - u_i \\ \theta_j - \theta_i \end{Bmatrix} = C_{ovl} \begin{Bmatrix} Uj \\ \emptyset j \end{Bmatrix} \tag{4.1}$$

Where overall flexibility matrix C_{ovl} can be expressed as;

$$C_{ovl} = \begin{pmatrix} R_{11} & -R_{12} \\ -R_{21} & R_{22} \end{pmatrix}$$

The displacement vector in equation (4.1) is due to the damage.

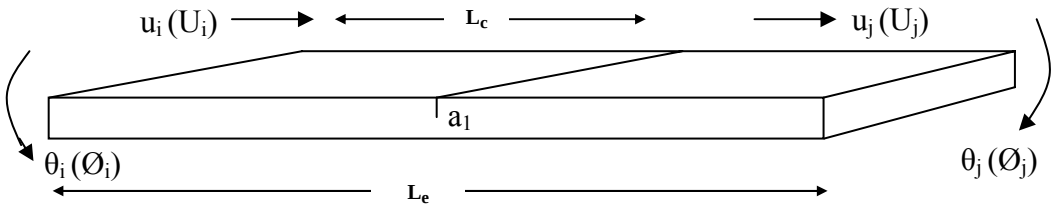

Fig. 4.1 Damaged beam element subjected to axial and bending forces.

The forces acting on the beam element for finite element analysis are shown in Fig. 4.1.

Where,

R_{11}: Deflection in direction 1 due to load in direction 1
$R_{12}= R_{21}$: Deflection in direction 1 due to load in direction 2
R_{22}: Deflection in direction 2 due to load in direction 2.

Under this system, the flexibility matrix C_{intact} of the intact beam element can be expressed as;

$$\begin{Bmatrix} u_j - u_i \\ \theta_j - \theta_i \end{Bmatrix} = C_{intact} \begin{Bmatrix} Uj \\ \emptyset j \end{Bmatrix} \tag{4.2}$$

Where. $C_{intact} = \begin{pmatrix} Le/EA & 0 \\ 0 & Le/EI \end{pmatrix}$

The displacement vector in equation (4.2) is for the intact beam.

The total flexibility matrix C_{tot} of the damaged beam element can now be obtained by

$$C_{tot} = C_{intact} + C_{ovl} = \begin{bmatrix} Le/EA + R_{11} & -R_{12} \\ -R_{21} & Le/EI + R_{22} \end{bmatrix} \quad (4.3)$$

Through the equilibrium conditions, the stiffness matrix K_c of a damaged beam element can be obtained as [30]

$$K_c = DC_{tot}^{-1} D^T \quad (4.4)$$

Where D is the transformation matrix and expressed as;

$$D = \begin{pmatrix} -1 & 0 \\ 0 & -1 \\ 1 & 0 \\ 0 & 1 \end{pmatrix}$$

By solving the stiffness matrix Kc, the natural frequencies and mode shapes of the damaged cantilever beam can be obtained. Similarly, for fixed-fixed beam the stiffness matrix and subsequently the natural frequencies and mode shapes can be obtained. This mathematical approach has been conceived by ANSYS commercial package to estimate the natural frequencies and mode shapes of beam structures. In the current analysis, ANSYS (Version 10) has been used to determine the vibration responses of damaged and undamaged cantilever and fixed-fixed of different materials such as Al, composite and steel. The FEA model of the meshed composite cantilever & fixed-fixed beam and the ANSYS generated beam models of first three modes of vibration are shown in the fig.A.1 to fig.A.12. .The results of the finite element analysis for the first three modes of the damaged beam are compared with that of the numerical analysis and experimental analysis of the damaged beam and are presented in Table 4.1 to Table 4.6.

4.3 Results and discussion of finite element analysis

This section presents an in depth analysis of the results obtained from finite element analysis and briefly discusses the outcome from the proposed methodologies.

It is observed that, the presence of damage in the cantilever beam model have noticeable effect on the vibration characteristics of the beam. A beam element with a crack subjected to axial and bending forces for Finite Element Analysis has been presented in Figure 4.1. The displacement vector and force vector have been applied to calculate the overall matrix. The total flexibility matrix that is produced due to the presence of cracks on the cantilever beam

has been derived, which is subsequently used to formulate the stiffness matrix for the multi cracked beam. Finally, the formulated matrices are used to calculate the first three natural frequencies and first three mode shapes of the cantilever beam structure. These vibration parameters obtained from the finite element analysis have been used to estimate the crack characteristics present on the structural member. The results from the FEA have been validated using the results from experimental and theoretical analysis for multiple crack identification. The results obtained from Finite Element Analysis are presented in fig.A.1 to fig.A.12. Table 4.1 to Table 4.6 presents relative damage positions and relative damage severities of Al, composite and steel cantilever & fixed-fixed beam obtained from FEA, numerical analysis and experimental analysis corresponds to nine set of relative deviation of first three natural frequencies and first three mode shape differences. The results are found to be well in agreement showing the effectiveness of the developed FEA methodology.

Table 4.1 Comparison of modal parameters and damage characteristics of Al cantilever beam obtained from FEA, numerical and experimental analysis

FNF	SNF	TNF	FMD	SMD	TMD	FEA		Numerical		Experimental	
						RDS	RDP	RDS	RDP	RDS	RDP
0.9979	0.9986	0.9992	0.0021	0.0075	0.0037	0.375	0.49	0.373	0.49	0.375	0.50
0.9956	0.9885	0.9986	0.0043	0.0011	0.0036	0.489	0.48	0.487	0.49	0.500	0.50
0.9910	0.9702	0.9983	0.0083	0.0140	0.0097	0.624	0.48	0.628	0.48	0.625	0.50
0.9924	0.9964	0.9944	0.0016	0.0301	0.0161	0.376	0.27	0.376	0.26	0.375	0.25
0.9837	0.9918	0.9880	0.0039	0.0094	0.0373	0.496	0.27	0.494	0.24	0.500	0.25
0.9661	0.9841	0.9752	0.0089	0.0147	0.0293	0.624	0.26	0.623	0.26	0.625	0.25
0.9999	0.9999	0.9908	0.0169	0.0682	0.0435	0.371	0.74	0.369	0.73	0.375	0.75
.9998	0.9996	0.9805	0.0359	0.0429	0.0711	0.497	0.72	0.497	0.73	0.500	0.75
0.9995	0.9931	0.9604	0.0724	0.0465	0.0313	0.622	0.73	0.619	0.74	0.625	0.75

Table 4.2 Comparison of modal parameters and damage characteristics of Al fixed-fixed beam obtained from FEA, numerical and experimental analysis

FNF	SNF	TNF	FMD	SMD	TMD	FEA		Numerical		Experimental	
						RDS	RDP	RDS	RDP	RDS	RDP
0.9939	0.9996	0.9916	0.1484	0.0043	0.0039	0.370	0.49	0.368	0.49	0.375	0.50
0.9868	0.9991	0.9823	0.1727	0.0078	0.0103	0.488	0.51	0.489	0.51	0.500	0.50
0.9745	0.9987	0.9666	0.2679	0.0156	0.0094	0.626	0.49	0.627	0.51	0.625	0.50
0.9999	0.9943	0.9936	0.1388	0.0333	0.0257	0.374	0.26	0.373	0.27	0.375	0.25
0.9998	0.9879	0.9867	0.3955	0.0572	0.0227	0.497	0.27	0.495	0.26	0.500	0.25
0.9994	0.9757	0.9742	0.4135	0.0667	0.0496	0.621	0.24	0.620	0.24	0.625	0.25

Table 4.3 Comparison of modal parameters and damage characteristics of composite cantilever beam obtained from FEA, numerical and experimental analysis

FNF	SNF	TNF	FMD	SMD	TMD	FEA		Numerical		Experimental	
						RDS	RDP	RDS	RDP	RDS	RDP
0.9964	0.9990	0.9999	0.0075	0.0031	0.0015	0.374	0.51	0.373	0.52	0.375	0.50
0.9957	0.9903	0.9998	0.0017	0.0053	0.0063	0.504	0.49	0.508	0.48	0.500	0.50
0.9914	0.9726	0.9998	0.0030	0.0074	0.0057	0.621	0.49	0.619	0.51	0.625	0.50
0.9926	0.9964	0.9946	0.0051	0.0082	0.0137	0.363	0.24	0.362	0.24	0.375	0.25
0.9843	0.9919	0.9885	0.0076	0.0014	0.0125	0.503	0.26	0.507	0.25	0.500	0.25
0.9671	0.9841	0.9761	0.0087	0.0024	0.0491	0.623	0.26	0.621	0.27	0.625	0.25
0.9999	0.9999	0.9911	0.0165	0.0110	0.0312	0.379	0.74	0.381	0.73	0.375	0.75
0.9997	0.9997	0.9811	0.0350	0.0233	0.0264	0.509	0.73	0.511	0.73	0.500	0.75
0.9995	0.9947	0.9616	0.0704	0.0561	0.0533	0620	0.73	0.617	0.74	0.625	0.75

Table 4.4 Comparison of modal parameters and damage characteristics of composite fixed-fixed beam obtained from FEA, numerical and experimental analysis

FNF	SNF	TNF	FMD	SMD	TMD	FEA		Numerical		Experimental	
						RDS	RDP	RDS	RDP	RDS	RDP
0.9940	0.9999	0.9918	0.0043	0.0091	0.0066	0.368	0.49	0.361	0.49	0.375	0.50
0.9872	0.9998	0.9828	0.0080	0.0123	0.0237	0.503	0.51	0.509	0.52	0.500	0.50
0.9753	0.9997	0.9676	0.0119	0.0087	0.0411	0.628	0.51	0.631	0.52	0.625	0.50
0.9998	0.9944	0.9937	0.1237	0.0265	0.0761	0.374	0.24	0.372	0.23	0.375	0.25
0.9997	0.9883	0.9869	0.3741	0.0465	0.0379	0.502	0.23	0.502	0.21	0.500	0.25
0.9994	0.9768	0.9751	0.3699	0.0823	0.0531	0.630	0.26	0.634	0.27	0.625	0.25

Table 4.5 Comparison of modal parameters and damage characteristics of steel cantilever beam obtained from FEA, numerical and experimental analysis

FNF	SNF	TNF	FMD	SMD	TMD	FEA		Numerical		Experimental	
						RDS	RDP	RDS	RDP	RDS	RDP
0.9979	0.9969	0.9996	0.0021	0.0069	0.0044	0.374	0.49	0.374	0.50	0.375	0.50
0.9955	0.9866	0.9992	0.0043	0.0019	0.0045	0.499	0.49	0.498	0.49	0.500	0.50
0.9908	0.9676	0.9988	0.0081	0.0138	0.0105	0.624	0.48	0.623	0.49	0.625	0.50
0.9921	0.9963	0.9941	0.0018	0.0288	0.0179	0.373	0.27	0.374	0.26	0.375	0.25
0.9833	0.9918	0.9875	0.0041	0.0129	0.0341	0.498	0.24	0.499	0.26	0.500	0.25
0.9653	0.9842	0.9744	0.0094	0.0122	0.0274	0.623	0.26	0.622	0.24	0.625	0.25
0.9999	0.9999	0.9905	0.0174	0.0607	0.0461	0.377	0.76	0.376	0.76	0.375	0.75
0.9998	0.9989	0.9798	0.0099	0.0477	0.0693	0.501	0.73	0.502	0.74	0.500	0.75
0.9994	0.9913	0.9593	0.0743	0.0419	0.0375	0.623	0.74	0.622	0.74	0.625	0.75

Table 4.6 Comparison of modal parameters and damage characteristics of steel fixed-fixed beam obtained from FEA, numerical and experimental analysis

FNF	SNF	TNF	FMD	SMD	TMD	FEA		Numerical		Experimental	
						RDS	RDP	RDS	RDP	RDS	RDP
0.9936	0.9997	0.9913	0.1444	0.0137	0.0153	0.376	0.49	0.377	0.49	0.375	0.50
0.9864	0.9992	0.9817	0.1713	0.1265	0.1117	0.498	0.49	0.499	0.48	0.500	0.50
0.9736	0.9989	0.9656	0.2627	0.2137	0.2106	0.627	0.48	0.628	0.49	0.625	0.50
0.9999	0.9941	0.9933	0.1354	0.1366	0.1291	0.377	0.27	0.376	0.26	0.375	0.25
0.9997	0.9875	0.9863	0.3899	0.3528	0.2205	0.503	0.26	0.502	0.27	0.500	0.25
0.9994	0.9751	0.9736	0.4082	0.3167	0.2496	0.623	0.26	0.623	0.24	0.625	0.25

4.4 Summary

In the present study, an effective and compatible method for damage detection for structural beam members has been presented. From the diagnosis of the vibration responses, it is observed that there is deviation of mode shapes and natural frequencies for the damaged beam in contrast to the undamaged beam. The vibration responses i.e. the natural frequencies and mode shapes obtained from the FE analysis are found to be in good agreement with theoretical and experimental analysis. The proposed method can be utilized to model any practical engineering structure and on-line condition monitoring of damaged structures.

Chapter 5

ANALYSIS OF FUZZY INFERENCE SYSTEM FOR DAMAGE DIAGNOSIS

Most of the structural failures encountered are caused by material fatigue and presence of damages in structures. Therefore, damages of any form are to be diagnosed as earliest as possible to maintain the integrity of the structures. In spite of the existence so many traditional methods, but presence of any damage can't be ensured without diagnosing the entire structure. In the current section, a fuzzy logic based technique has been proposed for structural damage identification. The proposed methodology utilizes the modal characteristics of the beam structure using reverse engineering techniques and anticipates the position and severities of the damage present in the system.

5.1 Introduction

By definition, fuzzy logic (FL) is a multi valued logic, which allows intermediate values to be defined between linguistic expressions like yes/no, high/low, true/false. In the last few decades, researchers have used the FL methodology for applications such as feature extraction, classification and detection of geometrical features in objects etc. Fuzzy system has the capability to imitate the human behavior by following the different reasoning phases in order to make the computer program behave like humans. In traditional computing, actions are taken based on data with precision and certainty. In soft computing, erroneous data are employed for decision making. The exploration of the erroneous and uncertainty influences the remarkable human ability to understand various engineering applications. FL can specify mapping rules in terms of words rather than numbers. Another basic concept in FL is the fuzzy if–then rule which is mostly used in development of fuzzy rule based systems. FL can model nonlinear functions of arbitrary complexity to a desired degree of accuracy. FL is a convenient way to map an input space to an output space and is one of the tools used to model a multi-input, multi-output system. Hence the fuzzy approach can be effectively employed to develop a damage diagnostic tool using the vibration responses of structures.

In the present chapter, a damage diagnosis algorithm using fuzzy inference system has been formulated and the performance has been evaluated. The fuzzy system for damage diagnosis has been designed with six inputs (first three relative natural frequencies and first three relative mode shape differences) and two outputs (relative damage position, relative damage severity). A number of fuzzy linguistic terms and fuzzy membership functions (triangular, trapezoidal and Gaussian) have been used to develop the proposed damage identification technique. The modal parameters obtained from the numerical, finite element and experimental analyses have been used to establish the rule base for designing of the fuzzy system. The performance of the proposed fuzzy based system for damage diagnosis have been compared with the results obtained from FEA, numerical and experimental analysis and it is observed that, the proposed fuzzy model can be effectively exploited for structural health monitoring.

5.2 Fuzzy inference system

A fuzzy logic system (FLS) essentially takes a decision by nonlinear mapping of the input data into a scalar output, using fuzzy rules. The mapping can be done through input/output membership functions, fuzzy if–then rules, aggregation of output sets, and defuzzification. An FLS can be considered as a collection of independent multi-input, single-output systems. The FLS maps crisp inputs into crisp outputs. It can be seen from the figure that the FIS contains four components: the fuzzifier, inference engine, rule base, and defuzzifier. The rule base of the FLS system can be developed using the numeric data. Once the rules have been established, the FLS can be viewed as a system that utilizes inputs and process them using the fuzzy rule database and fuzzy linguistic terms to get output vector. The fuzzifier takes input values and verifies the degree of association to each of the fuzzy sets through membership functions.

The fuzzy system generally consists of five steps. They are as follows,

Step 1

Inputs to fuzzy system: The fuzzy system at first is fed with the input parameters and then the system recognizes the degree of association of the data with the corresponding fuzzy set through the membership functions.

Step 2

Application of fuzzy operator: After the fuzzification of the inputs, the fuzzy model measures the degree to which each of the antecedents satisfies for each rule of the fuzzy rule data base. If the rule has a more than one part, the fuzzy operator is employed to obtain a single value for the given rule.

Step 3

Application of method for fulfillment of rules: Method is applied to reshape the output of the membership functions, which is represented by a fuzzy set. The reshaping of the output is done by a function related to the antecedent.

Step 4

Aggregation of results: The results obtained from each rule are unified to get a decision from the system. Aggregation process leads to a combined fuzzy set as output.

Step 5

Defuzzification: In this process the defuzzification layer of the fuzzy system incorporate method like centroid, maxima etc in order to convert the fuzzy set into crisp value, which will be easier to analyze.

5.2.1 Modeling of fuzzy membership functions

One of the most important features in designing a fuzzy inference system is to determine the fuzzy membership functions. The membership function defines the fuzzy set and also provides a measure of degree of imprecise dependencies or analogy of an element to a fuzzy set. The membership function can take any shape, but some commonly used examples for real applications are Gaussian, triangular, trapezoidal, bell shape etc. In a fuzzy set, elements with non zero degree membership are known as support and elements with degree of one are known as core of the fuzzy set. The membership functions are generally represented as $\mu_F(x)$. Where, μ is the degree of weight of the element x to the fuzzy set F. The height or magnitude of the membership function is usually referred to zero to one. Hence, any element from the fuzzy set belongs to the set with a degree ranging from [0, 1].

From the Fig. 5.1(a) (triangular membership function) the point ‘c’, ‘d’, ‘e’ represents the three vertices of the triangular membership function $\mu_F(x)$ of the fuzzy set ‘F’. It is observed

that the element at ‘c’ and ‘e’ is having membership degree equivalent to zero and the element at ‘d’ is having membership degree equivalent to one. The mathematical representation of the fuzzy triangular membership function of $\mu_F(x)$ can be explained as follows.

$$\mu_F(x) = \begin{cases} 0 \text{ if } x \le c \\ (x- c) / (d- c) \text{ if } c \le x \le d \\ (e- x) / (e- d) \text{ if } d \le x \le e \\ 0 \text{ if } x \ge e \end{cases}$$

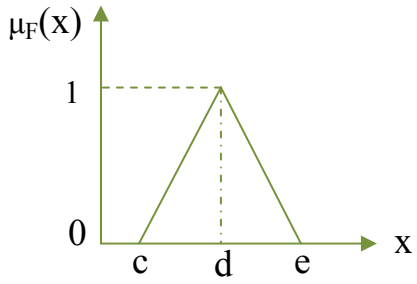

Fig. 5.1(a) Triangular membership function

Where c, w, n are the center, width and fuzzification factor respectively. The graphical presentation of the fuzzy Gaussian membership function can be seen in Fig. 5.1(b).

$$\mu_F(x, c, w, n) = \text{Exp}\left[-0.5\{(x - c) / w\}^n\right]$$

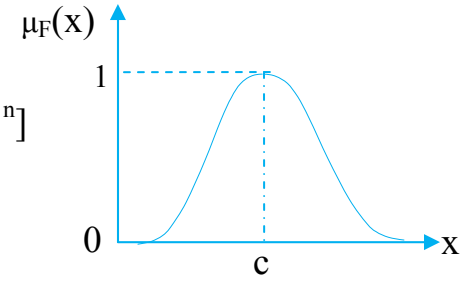

Fig. 5.1(b) Gaussian membership function

The trapezoidal membership function (Fig. 5.1 (c)) has two base points (0.2, 0.5) and two shoulder points (0.3, 0.4). A mathematical expression for the trapezoidal membership function is presented below. A graphical representation of the trapezoidal membership function has been shown in Fig. 5.1 (c).

$$\mu_F(x, 0.2, 0.3, 0.4, 0.5) = \begin{cases} 0 \text{ when } x \le 0.2 \\ (x - 0.2) / (0.3 - 0.2) \text{ when } 0.2 \le x \le 0.3 \\ 1 \text{ when } 0.3 \le x \le 0.0.4 \\ (0.5 - x) / (0.5 - 0.4) \text{ when } 0.4 \le x \le 0.5 \end{cases}$$

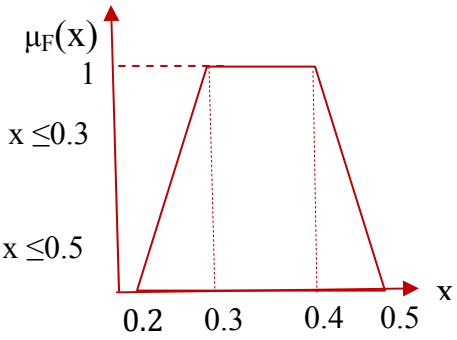

Fig.5.1(c) Trapezoidal membership function

5.2.2 Modeling of fuzzy controller using fuzzy rules

The understanding of the input data and the output data for a real application is often vague due to the intricate dependencies of the input and output variables of the working domain. Fuzzy inference system posses the approximation features by the help of fuzzy membership functions and fuzzy IF-THEN rules. In the process of development of a fuzzy model, the domain knowledge helps in selecting the appropriate membership functions and development of fuzzy rules. This membership functions are designed by using the suitable fuzzy linguistic terms and fuzzy rule base. The fuzzy rule base or the conditional statements are used for fuzzification of the input parameters and defuzzification of the output parameters. The fuzzy model can be designed with single input and multi output (SIMO), multi input and single output (MISO), multi input and multi output (MIMO). During the design of the fuzzy model, the fuzzy operations like fuzzy intersection, union and complement are used to develop the membership functions. Hence, the fuzzy model takes the input parameters from the application at a certain state of condition and using the rules it will provide a controlled action as desired by the system. A general model of a fuzzy inference system (FIS) is shown in Fig. 5.2.

The inputs to the fuzzy model for damage identification in the current analysis comprises
Relative first natural frequency = “FNF”; Relative second natural frequency = “SNF”;
Relative third natural frequency = “TNF”; Relative first mode shape difference = “FMD”;
Relative second mode shape difference = “SMD”; Relative third mode shape difference = “TMD”

The linguistic term used for the outputs are as follows;
Relative damage position = “RDP”
Relative damage severity = “RDS”

5.2.3 Modelling of defuzzifier

The final step in building of a fuzzy system is to convert the fuzzy output set into a crisp output. So, the input to the defuzzifier is the aggregate output fuzzy set and output is a single number. The crisp output represents the possible distribution of the inferred fuzzy control action. Selection of the defuzzification strategy depends on the features of the application.

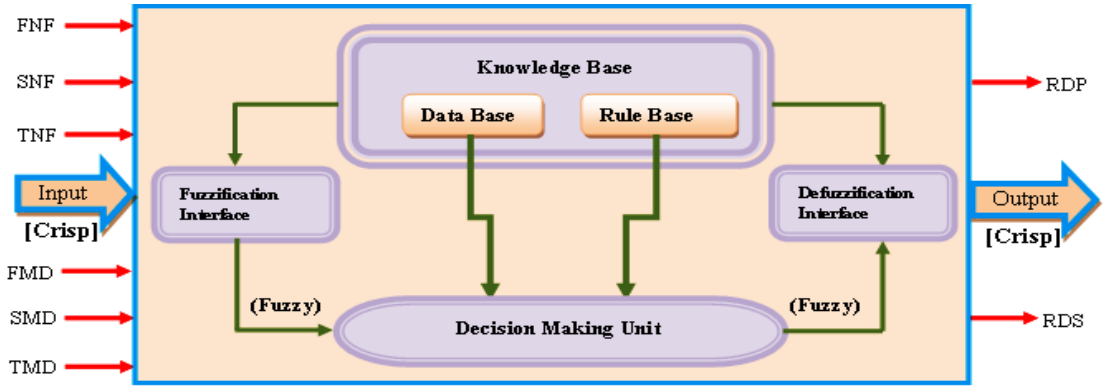

Fig.5.2 Fuzzy controller for current analysis

The relationship between the fuzzy output set (F), defuzzifier and crisp output (K_0) can be established in the following equation;

K_0 = defuzzifier (F);

There are several defuzzification methods used for development of fuzzy system. Some of them are listed below;

- Centroid of the area,
- Mean of maximum
- Weighted average method
- Height method

5.3 Analysis of the fuzzy controller used for damage identification

The fuzzy models developed in the current analysis, based on triangular, Gaussian and trapezoidal membership functions have got six input parameters and four output parameters. The linguistic term used for the inputs are as follows;

- Relative first natural frequency = "FNF";
- Relative second natural frequency = "SNF";
- Relative third natural frequency = "TNF";
- Average relative first mode shape difference = "FMD";
- Average relative second mode shape difference = "SMD";
- Average relative third mode shape difference = "TMD".

The linguistic term used for the outputs are as follows;

- Relative damage position = "RDP"

- Relative damage severity = “RDS”

The pictorial view of the triangular membership, Gaussian membership, trapezoidal membership fuzzy models are shown in Fig. Fig. 5.3 (a), Fig. 5.3 (b) and Fig. 5.3 (c) respectively. Some of the fuzzy linguistic terms and fuzzy rules (Twenty numbers) used to design and train the knowledge based fuzzy logic systems are represented in Table 5.1 and Table 5.2 respectively. The membership functions used in developing the fuzzy inference system for damage diagnosis are shown in Fig.5.4 to Fig.5.6. Nine membership functions have been used for each input parameters to the fuzzy model. In designing the output membership functions for the output parameters such as relative damage position (RDP) and relative damage severity (RDS), twelve membership functions are considered. The defuzzification process of the triangular, Gaussian, trapezoidal membership functions are presented in Fig 5.7, Fig. 5.8 and Fig. 5.9 respectively by activating the rule no 5 and rule no 15 from Table 5.2.

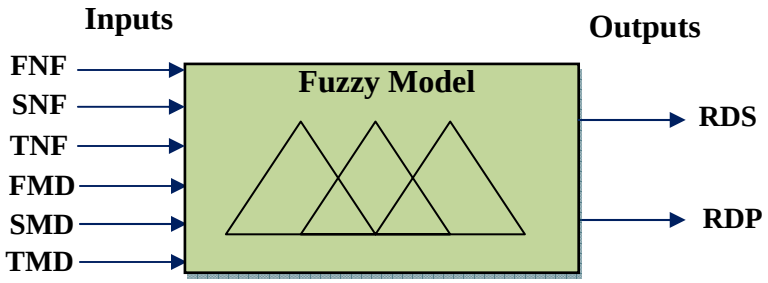

Fig. 5.3(a) Triangular fuzzy model

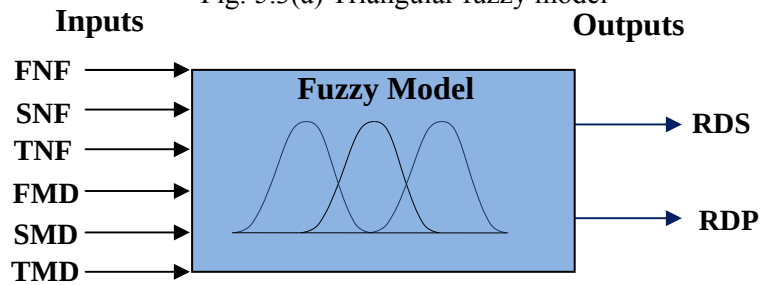

Fig. 5.3(b) Gaussian fuzzy model

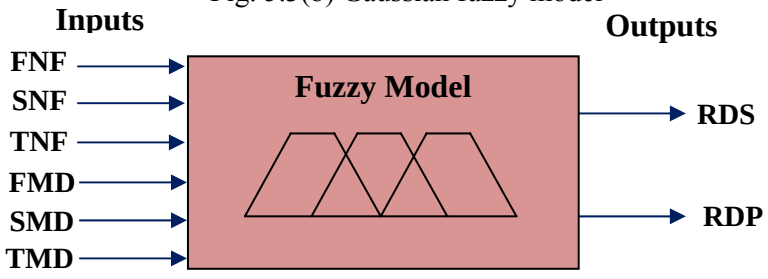

Fig. 5.3(c) Trapezoidal fuzzy model

5.3.1 Fuzzy mechanism for damage identification

Based on the above fuzzy subsets, the fuzzy control rules are defined in a general form as follows:

$$\text{If (FNF is } FNF_i \text{ and SNF is } SNF_j \text{ and TNF is } TNF_k \text{ and FMD is } FMD_l \text{ and SMD is } SMD_m \text{ and TMD is } TMD_n) \text{ then RDP is } RDP_{ijklmn} \text{ and RDS is } RDS_{ijklmn} \quad (4.1)$$

where i=1 to 9, j=1 to 9, k = 1 to 9, l= 1 to 9, m= 1 to 9, n= 1 to 9

As "FNF", "SNF", "TNF", "FMD", "SMD", "TMD" have ten membership functions each. From equation (4.1), two set of rules can be written

$$\left.\begin{array}{l}\text{If (FNF is } FNF_i \text{ and SNF is } SNF_j \text{ and TNF is } TNF_k \text{ and FMD is } FMD_l \text{ and SMD is } SMD_m \text{ and TMD is } TMD_n) \text{ then RDS is } RDS_{ijklmn} \\ \text{If (FNF is } FNF_i \text{ and SNF is } SNF_j \text{ and TNF is } TNF_k \text{ and FMD is } FMD_l \text{ and SMD is } SMD_m \text{ and TMD is } TMD_n) \text{ then RDP is } RDP_{ijklmn}\end{array}\right\} \quad (4.2)$$

According to the usual fuzzy logic control method [91,205], a factor W_{ijklmn} is defined for the rules as follows:

$$W_{ijklmn} = \mu_{fnf_i}(freq_i) \wedge \mu_{snf_j}(freq_j) \wedge \mu_{tnf_k}(freq_k) \wedge \mu_{fmd_l}(moddif_l) \wedge \mu_{smd_m}(moddif_m) \wedge \mu_{tmd_n}(moddif_n)$$

Where $freq_i$, $freq_j$ and $freq_k$ are the first, second and third relative natural frequencies of the cantilever beam with damage respectively ; $moddif_l$, $moddif_m$ and $moddif_n$ are the average first, second and third relative mode shape differences of the cantilever beam with damage respectively. By applying the composition rule of inference [36, 42], the membership values of the relative damage position and relative damage severity, $(position)_{RDP}$ and $(severity)_{RDS}$ can be computed as;

$$\left.\begin{array}{l}\mu_{RDP_{ijklmn}}(\text{position}) = W_{ijklmn} \wedge \mu_{RDP_{ijklmn}}(\text{position}) \\ \mu_{RDS_{ijklmn}}(severity) = W_{ijklmn} \wedge \mu_{RDS_{ijklmn}}(severity)\end{array}\right\} \quad (4.3)$$

The overall conclusion by combining the outputs of all the fuzzy rules can be written as follows:

$$\left.\begin{array}{l}\mu_{RDP}(\text{position}) = \mu_{RDP_{111111}}(\text{position}) \vee \ldots \vee \mu_{RDP_{ijklmn}}(\text{position}) \vee \ldots \vee \mu_{RDP_{10\ 10\ 10\ 10\ 10\ 10}}(\text{position}) \\ \mu_{RDS}(severity) = \mu_{RDS_{111111}}(severity) \vee \ldots \vee \mu_{RDS_{ijklmn}}(severity) \vee \ldots \vee \mu_{RDS_{10\ 10\ 10\ 10\ 10\ 10}}(severity)\end{array}\right\} \quad (4.4)$$

The crisp values of relative damage position and relative damage severity are evaluated using the centre of gravity method [42] as:

$$\left.\begin{aligned} \text{Relative damage position} = RDP = \frac{\int (position \cdot \mu_{RDP}(position) \cdot d(position)}{\int \mu_{RDP}(position) \cdot d(position)} \\ \text{Relative damage severity} = RDS = \frac{\int (severity) \cdot \mu_{RDS}(severity) \cdot d(severity)}{\int \mu_{RDS}(severity) \cdot d(severity)} \end{aligned}\right\} \quad (4.5)$$

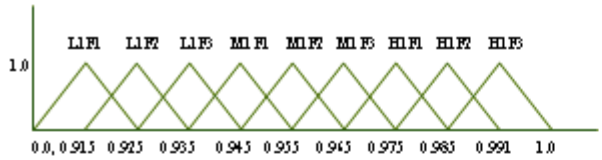

Fig. 5.4(a) Membership functions for relative natural frequency for first mode of vibration.

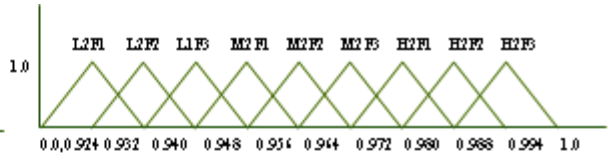

Fig. 5.4(b) Membership functions for relative natural frequency for second mode of vibration.

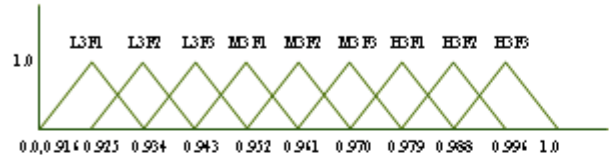

Fig. 5.4(c) Membership functions for relative natural frequency for third mode of vibration.

Fig. 5.4(d) Membership functions for relative mode shape difference for first mode of vibration.

Fig. 5.4(e) Membership functions for relative mode shape difference for second mode of vibration.

Fig. 5.4(f) Membership functions for relative mode shape difference for first mode of vibration.

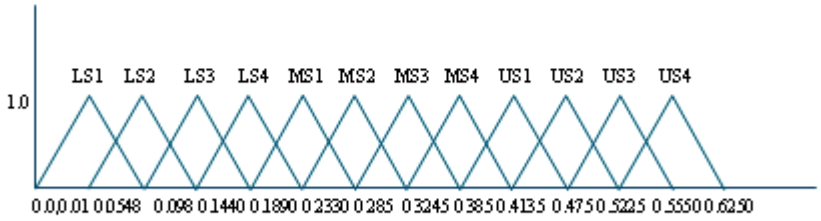

Fig. 5.4 (g) Membership functions for relative damage severity.

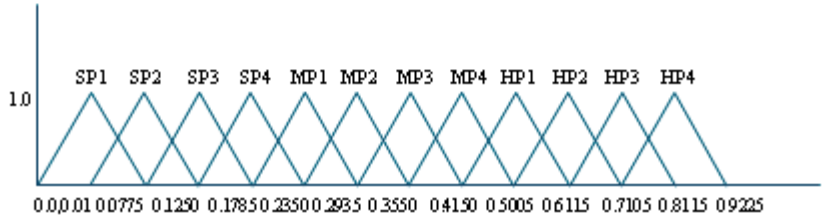

Fig. 5.4 (h) Membership functions for relative damage position.

Fig. 5.4 (a) - (h) Membership functions for triangular fuzzy model.

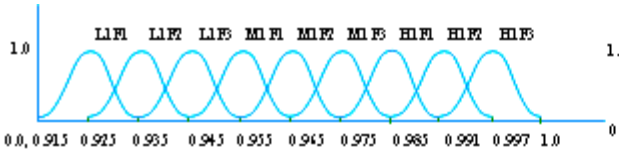

Fig. 5.5(a) Membership functions for relative natural frequency for first mode of vibration.

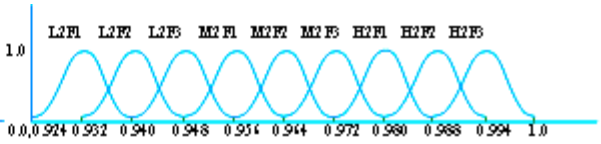

Fig. 5.5(b) Membership functions for relative natural frequency for second mode of vibration.

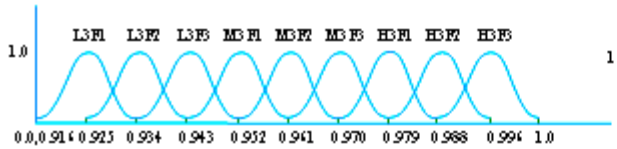

Fig. 5.5(c) Membership functions for relative natural frequency for third mode of vibration.

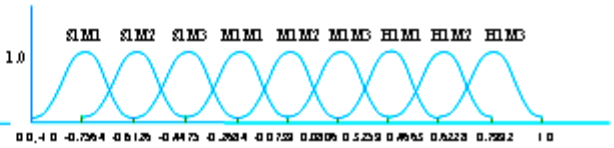

Fig. 5.5(d) Membership functions for relative mode shape difference for first mode of vibration.

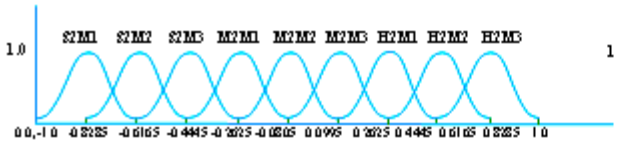

Fig. 5.5(e) Membership functions for relative mode shape difference for second mode of vibration.

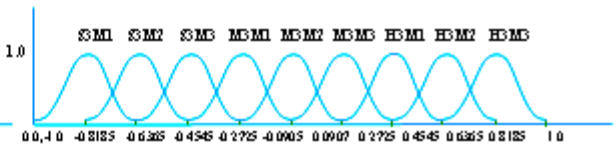

Fig. 5.5(f) Membership functions for relative mode shape difference for first mode of vibration.

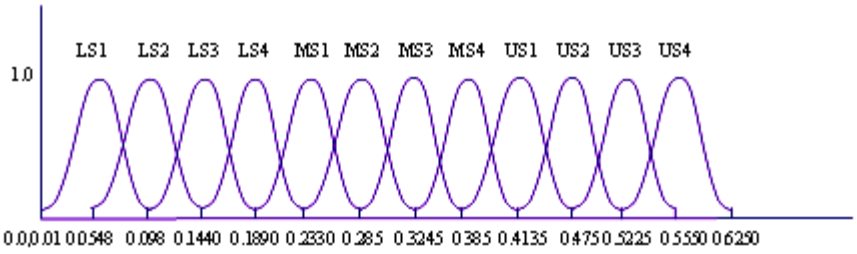

Fig. 5.5 (g) Membership functions for relative damage severity.

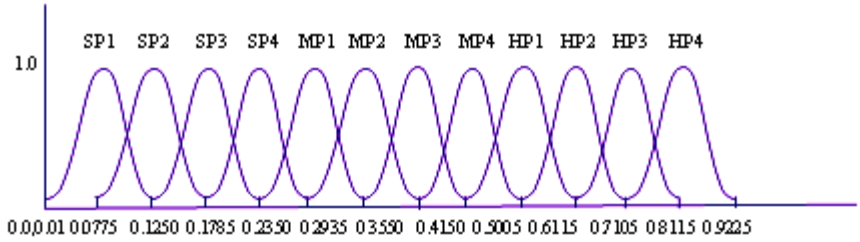

Fig. 5.5 (h) Membership functions for relative damage position.

Fig. 5.5 (a) - (h) Membership functions for triangular fuzzy model.

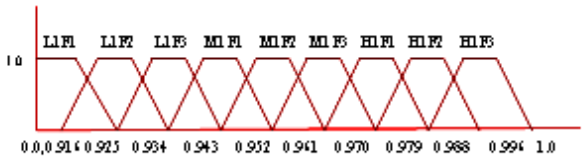

Fig. 5.6(a) Membership functions for relative natural frequency for first mode of vibration.

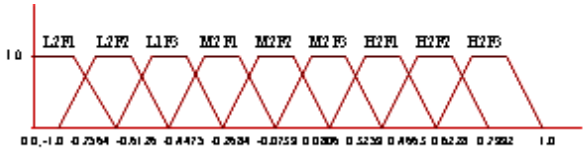

Fig. 5.6(b) Membership functions for relative natural frequency for second mode of vibration.

Fig. 5.6(c) Membership functions for relative natural frequency for third mode of vibration.

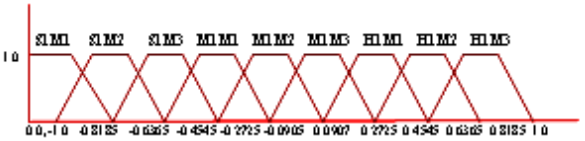

Fig. 5.6(d) Membership functions for relative mode shape difference for first mode of vibration.

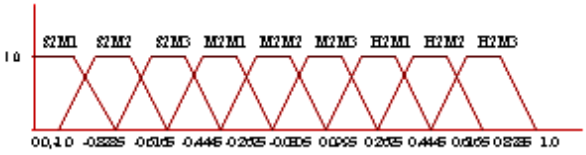

Fig. 5.6(e) Membership functions for relative mode shape difference for second mode of vibration.

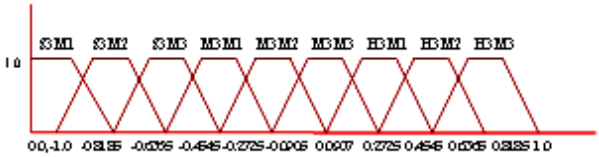

Fig. 5.6(f) Membership functions for relative mode shape difference for first mode of vibration.

Fig. 5.6 (g) Membership functions for relative damage severity.

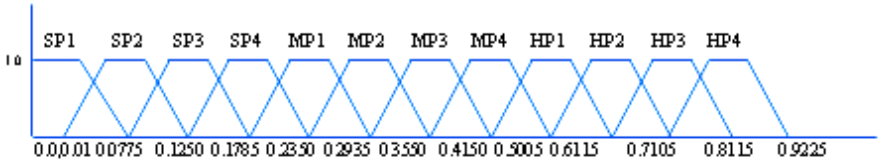

Fig. 5.6 (h) Membership functions for relative damage position.

Fig. 5.6 (a) - (h) Membership functions for trapezoidal fuzzy model.

Table 5.1 Description of fuzzy linguistic terms.

Membership Functions Name	Linguistic Terms	Definition of the Linguistic terms
L1F1,L1F2,L1F3	FNF $_{1 \text{ to } 3}$	Low ranges of relative natural frequency for first mode of vibration
M1F1,M1F2, M1F3	FNF $_{4 \text{ to } 6}$	Medium ranges of relative natural frequency for first mode of vibration
H1F1,H1F2,H1F3	FNF $_{7 \text{ to } 9}$	Higher ranges of relative natural frequency for first mode of vibration
L2F1,L2F2,L2F3	SNF $_{1 \text{ to } 3}$	Low ranges of relative natural frequency for second mode of vibration
M2F1,M2F2,M2F3	SNF $_{4 \text{ to } 6}$	Medium ranges of relative natural frequency for second mode of vibration
H2F1,H2F2,H2F3	SNF $_{7 \text{ to } 9}$	Higher ranges of relative natural frequencies for second mode of vibration
L3F1,L3F2,L3F3	TNF $_{1 \text{ to } 3}$	Low ranges of relative natural frequencies for third mode of vibration
M3F1,M3F2,M3F3	TNF $_{4 \text{ to } 6}$	Medium ranges of relative natural frequencies for third mode of vibration
H3F1,H3F2,H3F3	TNF $_{7 \text{ to } 9}$	Higher ranges of relative natural frequencies for third mode of vibration
S1M1,S1M2,S1M3	FMD $_{1 \text{ to } 3}$	Small ranges of first relative mode shape difference
M1M1,M1M2,M1M3	FMD $_{4 \text{ to } 6}$	medium ranges of first relative mode shape difference
H1M1,H1M2,H1M3	FMD $_{7 \text{ to } 10}$	Higher ranges of first relative mode shape difference
S2M1,S2M2,S2M3	SMD $_{1 \text{ to } 3}$	Small ranges of second relative mode shape difference
M2M1,M2M2,M2M3	SMD $_{4 \text{ to } 6}$	medium ranges of second relative mode shape difference
H2M1,H2M2,H2M3	SMD $_{7 \text{ to} 10}$	Higher ranges of second relative mode shape difference
S3M1,S3M2,S3M3	TMD $_{1 \text{ to } 3}$	Small ranges of third relative mode shape difference
M3M1,M3M2,M3M3	TMD $_{4 \text{ to } 6}$	medium ranges of third relative mode shape difference
H3M1,H3M2,H3M3	TMD $_{7 \text{ to } 10}$	Higher ranges of third relative mode shape difference
SP1,SP2,SP3,SP4	RDP $_{1 \text{ to } 4}$	Small ranges of relative damage position
MP1,MP2,MP3,MP4	RDP $_{5 \text{ to } 8}$	Medium ranges of relative damage position
HP1,HP2, HP3,HP4	RDP $_{9 \text{ to } 12}$	Higher ranges of relative damage position
LS1,LS2,LS3,LS4	RDS $_{1 \text{ to } 4}$	Lower ranges of relative damage severity
MS1,MS2,MS3,MS4	RDS$_{5 \text{ to } 8}$	Medium ranges of relative damage severity
US1,US2,US3,US4	RDS $_{9 \text{ to } 12}$	Upper ranges of relative damage severity

Table 5.2 Examples of twenty fuzzy rules to be implemented in fuzzy model.

Sl. No.	Examples of some rules used in the fuzzy model
1	If FNF is H1F1, SNF is M2F2, TNF is M3F1, FMD is H1M2, SMD is H2M4, TMD is H3M3, then RDS is LS4 and RDP is SP3.
2	If FNF is L1F4, SNF is L2F4, TNF is L3F4, FMD is H1M1, SMD is H2M1, TMD is H3M2, then RDS is LS2 and RDP is SP4.
3	If FNF is L1F3, SNF is L2F4, TNF is L3F4, FMD is M1M2, SMD is H2M2, TMD is H3M3, then RDS is LS3 and RDP is SP2.
4	If FNF is H1F2, SNF is H2F1, TNF is H3F1, FMD is H1M3, SMD is H2M4, TMD is H3M4, then RDS is MS2 and RDP is SP3.
5	If FNF is M1F1, SNF is L2F2, TNF is L3F3, FMD is H1M1, SMD is H2M1, TMD is H3M2, then RDS is MS1 and RDP is SP2.
6	If FNF is L1F1, SNF is L2F2, TNF is L3F3, FMD is H1M3, SMD is M2M1, TMD is H3M4, then RDS is MS2 and RDP is MP1.
7	If FNF is L1F4, SNF is L2F4, TNF is L3F4, FMD is M1M2, SMD is H2M1, TMD is H3M1, then RDS is MS1 and RDP is SP1.
8	If FNF is H1F1, SNF is M2F2, TNF is M3F1, FMD is H1M2, SMD is H2M2, TMD is H3M2, then RDS is MS2 and RDP is SP2.
9	If FNF is L1F1, SNF is L2F4, TNF is L3F4, FMD is M1M1, SMD is M2M1, TMD is M3M2, then RDS is LS1 and RDP is MP2.
10	If FNF is M1F1, SNF is L2F2, TNF is L3F1, FMD is M1M2, SMD is M2M2, TMD is H3M1, then RDS is LS1 and RDP is SP2.
11	If FNF is M1F1, SNF is M2F1, TNF is M3F1, FMD is H1M3, SMD is H2M3, TMD is H3M4, then RDS is MS1 and RDP is SP4.
12	If FNF is M1F1, SNF is L2F1, TNF is L3F1, FMD is H1M3, SMD is H2M2, TMD is H3M3, then RDS is LS2 and RDP is MP1.
13	If FNF is M1F2, SNF is M2F1, TNF is M3F1, FMD is M1M1, SMD is H2M1, TMD is H3M2, then RDS is MS2 and RDP is MP2.
14	If FNF is H1F2, SNF is H2F1, TNF is H3F1, FMD is H1M4, SMD is H2M1, TMD is H3M1, then RDS is MS1 and RDP is SP4.
15	If FNF is M1F1, SNF is L2F1, TNF is L3F2, FMD is S1M1, SMD is S2M2, TMD is H3M1, then RDS is LS2 and RDP is MP1.
16	If FNF is L1F4, SNF is L2F4, TNF is L3F4, FMD is H1M2, SMD is S2M1, TMD is H3M2, then RDS is LS1 and RDP is MP3.
17	If FNF is M1F1, SNF is L2F3, TNF is L3F1, FMD is S1M2, SMD is M2M1, TMD is S3M1, then RDS is LS2 and RDP is MP3.
18	If FNF is L1F1, SNF is L2F1, TNF is L3F1, FMD is H1M2, SMD is H2M2, TMD is H3M2, then RDS is LS3 and RDP is MP2.
19	If FNF is H1F2, SNF is H2F1, TNF is H3F1, FMD is S1M2, SMD is H2M3, TMD is H3M1, then RDS is LS4 and RDP is MP1.
20	If FNF is L1F3, SNF is L2F4, TNF is L3F4, FMD is S1M3, SMD is S2M2, TMD is S3M3, then RDS is LS3 and RDP is SP3.

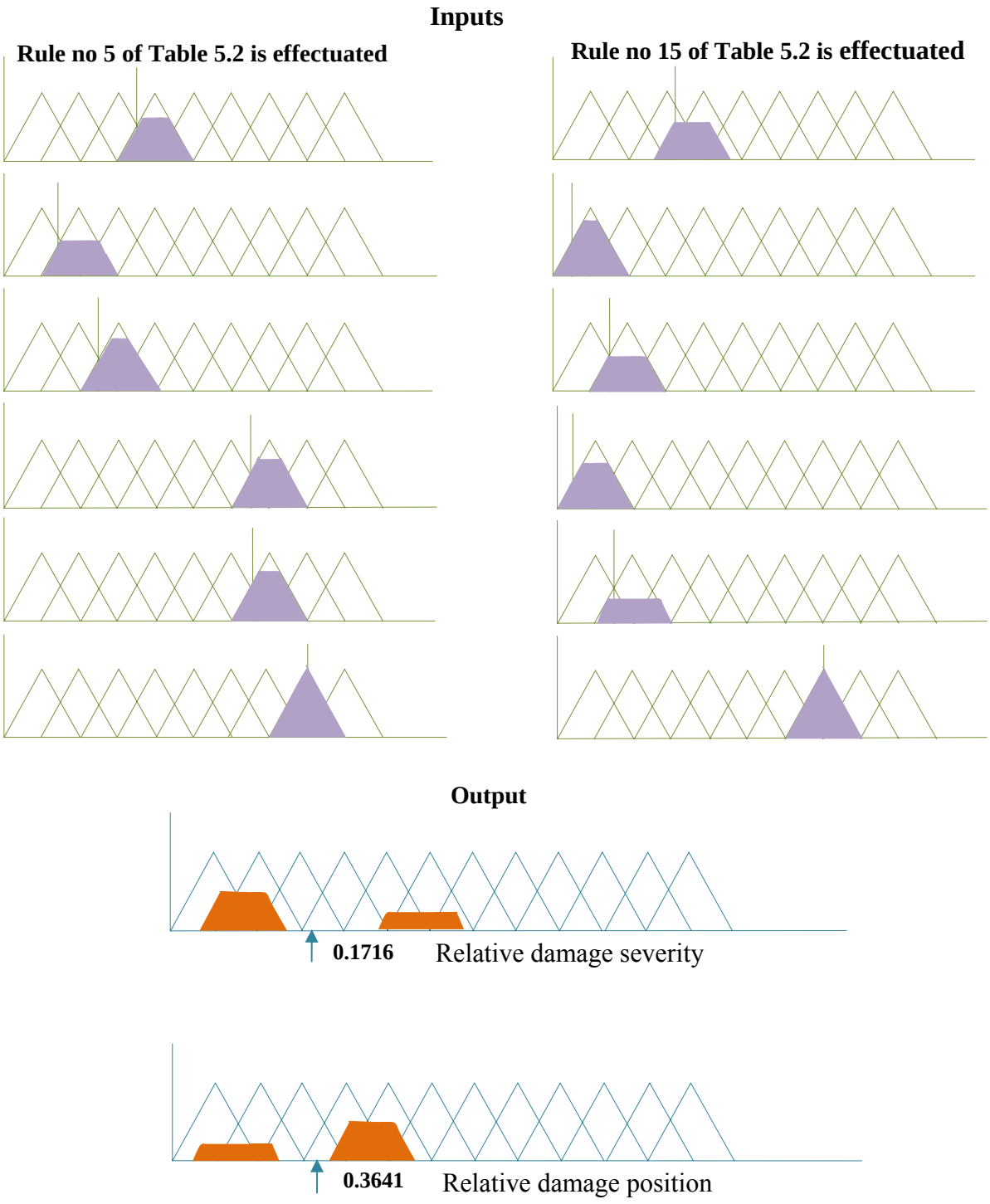

Fig. 5.7 Resultant values of relative damage severity and relative damage position from triangular fuzzy model when Rules 5 and 15 of Table 5.2 are effectuated.

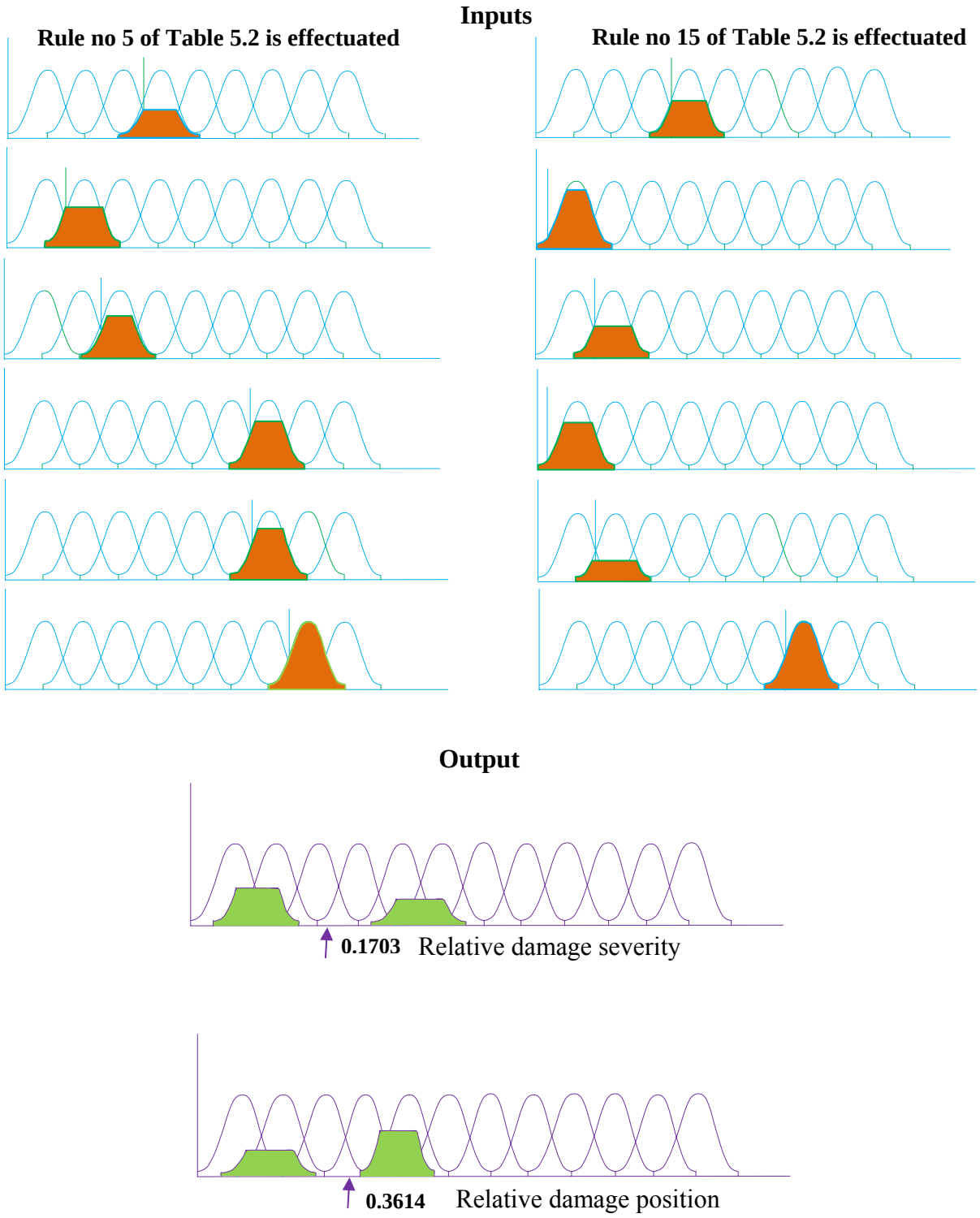

Fig.5.8 Resultant values of relative damage severity and relative damage position from Guassian fuzzy model when Rules 5 and 15 of Table 5.2 are effectuated.

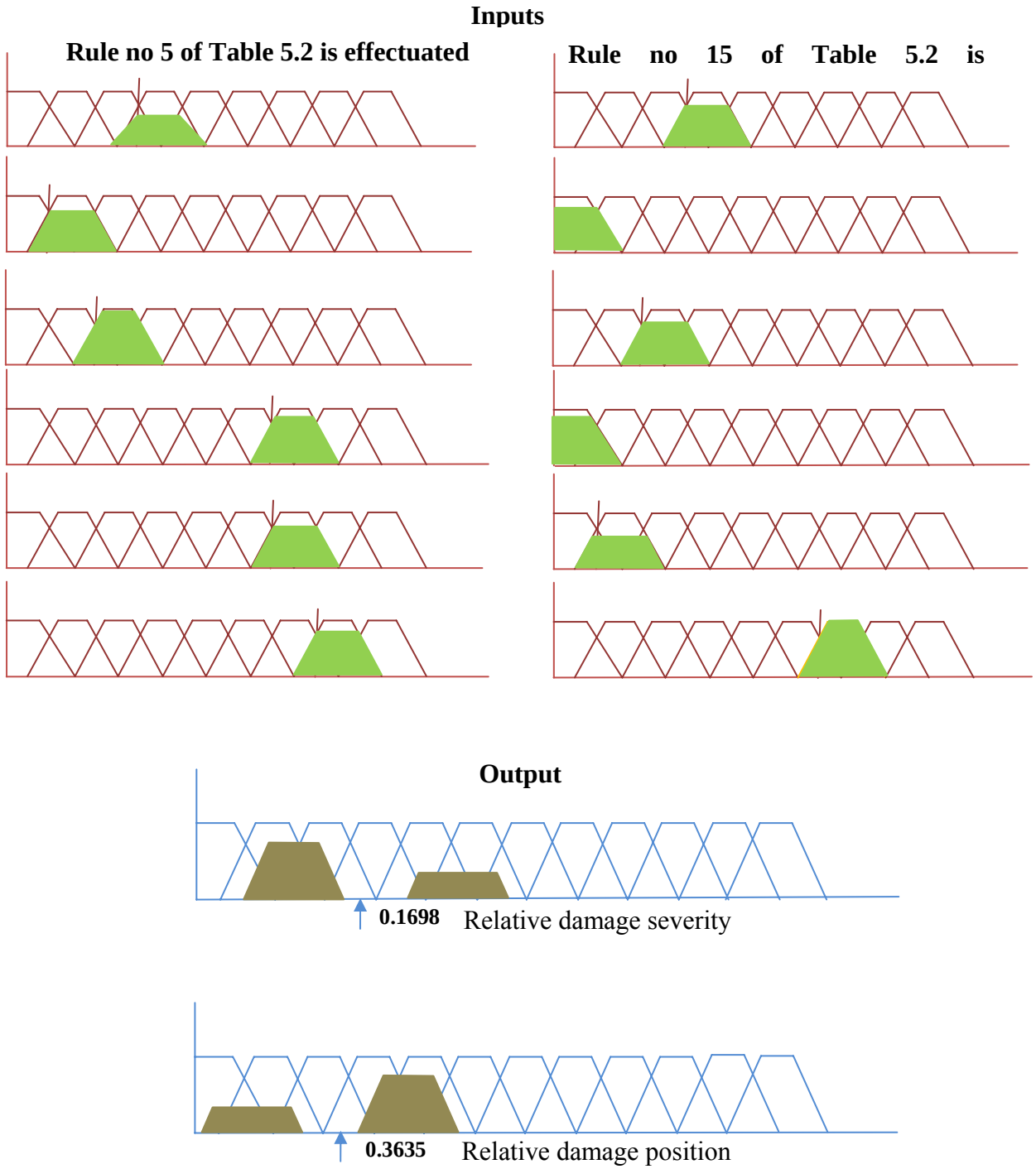

Fig. 5.9 Resultant values of relative damage severity and relative damage position from trapezoidal fuzzy model when Rules 5 and 15 of Table 5.2 are effectuated.

5.3.2 Results of fuzzy model

In the current section, the fuzzy system based damage diagnosis is realized. The fuzzy model (Fig. 5.2) has been designed for Al cantilever beam with six inputs as first three relative natural frequencies and first three relative mode shape differences and two outputs as relative damage position and relative damage severity. Three types of membership functions (triangular, Gaussian and trapezoidal) has been employed to develop the fuzzy model (Fig.5.4, Fig.5.5, Fig.5.6). Defuzzification (Fig.5.7, Fig.5.8, Fig.5.9) of the inputs using triangular, Gaussian and trapezoidal membership functions have been done by activating the rule no. 5 and rule no. 15 form the Table 5.2. Similarly, fuzzy model for fixed-fixed beam can be modeled. Moreover, different fuzzy models can be designed for composite and steel beam structures. The results obtained for cantilever and fixed-fixed beam structures with three different materials from numerical, finite element, fuzzy triangular, fuzzy Gaussian, fuzzy trapezoidal model and experimental analysis are compared in Table 5.1 to Table 5.12. Nine sets of data from the Table 5.1 to Table 5.6 represents the first three relative natural frequencies and first three relative mode shape differences in the first six columns and rest of the columns represents the corresponding values of relative damage positions and relative damage severity obtained from numerical, finite element, fuzzy triangular, fuzzy Gaussian, fuzzy trapezoidal model and experimental analysis.

5.4 Discussion

The fuzzy system designed in the current research has been adopted for damage diagnosis in structural members of different materials such as Al, composite & steel. The various types of membership functions used for development of the knowledge based system are triangular, Gaussian trapezoidal as depicted in Fig. 5.1 (a) to Fig. 5.1 (c). The different schemes complemented in designing of the proposed system are presented in Fig. 5.2. The various linguistic terms and some of the fuzzy rules used for developing the fuzzy damage diagnostic tool have been exhibited in Table 5.1 and Table 5.2 respectively. The complete architecture of different types of membership functions with the linguistic terms have been presented in Fig. 5.4 to Fig. 5.6. The results obtained for all three materials from fuzzy model with triangular, Gaussian and trapezoidal membership functions and experimental analyses are compared in Table 5.1 to Table 5.6 .The results from numerical, finite element and Gaussian fuzzy model analysis are shown in Table 5.7 to Table 5.12 and the results are found to be in very good agreement. From the analysis of the results presented in Table 5.1 to Table

5.6, it is observed that the percentage deviation of the results of the triangular membership function fuzzy model for Al, composite & steel cantilever and fixed-fixed beam structures are 7.65%, 7.59%, 7.15%, 7.21%, 8.03%, 8.11%. For Gaussian membership function percentage deviation of the results are found to be 5.10%, 5.16%, 4.95%, 5.02%, 6.19%, 6.63% and for trapezoidal membership function, deviation of the results are 7.38%, 7.45%, 6.93%, 6.98%, 7.68%, 7.72%.

Table 5.3 Comparison of modal parameters and damage characteristics of Al cantilever beam obtained from Fuzzy logic (Gaussian, Trapezoidal, Triangular) based model and experimental analysis

FNF	SNF	TNF	FMD	SNF	TNF	Fuzzy Gaussian		Fuzzy Trapezoidal		Fuzzy Triangular		Experimental	
						RDS	RDP	RDS	RDP	RDS	RDP	RDS	RDP
0.9964	0.9990	0.9999	0.0075	0.0031	0.0015	0.374	0.50	0.374	0.49	0.372	0.48	0.375	0.50
0.9957	0.9903	0.9998	0.0017	0.0053	0.0063	0499	0.49	0.498	0.48	0.497	0.51	0.500	0.50
0.9914	0.9726	0.9998	0.0030	0.0074	0.0057	0.624	0.49	0.622	0.48	0.622	0.48	0.625	0.50
0.9926	0.9964	0.9946	0.0051	0.0082	0.0137	0.376	0.26	0.377	0.27	0.378	0.27	0.375	0.25
0.9843	0.9919	0.9885	0.0076	0.0014	0.0125	0.501	0.26	0.498	0.27	0.497	0.28	0.500	0.25
0.9671	0.9841	0.9761	0.0087	0.0024	0.0491	0.626	0.25	0.627	0.26	0.627	0.27	0.625	0.25
0.9999	0.9999	0.9911	0.0165	0.0110	0.0312	0.374	0.76	0.373	0.73	0.372	0.72	0.375	0.75
0.9997	0.9997	0.9811	0.0350	0.0233	0.0264	0.499	0.76	0.497	0.74	0.502	0.73	0.500	0.75
0.9995	0.9947	0.9616	0.0704	0.0561	0.0533	0.626	0.74	0.627	0.73	0.628	0.73	0.625	0.75

Table 5.4 Comparison of modal parameters and damage characteristics of Al fixed-fixed beam obtained from Fuzzy logic (Gaussian, Trapezoidal, Triangular) based model and experimental analysis

FNF	SNF	TNF	FMD	SNF	TNF	Fuzzy Gaussian		Fuzzy Trapezoidal		Fuzzy Triangular		Experimental	
						RDS	RDP	RDS	RDP	RDS	RDP	RDS	RDP
0.9939	0.9996	0.9916	0.1484	0.0043	0.0039	0.375	0.51	0.374	0.48	0.377	0.52	0.375	0.50
0.9868	0.9991	0.9823	0.1727	0.0078	0.0103	0.501	0.51	0.502	0.48	0.503	0.51	0.500	0.50
0.9745	0.9987	0.9666	0.2679	0.0156	0.0094	0.626	0.49	0.624	0.51	0.624	0.48	0.625	0.50
0.9999	0.9943	0.9936	0.1388	0.0333	0.0257	0.374	0.26	0.377	0.26	0.379	0.27	0.375	0.25
0.9998	0.9879	0.9867	0.3955	0.0572	0.0227	0.499	0.27	0.503	0.23	0.497	027	0.500	0.25
0.9994	0.9757	0.9742	0.4135	0.0667	0.0496	0.626	0.24	0.623	0.24	0.627	0.26	0.625	0.25

Table 5.5 Comparison of modal parameters and damage characteristics of composite cantilever beam obtained from Fuzzy logic (Gaussian, Trapezoidal, Triangular) based model and experimental analysis

FNF	SNF	TNF	FMD	SNF	TNF	Fuzzy Gaussian		Fuzzy Trapezoidal		Fuzzy Triangular		Experimental	
						RDS	RDP	RDS	RDP	RDS	RDP	RDS	RDP
0.9979	0.9986	0.9992	0.0021	0.0075	0.0037	0.375	0.49	0.373	0.48	0.373	0.48	0.375	0.50
0.9956	0.9885	0.9986	0.0043	0.0011	0.0036	0.501	0.49	0.497	0.47	0.502	0.52	0.500	0.50
0.9910	0.9702	0.9983	0.0083	0.0140	0.0097	0.625	0.51	0.623	0.49	0.623	0.48	0.625	0.50
0.9924	0.9964	0.9944	0.0016	0.0301	0.0161	0.374	0.24	0.376	0.23	0.373	0.23	0.375	0.25
0.9837	0.9918	0.9880	0.0039	0.0094	0.0373	0.499	0.24	0.502	0.23	0.496	0.23	0.500	0.25
0.9661	0.9841	0.9752	0.0089	0.0147	0.0293	0.626	0.26	0.626	0.27	0.629	0.28	0.625	0.25
0.9999	0.9999	0.9908	0.0169	0.0682	0.0435	0.374	0.75	0.372	0.73	0.371	0.71	0.375	0.75
0.9998	0.9996	0.9805	0.0359	0.0429	0.0711	0.501	0.74	0.498	0.76	0.503	0.72	0.500	0.75
0.9995	0.9931	0.9604	0.0724	0.0465	0.0313	0.626	0.74	0.628	0.77	0.628	0.76	0.625	0.75

Table 5.6 Comparison of modal parameters and damage characteristics of composite fixed-fixed beam obtained from Fuzzy logic (Gaussian, Trapezoidal, Triangular) based model and experimental analysis

FNF	SNF	TNF	FMD	SNF	TNF	Fuzzy Gaussian		Fuzzy Trapezoidal		Fuzzy Triangular		Experimental	
						RDS	RDP	RDS	RDP	RDS	RDP	RDS	RDP
0.9940	0.9999	0.9918	0.0043	0.0091	0.0066	0.374	0.50	0.373	0.48	0.378	0.47	0.375	0.50
0.9872	0.9998	0.9828	0.0080	0.0123	0.0237	0.498	0.51	0.498	0.49	0.497	0.48	0.500	0.50
0.9753	0.9997	0.9676	0.0119	0.0087	0.0411	0.624	0.51	0.623	0.49	0.627	0.52	0.625	0.50
0.9998	0.9944	0.9937	0.1237	0.0265	0.0761	0.376	0.25	0.373	0.27	0.378	0.23	0.375	0.25
0.9997	0.9883	0.9869	0.3741	0.0465	0.0379	0.501	0.26	0.502	0.24	0.503	0.23	0.500	0.25
0.9994	0.9768	0.9751	0.3699	0.0823	0.0531	0.626	0.24	0.622	0.26	0.628	0.27	0.625	0.25

Table 5.7 Comparison of modal parameters and damage characteristics of steel cantilever beam obtained from Fuzzy logic (Gaussian, Trapezoidal, Triangular) based model and experimental analysis

FNF	SNF	TNF	FMD	SNF	TNF	Fuzzy Gaussian		Fuzzy Trapezoidal		Fuzzy Triangular		Experimental	
						RDS	RDP	RDS	RDP	RDS	RDP	RDS	RDP
0.9979	0.9969	0.9996	0.0021	0.0069	0.0044	0.374	0.49	0.373	0.48	0.372	0.48	0.375	0.50
0.9955	0.9866	0.9992	0.0043	0.0019	0.0045	0.501	0.49	0.502	0.48	0.503	0.47	0.500	0.50
0.9908	0.9676	0.9988	0.0081	0.0138	0.0105	0.624	0.51	0.624	0.49	0.622	0.51	0.625	0.50
0.9921	0.9963	0.9941	0.0018	0.0288	0.0179	0.376	0.25	0.377	0.26	0.371	0.27	0.375	0.25
0.9833	0.9918	0.9875	0.0041	0.0129	0.0341	0.499	0.24	0.498	0.26	0.503	0.27	0.500	0.25
0.9653	0.9842	0.9744	0.0094	0.0122	0.0274	0.626	0.24	0.627	0.24	0.628	0.22	0.625	0.25
0.9999	0.9999	0.9905	0.0174	0.0607	0.0461	0.374	0.74	0.373	0.73	0.377	0.22	0.375	0.75
0.9998	0.9989	0.9798	0.0099	0.0477	0.0693	0.499	0.74	0.502	0.76	0.497	0.78	0.500	0.75
0.9994	0.9913	0.9593	0.0743	0.0419	0.0375	0.624	0.76	0.623	0.77	0.621	0.72	0.625	0.75

Table 5.8 Comparison of modal parameters and damage characteristics of steel fixed-fixed beam obtained from Fuzzy logic (Gaussian, Trapezoidal, Triangular) based model and experimental analysis

FNF	SNF	TNF	FMD	SNF	TNF	Fuzzy Gaussian		Fuzzy Trapezoidal		Fuzzy Triangular		Experimental	
						RDS	RDP	RDS	RDP	RDS	RDP	RDS	RDP
0.9936	0.9997	0.9913	0.1444	0.0137	0.0153	0.374	0.50	0.373	0.48	0.371	0.47	0.375	0.50
0.9864	0.9992	0.9817	0.1713	0.1265	0.1117	0.502	0.51	0.502	0.48	0.504	0.49	0.500	0.50
0.9736	0.9989	0.9656	0.2627	0.2137	0.2106	0.624	0.49	0.622	0.51	0.621	0.52	0.625	0.50
0.9999	0.9941	0.9933	0.1354	0.1366	0.1291	0.376	0.51	0.373	0.26	0.377	0.28	0.375	0.25
0.9997	0.9875	0.9863	0.3899	0.3528	0.2205	0.501	0.51	0.502	0.26	0.503	0.28	0.500	0.25
0.9994	0.9751	0.9736	0.4082	0.3167	0.2496	0.624	0.49	0.623	0.24	0.628	0.27	0.625	0.25

Table 5.9 Comparison of modal parameters and damage characteristics of Al cantilever beam obtained from Fuzzy Gaussian based model, FEA, numerical and experimental analysis

FNF	SNF	TNF	FMD	SNF	TNF	Fuzzy Gaussian		FEA		Numerical		Experimental	
						RDS	RDP	RDS	RDP	RDS	RDP	RDS	RDP
0.9979	0.9986	0.9992	0.0021	0.0075	0.0037	0.374	0.50	0.375	0.49	0.373	0.49	0.375	0.50
0.9956	0.9885	0.9986	0.0043	0.0011	0.0036	0499	0.49	0.489	0.48	0.487	0.49	0.500	0.50
0.9910	0.9702	0.9983	0.0083	0.0140	0.0097	0.624	0.49	0.624	0.48	0.628	0.48	0.625	0.50
0.9924	0.9964	0.9944	0.0016	0.0301	0.0161	0.376	0.26	0.376	0.27	0.376	0.26	0.375	0.25
0.9837	0.9918	0.9880	0.0039	0.0094	0.0373	0.501	0.26	0.496	0.27	0.494	0.24	0.500	0.25
0.9661	0.9841	0.9752	0.0089	0.0147	0.0293	0.626	0.25	0.624	0.26	0.623	0.26	0.625	0.25
0.9999	0.9999	0.9908	0.0169	0.0682	0.0435	0.374	0.76	0.371	0.74	0.369	0.73	0.375	0.75
0.9998	0.9996	0.9805	0.0359	0.0429	0.0711	0.499	0.76	0.497	0.72	0.497	0.73	0.500	0.75
0.9995	0.9931	0.9604	0.0724	0.0465	0.0313	0.626	0.74	0.622	0.73	0.619	0.74	0.625	0.75

Table 5.10 Comparison of modal parameters and damage characteristics of Al fixed-fixed beam obtained from Fuzzy Gaussian based model, FEA, numerical and experimental analysis

FNF	SNF	TNF	FMD	SNF	TNF	Fuzzy Gaussian		FEA		Numerical		Experimental	
						RDS	RDP	RDS	RDP	RDS	RDP	RDS	RDP
0.9939	0.9996	0.9916	0.1484	0.0043	0.0039	0.375	0.51	0.370	0.49	0.368	0.49	0.375	0.50
0.9868	0.9991	0.9823	0.1727	0.0078	0.0103	0.501	0.51	0.488	0.51	0.489	0.51	0.500	0.50
0.9745	0.9987	0.9666	0.2679	0.0156	0.0094	0.626	0.49	0.626	0.49	0.627	0.51	0.625	0.50
0.9999	0.9943	0.9936	0.1388	0.0333	0.0257	0.374	0.26	0.374	0.26	0.373	0.27	0.375	0.25
0.9998	0.9879	0.9867	0.3955	0.0572	0.0227	0.499	0.27	0.497	0.27	0.495	0.26	0.500	0.25
0.9994	0.9757	0.9742	0.4135	0.0667	0.0496	0.626	0.24	0.621	0.24	0.620	0.24	0.625	0.25

Table 5.11 Comparison of modal parameters and damage characteristics of composite cantilever beam obtained from Fuzzy Gaussian based model, FEA, numerical and experimental analysis

FNF	SNF	TNF	FMD	SNF	TNF	Fuzzy Gaussian		FEA		Numerical		Experimental	
						RDS	RDP	RDS	RDP	RDS	RDP	RDS	RDP
0.9964	0.9990	0.9999	0.0075	0.0031	0.0015	0.375	0.49	0.374	0.51	0.373	0.52	0.375	0.50
0.9957	0.9903	0.9998	0.0017	0.0053	0.0063	0.501	0.49	0.504	0.49	0.508	0.48	0.500	0.50
0.9914	0.9726	0.9998	0.0030	0.0074	0.0057	0.625	0.51	0.621	0.49	0.619	0.51	0.625	0.50
0.9926	0.9964	0.9946	0.0051	0.0082	0.0137	0.374	0.24	0.363	0.24	0.362	0.24	0.375	0.25
0.9843	0.9919	0.9885	0.0076	0.0014	0.0125	0.499	0.24	0.503	0.26	0.507	0.25	0.500	0.25
0.9671	0.9841	0.9761	0.0087	0.0024	0.0491	0.626	0.26	0.623	0.26	0.621	0.27	0.625	0.25
0.9999	0.9999	0.9911	0.0165	0.0110	0.0312	0.374	0.75	0.379	0.74	0.381	0.73	0.375	0.75
0.9997	0.9997	0.9811	0.0350	0.0233	0.0264	0.501	0.74	0.509	0.73	0.511	0.73	0.500	0.75
0.9995	0.9947	0.9616	0.0704	0.0561	0.0533	0.626	0.74	0620	0.73	0.617	0.74	0.625	0.75

Table 5.12 Comparison of modal parameters and damage characteristics of composite fixed-fixed beam obtained from Fuzzy Gaussian based model, FEA, numerical and experimental analysis

FNF	SNF	TNF	FMD	SNF	TNF	Fuzzy Gaussian		FEA		Numerical		Experimental	
						RDS	RDP	RDS	RDP	RDS	RDP	RDS	RDP
0.9940	0.9999	0.9918	0.0043	0.0091	0.0066	0.374	0.50	0.368	0.49	0.361	0.49	0.375	0.50
0.9872	0.9998	0.9828	0.0080	0.0123	0.0237	0.498	0.51	0.503	0.51	0.509	0.52	0.500	0.50
0.9753	0.9997	0.9676	0.0119	0.0087	0.0411	0.624	0.51	0.628	0.51	0.631	0.52	0.625	0.50
0.9998	0.9944	0.9937	0.1237	0.0265	0.0761	0.376	0.25	0.374	0.24	0.372	0.23	0.375	0.25
0.9997	0.9883	0.9869	0.3741	0.0465	0.0379	0.501	0.26	0.502	0.23	0.502	0.21	0.500	0.25
0.9994	0.9768	0.9751	0.3699	0.0823	0.0531	0.626	0.24	0.630	0.26	0.634	0.27	0.625	0.25

Table 5.13 Comparison of modal parameters and damage characteristics of steel cantilever beam obtained from Fuzzy Gaussian based model, FEA, numerical and experimental analysis

FNF	SNF	TNF	FMD	SNF	TNF	Fuzzy Gaussian		FEA		Numerical		Experimental	
						RDS	RDP	RDS	RDP	RDS	RDP	RDS	RDP
0.9979	0.9969	0.9996	0.0021	0.0069	0.0044	0.374	0.49	0.374	0.49	0.374	0.50	0.375	0.50
0.9955	0.9866	0.9992	0.0043	0.0019	0.0045	0.501	0.49	0.499	0.49	0.498	0.49	0.500	0.50
0.9908	0.9676	0.9988	0.0081	0.0138	0.0105	0.624	0.51	0.624	0.48	0.623	0.49	0.625	0.50
0.9921	0.9963	0.9941	0.0018	0.0288	0.0179	0.376	0.25	0.373	0.27	0.374	0.26	0.375	0.25
0.9833	0.9918	0.9875	0.0041	0.0129	0.0341	0.499	0.24	0.498	0.24	0.499	0.26	0.500	0.25
0.9653	0.9842	0.9744	0.0094	0.0122	0.0274	0.626	0.24	0.623	0.26	0.622	0.24	0.625	0.25
0.9999	0.9999	0.9905	0.0174	0.0607	0.0461	0.374	0.74	0.377	0.76	0.376	0.76	0.375	0.75
0.9998	0.9989	0.9798	0.0099	0.0477	0.0693	0.499	0.74	0.501	0.73	0.502	0.74	0.500	0.75
0.9994	0.9913	0.9593	0.0743	0.0419	0.0375	0.624	0.76	0.623	0.74	0.622	0.74	0.625	0.75

Table 5.14 Comparison of modal parameters and damage characteristics of steel fixed-fixed beam obtained from Fuzzy Gaussian based model, FEA, numerical and experimental analysis

FNF	SNF	TNF	FMD	SNF	TNF	Fuzzy Gaussian		FEA		Numerical		Experimental	
						RDS	RDP	RDS	RDP	RDS	RDP	RDS	RDP
0.9936	0.9997	0.9913	0.1444	0.0137	0.0153	0.374	0.50	0.376	0.49	0.377	0.49	0.375	0.50
0.9864	0.9992	0.9817	0.1713	0.1265	0.1117	0.502	0.51	0.498	0.49	0.499	0.48	0.500	0.50
0.9736	0.9989	0.9656	0.2627	0.2137	0.2106	0.624	0.49	0.627	0.48	0.628	0.49	0.625	0.50
0.9999	0.9941	0.9933	0.1354	0.1366	0.1291	0.376	0.51	0.377	0.27	0.376	0.26	0.375	0.25
0.9997	0.9875	0.9863	0.3899	0.3528	0.2205	0.501	0.51	0.503	0.26	0.502	0.27	0.500	0.25
0.9994	0.9751	0.9736	0.4082	0.3167	0.2496	0.624	0.49	0.623	0.26	0.623	0.24	0.625	0.25

5.5 Summary

The fuzzy modeling implemented in the current section has been analyzed to get the following conclusions. The presence of damages in structural member has remarkable impact on the modal parameters of the dynamic structure. The first three relative natural frequencies and first three relative mode shape differences are engaged as inputs to the fuzzy model and relative damage positions and relative damage severity are the output parameters. The reliability of the proposed model has been established by comparing the results from the fuzzy models (Gaussian, trapezoidal, triangular) with that of the numerical, finite element and experimental analysis. The results are found to be well in agreement. Moreover, Guassian membership function is found to deliver better results compared to the other membership function and numerical & finite element analysis. Hence, the proposed Gaussian fuzzy model can be effectively used as damage identification tools in vibrating structures.

Chapter 6

ARTIFICIAL NEURAL NETWORK BASED DAMAGE DIAGNOSIS FOR VIBRATING STRUCTURES

Though damage diagnosis is not a phenomena, the evolution of various techniques over the time has made a point that the smooth functioning of all structural members is only possible when the development of damage of any form is prohibited. Therefore estimating the potential of the damage is to be thoroughly diagnosed for maintaining the life span of the various structures. The change in dynamic characteristics of vibrating structures lay down the main platform for most of the damage diagnosis mechanism. In this section, artificial neural network based model is developed with requisite amount of trained data generated from back propagation technique. Finally, the results from the model have been compared with the experimental results to establish the robustness of the proposed neural method.

6.1 Introduction

This section of the thesis provides an introduction to basic neural network architectures and learning rules.

The complex biological neural network in a human body has highly interconnected set of neurons, facilitates for various kind of output such as thinking, breathing, driving etc. Generally the neurons are believed to store the biological neural functions and memory and learning of the neural system facilitates for establishment of new connections between the neurons. The most interesting feature of this artificial neural network (ANN) is the novel structure of the information processing system. It is composed of a large number of highly interconnected processing elements (neurons) working in parallel to solve specific applications, such as pattern recognition or data classification, through a learning process. Learning in biological systems involves adjustments to the synaptic weights that exist between the neurons. Neural networks, with their remarkable ability to derive meaning from complicated or imprecise data, can be used to recognize patterns and detect trends that are too

complex to be noticed by either humans or other computer techniques. Some of the advantages of the ANN are depicted below.

Adaptive learning: The ability of the neural system lies in the capacity to adapt to the changing environment by adjusting the synaptic weights and perform according to the situation. This feature makes the neural network a methodology to address industrial applications in dynamic environment.

Self-Organization: An artificial neural network can produce results for inputs that are not used during training by creating its own representation of the information it receives during learning time. This capability helps in solving problem of higher complexities.

Real Time Operation: The neural network is composed of a large number interconnected neurons working in parallel to solve a specific problem. Neural networks learn by example. For this special hardware devices are being designed and manufactured which take advantage of this capability.

Fault Tolerance: In case of failure of a neuron in neural network system there will be a partial destruction of a network which leads to only deterioration of quality of output rather than collapsing the system as a whole.

This section introduces a feed forward multilayer neural network trained with back propagation technique for online multiple damage detection in structural beam members. The proposed neural network system has been designed with six input parameters (first three relative natural frequencies, first three relative mode shape differences) and two output parameters (relative damage position, relative damage severity). A comparison of results obtained from fuzzy, numerical, FEA, neural and experimental analysis have been conducted and it is observed that the developed neural network provides more accurate results as compared to other mentioned methods. Subsequently, the outputs from neural network are validated by the experimentation.

6.2 Neural network technique

Given this the description of neural network, it has been successfully implemented in many industrial applications such as industrial process control, sales forecasting, electronic noses,

modeling, diagnosing the Cardiovascular System and etc. The parallel computing capability and the ability to perform under changing environment make the neural network a potential tool to address applications, which are hard to solve using analytical or numerical methods.

6.2.1 Model of a neural network

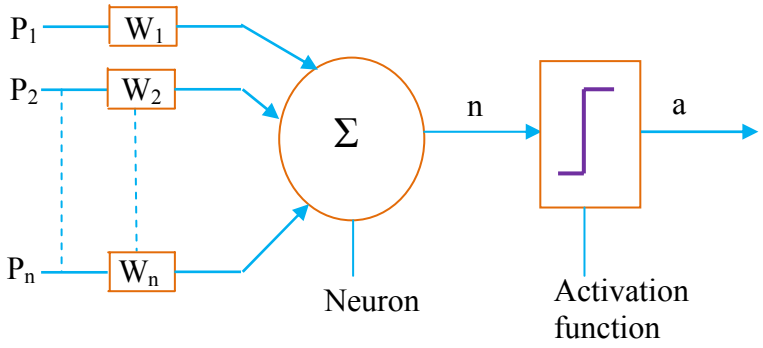

Fig. 6.1 Neuron Model

A neuron which can be used in a dynamic environment is shown in Fig. 6.1. An artificial neuron is a device with many inputs and one output. The neuron has two modes of operation; the training mode and the using mode. In the training mode, the neuron can be trained to fire (or not), for particular input patterns. In the using mode, when a taught input pattern is detected at the input, its associated output becomes the current output. If the input pattern does not belong in the taught list of input patterns, the firing rule is used to determine whether to fire or not.

The main features of the neural model are as follows,

- The inputs to the neuron are assigned with synaptic weights, which in turn affect the decision making ability of the neural network. The inputs to the neuron are called weighted inputs.
- These weighted inputs are then summed together in an adder and if they exceed a pre-set threshold value, the neuron fires. In any other case the neuron does not fire.
- An activation function for limiting the amplitude of the output of a neuron. Generally the normalized amplitude range of the output of a neuron is given as the closed unit interval [0,1] or alternatively [-1,1].

Learning process of ANN:

The learning for a neural network means following a methodology for modifying the weights to make the network adaptive in nature to changing environment. The learning rules may be broadly divided into three categories,

1. Supervised learning: The supervised learning rule is provided with set of training data for proper network behavior. When the inputs are applied to the network, the outputs from the network are compared with the targets. Through the learning process the network will adjust the weights of the network in order to bring the outputs closer to the targets.
2. Unsupervised learning: In this type of learning the network modifies the weights in response to the inputs to the network. This is suitable for applications requiring vector quantization.
3. Reinforcement learning: In the reinforcement learning instead of being provided with the correct output, for each network input, the algorithm is only given a score. The score is the measure of network performance over some sequence of inputs.

In mathematical terms, we can describe a neuron k by writing the following pair of equations:

$$u_k = \sum_{j=1}^{p} w_{kj} x_j \tag{6.1}$$

$$y_k = f(u_k) \tag{6.2}$$

Where $x_1, x_2, \ldots, x_p$ are the input signals; $w_{k1}, w_{k2}, \ldots, w_{kp}$ are the synaptic weights of neuron k; u_k is the linear combined output; $f(\cdot)$ is the activation function; and y_k is the output signal of the neuron.

6.2.2 Use of back propagation neural network

The back propagation technique (Fig. 6.2) can be used to train the multilayer networks. This technique is an approximate steepest gradient algorithm in which the performance of the network is based on mean square error. In order to train the neural network, the weights for each input to the neural system should be so adjusted that the error between the actual output

and desired output is minimum. The multilayer neural system would calculate the change in error due to increase or decrease in the weights. The algorithm first computes each error weight by computing the rate of the error changes with the change in synaptic weights. The error in each hidden layer just before the output layer in a direction opposite to the way activities propagate through the network have to be computed and fed to the network by back propagation algorithm to minimize the error in the actual output and desired output by adjusting the parameters of the network.

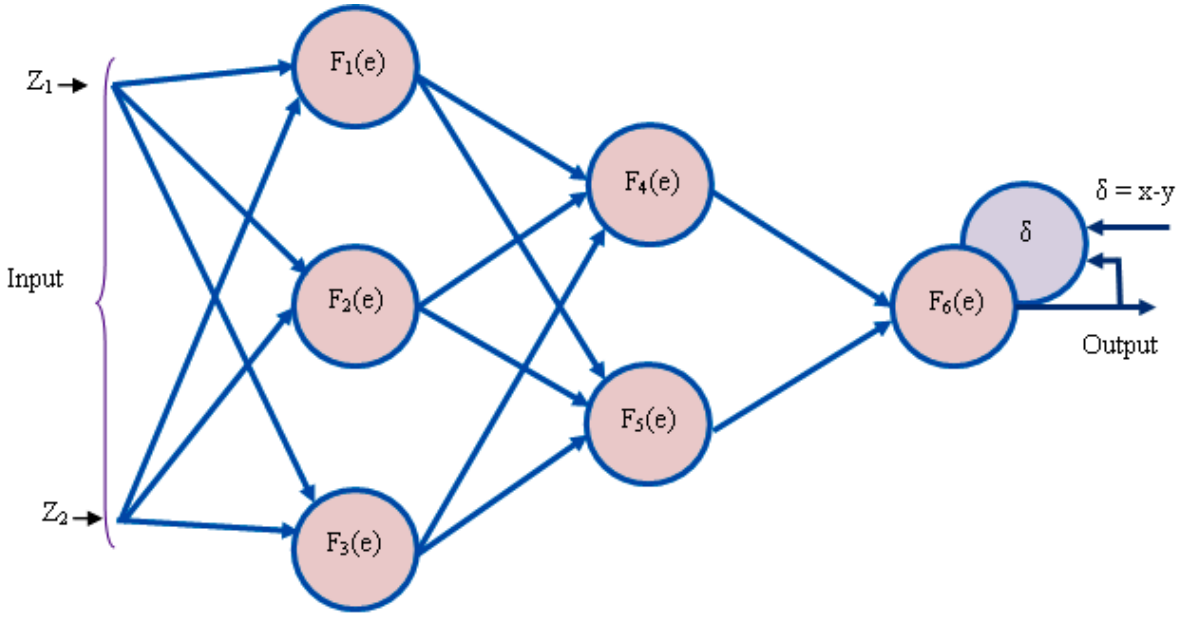

Fig. 6.2 Back propagation technique

6.3 Analysis of neural network model used for damage detection

A back propagation neural model [66] has been proposed for identification of damage (i.e. relative damage positions, relative damage severity) of structural beam members (Fig.6.3).The neural model has been designed with six input parameters and two output parameters.

The inputs to the neural network model are FNF, SNF, TNF, FMD, SMD and TMD.

The outputs from the neural model are as follows;

Relative damage position = “RDP”

Relative damage severity = “RDS”

The back propagation neural network has been made with one input layer, one output layer and eight hidden layers. The input layer contains six neurons, where as the output layer contains two neurons. The number of neurons in each hidden layers are different in order to give the neural network a diamond shape and for better convergence of results (Fig.6.4). The neurons associated with the input layer of the network represent the first three relative natural frequencies and first three average relative mode shape difference. The relative damage position, relative damage severityare represented by the two neurons of the output layer of the neural network.

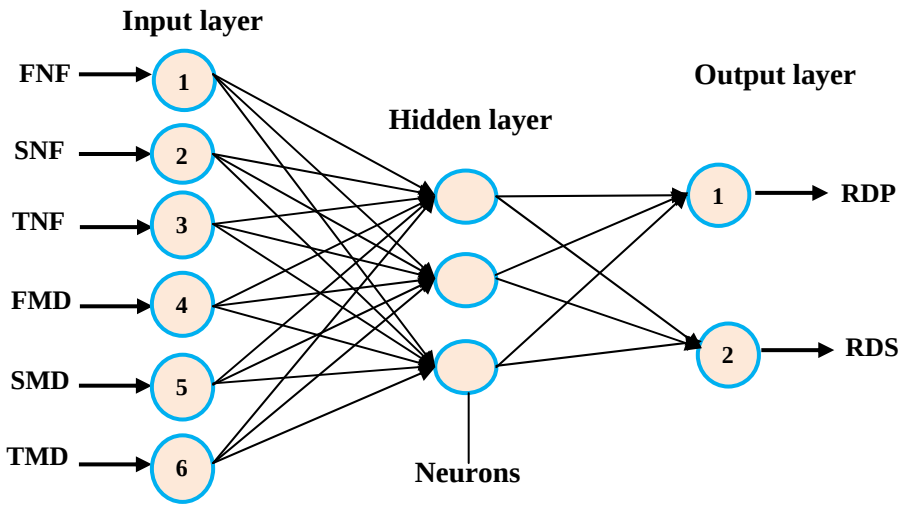

Fig. 6.3 Neural network model

6.3.1 Neural controller mechanism for damage detection

The neural network used in the current investigation is a five-layered feed forward neural network model trained with back propagation technique [66]. The training of neural data is realized using the number of chosen layers. The input layer of the neural network consists of six neurons for first three relative natural frequencies and first three relative mode shape difference and the output layer consists of two neurons for relative damage positions and relative damage severities. The hidden layers i.e. 2^{nd}, 3^{rd} and 4^{th} layer of the network comprises 9 neurons, 11 neurons and 9 neurons respectively. The number of neurons in each

hidden layer has been decided using the empirical relation. Fig. 6.4 illustrates the neural network with its input and output signals for Al cantilever beam. Similarly, for composite and steel cantilever beam structures, neural network model can be designed. Moreover for fixed-fixed beam of each material can also be integrated with the neural network model.

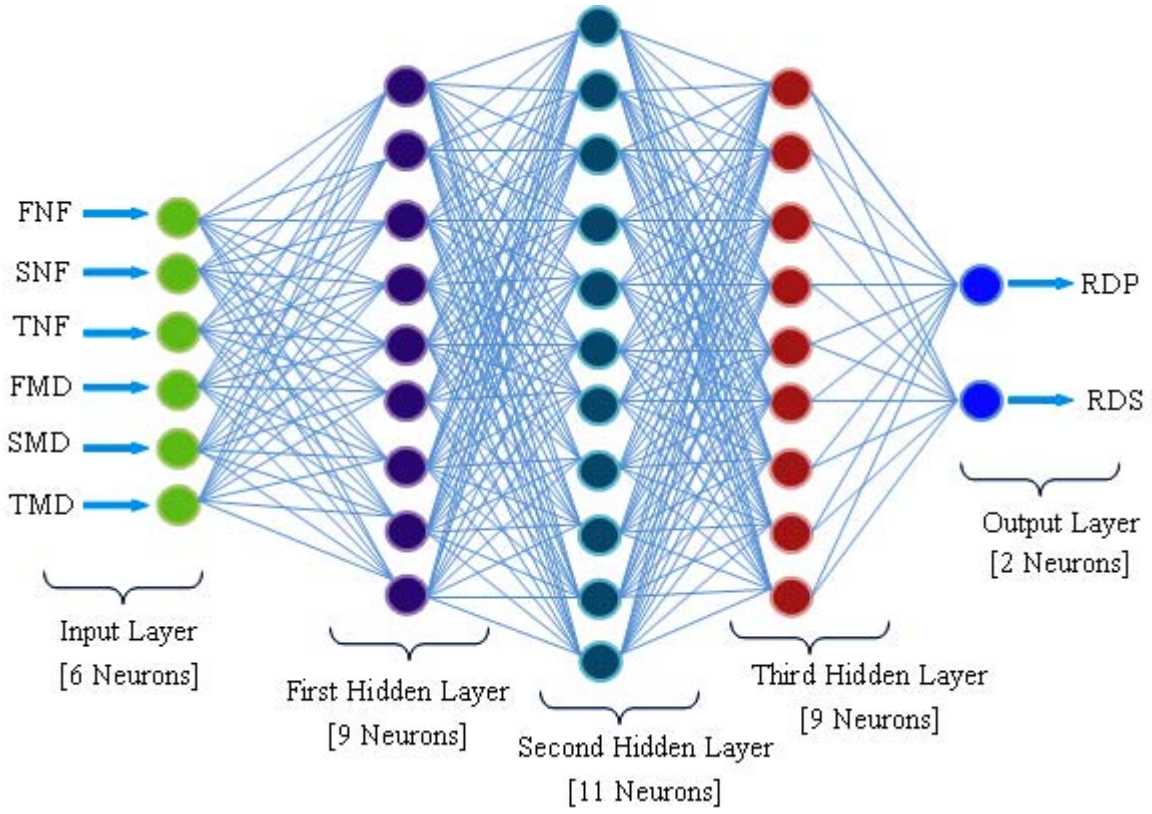

Fig. 6.4 Multi layered feed forward back propagation neural controller for damage identification

The proposed neural network model for damage identification has been trained with 600 patterns of data for each Al, composite & steel cantilever and fixed-fixed beam featuring various states of the beam members. Out of the several hundred testing data, some of them are presented for each material in Table 6.1 to Table 6.6. During the training, the models are fed with six input parameters i.e. first three relative natural frequencies and first three mode shape differences. The outputs are relative damage positions and relative damage severities.

During training and during normal operation, the input patterns fed to the neural network comprise the following components:

$$y_1^{\{1\}} = \text{relative deviation of first natural frequency} \qquad (6.3(a))$$

$y_2^{\{1\}}$ = relative deviation of second natural frequency (6.3(b))

$y_3^{\{1\}}$ = relative deviation of third natural frequency (6.3(c))

$y_4^{\{1\}}$ = relative deviation of first mode shape difference (6.3(d))

$y_5^{\{1\}}$ = relative deviation of second mode shape difference (6.3(e))

$y_6^{\{1\}}$ = relative deviation of third mode shape difference (6.3(f))

The outputs generated due to the distribution of the input to the hidden neurons are given by [66]:

$$f\left(V_j^{\{lay\}}\right) = y_j^{\{lay\}} \tag{6.4}$$

Where,

$$\sum_i W_{ji}^{\{lay\}} . y_i^{\{lay-1\}} = V_j^{\{lay\}} \tag{6.5}$$

layer number (2 or 4) = lay

label for j^{th} neuron in hidden layer 'lay'= j

label for i^{th} neuron in hidden layer 'lay-1'= i

Weight of the connection from neuron i in layer 'lay-1' to neuron j in layer 'lay'= $W_{ji}^{\{lay\}}$

Activation function, chosen in this work as the hyperbolic tangent function = f (.), where,

$$\frac{e^x - e^{-x}}{e^x + e^{-x}} = f(x) \tag{6.6}$$

In the process of training, the network output $\theta_{actual,\ n}$ (i=1 to 2) may differ from the desired output $\theta_{desired,n}$ (n=1 to 2) as specified in the training pattern presented to the network. The measure of performance of the network is the instantaneous sum-squared difference between $\theta_{desired,\ n}$ and $\theta_{actual,\ n}$ for the set of presented training patterns:

$$\mathrm{Err} = \frac{1}{2} \sum_{\substack{\text{all training} \\ \text{patterns}}} \left(\theta_{\text{desired,n}} - \theta_{\text{actual,n}}\right)^2 \tag{6.7}$$

Where $\theta_{\text{actual, n}}$ (n=1) represents relative damage position ("RDP")

$\theta_{\text{actual, n}}$ (n=2) represents relative damage severity ("RDS")

During the development of the neural model, the error back propagation method is employed to train the network [66]. This method requires the computation of local error gradients in order to determine appropriate weight corrections to reduce error. For the output layer, the error gradient $\delta^{\{5\}}$ is:

$$\delta^{\{5\}} = f'\left(V_1^{\{5\}}\right)\left(\theta_{desired,n} - \theta_{actual,n}\right) \tag{6.8}$$

Hence, the local gradient for neurons in hidden layer {lay} is given by:

$$\delta_j^{\{\text{lay}\}} = \mathrm{f}'\left(\mathrm{V}_j^{\{\text{lay}\}}\right)\left(\sum_k \delta_k^{\{\text{lay+1}\}} \mathrm{W}_{kj}^{\{\text{lay+1}\}}\right) \tag{6.9}$$

Synaptic weights are updated according to the following expressions:

$$\mathrm{W}_{ji}(\mathrm{t}+1) = \mathrm{W}_{ji}(\mathrm{t}) + \Delta \mathrm{W}_{ji}(\mathrm{t}+1) \tag{6.10}$$

and $$\Delta \mathrm{W}_{ji}(\mathrm{t}+1) = \alpha \Delta \mathrm{W}_{ji}(\mathrm{t}) + \eta \delta_j^{\{\text{lay}\}} \mathrm{y}_i^{\{\text{lay}-1\}} \tag{6.11}$$

Where

Momentum coefficient (chosen statistically as 0.2 in this work)= α

Learning rate (chosen statistically as 0.35 in this work) = η

Iteration number, each iteration consisting of the presentation of a training

pattern and correction of the weights = t

Following expression shows, the final output from the neural network as;

$$\theta_{actual,n} = f\left(V_n^{\{5\}}\right) \tag{6.12}$$

where $$V_n^{\{5\}} = \sum_i W_{ni}^{\{5\}} y_i^{\{4\}} \tag{6.13}$$

η = learning rate (chosen empirically as 0.35 in this work)

t = iteration number, each iteration consisting of the presentation of a training pattern and correction of the weights.

Table 6.1 Comparison of modal parameters and damage characteristics of Al cantilever beam obtained from Neural Network based model

Input to the Neural Network Model						Output from the Neural Network Model	
FNF	SNF	TNF	FMD	SMD	TMD	RDS	RDP
0.9979	0.9986	0.9992	0.0021	0.0075	0.0037	0.374	0.50
0.9956	0.9885	0.9986	0.0043	0.0011	0.0036	0.499	0.49
0.9910	0.9702	0.9983	0.0083	0.0140	0.0097	0.626	0.51
0.9924	0.9964	0.9944	0.0016	0.0301	0.0161	0.375	0.26
0.9837	0.9918	0.9880	0.0039	0.0094	0.0373	0.501	0.26
0.9661	0.9841	0.9752	0.0089	0.0147	0.0293	0.624	0.24
0.9999	0.9999	0.9908	0.0169	0.0682	0.0435	0.375	0.76
0.9998	0.9996	0.9805	0.0359	0.0429	0.0711	0.499	0.76
0.9995	0.9931	0.9604	0.0724	0.0465	0.0313	0.626	0.75

Table 6.2 Comparison of modal parameters and damage characteristics of Al fixed-fixed beam obtained from Neural Network based model

Input to the Neural Network Model						Output from the Neural Network Model	
FNF	SNF	TNF	FMD	SMD	TMD	RDS	RDP
0.9939	0.9996	0.9916	0.1484	0.0043	0.0039	0.374	0.50
0.9868	0.9991	0.9823	0.1727	0.0078	0.0103	0.501	0.49
0.9745	0.9987	0.9666	0.2679	0.0156	0.0094	0.625	0.49
0.9999	0.9943	0.9936	0.1388	0.0333	0.0257	0.374	0.50
0.9998	0.9879	0.9867	0.3955	0.0572	0.0227	0.502	0.49
0.9994	0.9757	0.9742	0.4135	0.0667	0.0496	0.626	0.51

Table 6.3 Comparison of modal parameters and damage characteristics of composite cantilever beam obtained from Neural Network based model

Input to the Neural Network Model						Output from the Neural Network Model	
FNF	SNF	TNF	FMD	SMD	TMD	RDS	RDP
0.9964	0.9990	0.9999	0.0075	0.0031	0.0015	0.375	0.49
0.9957	0.9903	0.9998	0.0017	0.0053	0.0063	0.498	0.49
0.9914	0.9726	0.9998	0.0030	0.0074	0.0057	0.624	0.51
0.9926	0.9964	0.9946	0.0051	0.0082	0.0137	0.376	0.25
0.9843	0.9919	0.9885	0.0076	0.0014	0.0125	0.499	0.25
0.9671	0.9841	0.9761	0.0087	0.0024	0.0491	0.625	0.25
0.9999	0.9999	0.9911	0.0165	0.0110	0.0312	0.374	0.75
0.9997	0.9997	0.9811	0.0350	0.0233	0.0264	0.498	0.75
0.9995	0.9947	0.9616	0.0704	0.0561	0.0533	0.626	0.76

Table 6.4 Comparison of modal parameters and damage characteristics of composite fixed-fixed beam obtained from Neural Network based model

Input to the Neural Network Model						Output from the Neural Network Model	
FNF	SNF	TNF	FMD	SMD	TMD	RDS	RDP
0.9940	0.9999	0.9918	0.0043	0.0091	0.0066	0.376	0.51
0.9872	0.9998	0.9828	0.0080	0.0123	0.0237	0.501	0.50
0.9753	0.9997	0.9676	0.0119	0.0087	0.0411	0.627	0.48
0.9998	0.9944	0.9937	0.1237	0.0265	0.0761	0.375	0.50
0.9997	0.9883	0.9869	0.3741	0.0465	0.0379	0.501	0.50
0.9994	0.9768	0.9751	0.3699	0.0823	0.0531	0.625	0.51

Table 6.5 Comparison of modal parameters and damage characteristics of steel cantilever beam obtained from Neural Network based model

Input to the Neural Network Model						Output from the Neural Network Model	
FNF	SNF	TNF	FMD	SMD	TMD	RDS	RDP
0.9979	0.9969	0.9996	0.0021	0.0069	0.0044	0.377	0.48
0.9955	0.9866	0.9992	0.0043	0.0019	0.0045	0.499	0.51
0.9908	0.9676	0.9988	0.0081	0.0138	0.0105	0.625	0.51
0.9921	0.9963	0.9941	0.0018	0.0288	0.0179	0.374	0.25
0.9833	0.9918	0.9875	0.0041	0.0129	0.0341	0.500	0.25
0.9653	0.9842	0.9744	0.0094	0.0122	0.0274	0.626	0.26
0.9999	0.9999	0.9905	0.0174	0.0607	0.0461	0.376	0.74
0.9998	0.9989	0.9798	0.0099	0.0477	0.0693	0.499	0.76
0.9994	0.9913	0.9593	0.0743	0.0419	0.0375	0.625	0.74

Table 6.6 Comparison of modal parameters and damage characteristics of steel fixed-fixed beam obtained from Neural Network based model

Input to the Neural Network Model						Output from the Neural Network Model	
FNF	SNF	TNF	FMD	SMD	TMD	RDS	RDP
0.9936	0.9997	0.9913	0.1444	0.0137	0.0153	0.375	0.50
0.9864	0.9992	0.9817	0.1713	0.1265	0.1117	0.499	0.49
0.9736	0.9989	0.9656	0.2627	0.2137	0.2106	0.624	0.50
0.9999	0.9941	0.9933	0.1354	0.1366	0.1291	0.376	0.51
0.9997	0.9875	0.9863	0.3899	0.3528	0.2205	0.501	0.50
0.9994	0.9751	0.9736	0.4082	0.3167	0.2496	0.625	0.49

Table 6.7 Comparison of modal parameters and damage characteristics of Al cantilever beam obtained from Neural Network based model, Fuzzy Gaussian based model, FEA and Experimental analysis

FNF	SNF	TNF	FMD	SNF	TNF	Neural Network		Fuzzy Gaussian		FEA		Experimental	
						RDS	RDP	RDS	RDP	RDS	RDP	RDS	RDP
0.9979	0.9986	0.9992	0.0021	0.0075	0.0037	0.374	0.50	0.374	0.50	0.375	0.49	0.375	0.50
0.9956	0.9885	0.9986	0.0043	0.0011	0.0036	0.499	0.49	0499	0.49	0.489	0.48	0.500	0.50
0.9910	0.9702	0.9983	0.0083	0.0140	0.0097	0.626	0.51	0.624	0.49	0.624	0.48	0.625	0.50
0.9924	0.9964	0.9944	0.0016	0.0301	0.0161	0.375	0.26	0.376	0.26	0.376	0.27	0.375	0.25
0.9837	0.9918	0.9880	0.0039	0.0094	0.0373	0.501	0.26	0.501	0.26	0.496	0.27	0.500	0.25
0.9661	0.9841	0.9752	0.0089	0.0147	0.0293	0.624	0.24	0.626	0.25	0.624	0.26	0.625	0.25
0.9999	0.9999	0.9908	0.0169	0.0682	0.0435	0.375	0.76	0.374	0.76	0.371	0.74	0.375	0.75
0.9998	0.9996	0.9805	0.0359	0.0429	0.0711	0.499	0.76	0.499	0.76	0.497	0.72	0.500	0.75
0.9995	0.9931	0.9604	0.0724	0.0465	0.0313	0.626	0.75	0.626	0.74	0.622	0.73	0.625	0.75

Table 6.8 Comparison of modal parameters and damage characteristics of Al fixed-fixed beam obtained from Neural Network based model, Fuzzy Gaussian based model, FEA and Experimental analysis

FNF	SNF	TNF	FMD	SNF	TNF	Neural Network		Fuzzy Gaussian		FEA		Experimental	
						RDS	RDP	RDS	RDP	RDS	RDP	RDS	RDP
0.9939	0.9996	0.9916	0.1484	0.0043	0.0039	0.374	0.50	0.370	0.49	0.368	0.49	0.375	0.50
0.9868	0.9991	0.9823	0.1727	0.0078	0.0103	0.501	0.49	0.488	0.51	0.489	0.51	0.500	0.50
0.9745	0.9987	0.9666	0.2679	0.0156	0.0094	0.625	0.49	0.626	0.49	0.627	0.51	0.625	0.50
0.9999	0.9943	0.9936	0.1388	0.0333	0.0257	0.374	0.50	0.374	0.26	0.373	0.27	0.375	0.25
0.9998	0.9879	0.9867	0.3955	0.0572	0.0227	0.502	0.49	0.497	0.27	0.495	0.26	0.500	0.25
0.9994	0.9757	0.9742	0.4135	0.0667	0.0496	0.626	0.51	0.621	0.24	0.620	0.24	0.625	0.25

Table 6.9 Comparison of modal parameters and damage characteristics of composite cantilever beam obtained from Neural Network based model, Fuzzy Gaussian based model, FEA and Experimental analysis

FNF	SNF	TNF	FMD	SNF	TNF	Neural Network		Fuzzy Gaussian		FEA		Experimental	
						RDS	RDP	RDS	RDP	RDS	RDP	RDS	RDP
0.9964	0.9990	0.9999	0.0075	0.0031	0.0015	0.375	0.49	0.375	0.49	0.374	0.51	0.375	0.50
0.9957	0.9903	0.9998	0.0017	0.0053	0.0063	0.501	0.49	0.501	0.49	0.504	0.49	0.500	0.50
0.9914	0.9726	0.9998	0.0030	0.0074	0.0057	0.625	0.51	0.625	0.51	0.621	0.49	0.625	0.50
0.9926	0.9964	0.9946	0.0051	0.0082	0.0137	0.374	0.24	0.374	0.24	0.363	0.24	0.375	0.25
0.9843	0.9919	0.9885	0.0076	0.0014	0.0125	0.499	0.24	0.499	0.24	0.503	0.26	0.500	0.25
0.9671	0.9841	0.9761	0.0087	0.0024	0.0491	0.626	0.26	0.626	0.26	0.623	0.26	0.625	0.25
0.9999	0.9999	0.9911	0.0165	0.0110	0.0312	0.374	0.75	0.374	0.75	0.379	0.74	0.375	0.75
0.9997	0.9997	0.9811	0.0350	0.0233	0.0264	0.501	0.74	0.501	0.74	0.509	0.73	0.500	0.75
0.9995	0.9947	0.9616	0.0704	0.0561	0.0533	0.626	0.74	0.626	0.74	0620	0.73	0.625	0.75

Table 6.10 Comparison of modal parameters and damage characteristics of composite fixed-fixed beam obtained from Neural Network based model, Fuzzy Gaussian based model, FEA and Experimental

FNF	SNF	TNF	FMD	SNF	TNF	Neural Network		Fuzzy Gaussian		FEA		Experimental	
						RDS	RDP	RDS	RDP	RDS	RDP	RDS	RDP
0.9940	0.9999	0.9918	0.0043	0.0091	0.0066	0.374	0.50	0.368	0.49	0.361	0.49	0.375	0.50
0.9872	0.9998	0.9828	0.0080	0.0123	0.0237	0.498	0.51	0.503	0.51	0.509	0.52	0.500	0.50
0.9753	0.9997	0.9676	0.0119	0.0087	0.0411	0.624	0.51	0.628	0.51	0.631	0.52	0.625	0.50
0.9998	0.9944	0.9937	0.1237	0.0265	0.0761	0.376	0.25	0.374	0.24	0.372	0.23	0.375	0.25
0.9997	0.9883	0.9869	0.3741	0.0465	0.0379	0.501	0.26	0.502	0.23	0.502	0.21	0.500	0.25
0.9994	0.9768	0.9751	0.3699	0.0823	0.0531	0.626	0.24	0.630	0.26	0.634	0.27	0.625	0.25

Table 6.11 Comparison of modal parameters and damage characteristics of steel cantilever beam obtained from Neural Network based model, Fuzzy Gaussian based model, FEA and Experimental analysis

FNF	SNF	TNF	FMD	SNF	TNF	Neural Network		Fuzzy Gaussian		FEA		Experimental	
						RDS	RDP	RDS	RDP	RDS	RDP	RDS	RDP
0.9979	0.9969	0.9996	0.0021	0.0069	0.0044	0.377	0.48	0.374	0.49	0.374	0.49	0.375	0.50
0.9955	0.9866	0.9992	0.0043	0.0019	0.0045	0.499	0.51	0.501	0.49	0.499	0.49	0.500	0.50
0.9908	0.9676	0.9988	0.0081	0.0138	0.0105	0.625	0.51	0.624	0.51	0.624	0.48	0.625	0.50
0.9921	0.9963	0.9941	0.0018	0.0288	0.0179	0.374	0.25	0.376	0.25	0.373	0.27	0.375	0.25
0.9833	0.9918	0.9875	0.0041	0.0129	0.0341	0.500	0.25	0.499	0.24	0.498	0.24	0.500	0.25
0.9653	0.9842	0.9744	0.0094	0.0122	0.0274	0.626	0.26	0.626	0.24	0.623	0.26	0.625	0.25
0.9999	0.9999	0.9905	0.0174	0.0607	0.0461	0.376	0.74	0.374	0.74	0.377	0.76	0.375	0.75
0.9998	0.9989	0.9798	0.0099	0.0477	0.0693	0.499	0.76	0.499	0.74	0.501	0.73	0.500	0.75
0.9994	0.9913	0.9593	0.0743	0.0419	0.0375	0.625	0.74	0.624	0.76	0.623	0.74	0.625	0.75

Table 6.12 Comparison of modal parameters and damage characteristics of steel fixed-fixed beam obtained from Neural Network based model, Fuzzy Gaussian based model, FEA and Experimental analysis

FNF	SNF	TNF	FMD	SNF	TNF	Neural Network		Fuzzy Gaussian		FEA		Experimental	
						RDS	RDP	RDS	RDP	RDS	RDP	RDS	RDP
0.9936	0.9997	0.9913	0.1444	0.0137	0.0153	0.375	0.50	0.374	0.50	0.376	0.49	0.375	0.50
0.9864	0.9992	0.9817	0.1713	0.1265	0.1117	0.499	0.49	0.502	0.51	0.498	0.49	0.500	0.50
0.9736	0.9989	0.9656	0.2627	0.2137	0.2106	0.624	0.50	0.624	0.49	0.627	0.48	0.625	0.50
0.9999	0.9941	0.9933	0.1354	0.1366	0.1291	0.376	0.51	0.376	0.51	0.377	0.27	0.375	0.25
0.9997	0.9875	0.9863	0.3899	0.3528	0.2205	0.501	0.50	0.501	0.51	0.503	0.26	0.500	0.25
0.9994	0.9751	0.9736	0.4082	0.3167	0.2496	0.625	0.49	0.624	0.49	0.623	0.26	0.625	0.25

6.3.2 Neural network contollerl for diagnosis of damage

The feed forward network has been trained with 600 different patterns of parameters to obtain the objective. Some of the test patterns are depicted in Table 6.1 to Table 6.6. The intelligent neural system has six numbers of input parameters in the input layer i.e. first three relative natural frequencies and first three average mode shape difference. The output layer has two outputs and they relative damage position and relative damage severity.

6.4 Results and discussion of neural controller

The five layer feed forward neural network model with back propagation technique for damage identification is shown with the complete architecture in Fig.6.4. This has been designed to predict the relative damage position and relative damage severity. The first three relative natural frequencies and first three average relative mode shape differences have been used as inputs to the input layer of the proposed network. These inputs are processed in the three hidden layers and finally the output layer provides the results for relative crack position and relative damage severity. The block diagram of the neural model with the input and output parameters is depicted in Fig.6.3. Out of several hundred training patterns that have been used to train the neural model, some of them along with the outputs from the model are shown in Table 6.1 to Table 6.6. Experiments have been carried out to validate the results obtained from different analyses performed on the damaged cantilever beam and fixed-fixed beam of Al, composite & steel. The results obtained from neural model, fuzzy Gaussian model, finite element analysis and experimental analysis are presented in Table 6.7 to Table 6.12 and are found to be in close agreement. The different parameters presented in various columns of the Table 6.7 to Table 6.12 are expressed as, relative first natural frequency (FNF), relative second natural frequency (SNF), relative of 3^{rd} natural frequency (TNF), relative first mode shape difference (FMD), relative second mode shape difference (SMD), relative third mode shape difference (TMD) as inputs and the rest columns represents the outputs as relative damage position and relative damage severity obtained from corresponding investigation. The percentage of deviations of the results from neural model

with respect to experimental results observed for Al, composite & steel cantilever and fixed-fixed beams as given in Table 6.2 (a) to Table 6.2 (f) are about 4.35%, 4.43%, 4.12%, 4.23%, 4.79% and 4.97% respectively which is better than the performance of fuzzy Gaussian model.

6.5 Summary

This section expresses the final conclusions drawn from the analysis carried out in the present chapter. The neural network model has been designed on the basis of change of modal parameters such as natural frequencies and modes shapes due to presence of damages in structural members. The input parameters to the diamond shaped feed forward neural network model is the first three natural frequencies and first three average mode shapes. The outputs from the model are relative damage position and relative damage severity. Hundreds of training patterns have been developed to train the neural model for damage detection. The neural system has different numbers of neurons in all the five layers for processing the inputs to the model. By adopting the back propagation algorithm, it is observed that the difference between the actual output and desired output has been successfully reduced. The results derived from the proposed neural network have been compared with the results obtained from numerical, FEA, fuzzy Gaussian model and experimental analysis to check the reliability of the model and the comparison results are found to be very encouraging.

Chapter 7

DESCRIPTION AND INSTALLATION OF EXPERIMENTAL SETUP

The experimental analysis has been carried out to measure the natural frequencies and mode shapes of the damaged beam structures. The experimental set up has been shown in Fig.7.1. Experiments have been performed on the damaged beam structures with different damage positions and damage severities to validate the results obtained from theoretical, finite element and other artificial intelligent techniques used for damage diagnosis as discussed in the previous chapters of the thesis. This chapter briefly describes the systematic procedures adopted for experimental investigation and the required instrumentation for measuring the vibration parameters of the cantilever beam and fixed-fixed beam of different materials such as Al, composite & steel.

7.1 Detail specifications of the vibration measuring instruments

Experiments have been performed using the developed experimental set up (Fig. 7.1) for measuring the vibration responses (natural frequencies and amplitude of vibration) of the cantilever beams and fixed-fixed beam specimens made from Aluminum, composite and steel with dimension 1000mm x 50mm x 8mm. During the experiment, the damaged and undamaged beams have been subjected to vibration at their 1^{st}, 2^{nd} and 3^{rd} mode of vibration by using an exciter and a function generator. The vibrations characteristics of the beams correspond to 1^{st}, 2^{nd} and 3^{rd} mode of vibration have been recorded by placing the accelerometer along the length of the beams. The signals from the accelerometer which contains the vibration parameters such as natural frequencies and mode shapes are analyzed and shown on the vibration indicator. The Table 7.1 shown below gives the detail specifications of the instruments used in the current experimental analysis.

Fig. 7.1 Experimental setup for current investigation

1.Vibration exciter 2. Delta Tron accelerometer 3. Composite cantilever beam platform

4. Vibration Analyzer 5. Vibration Monitor 6. Function Generator

7. Power amplifier 8. Power supply

7.2 Experimental procedure and its architecture

The authenticity of the results obtained from theoretical, finite element and AI based techniques for damage diagnosis have been validated by measuring the dynamic responses of the undamaged and damage Aluminum, composite & steel beam specimens through experimentation. The damages at various positions with different severities in the beam elements were introduced by wire EDM & Hack saw [32 teeth per inch] perpendicular in the transverse direction of the beam. The test specimens made from all three materials are of 1000 mm length and have cross section of 50 mm x 8 mm. The composite cantilever beam

test sample was clamped at its one end by clamping device as shown in the Fig. 7.1. The free end of the beam specimen was excited by an appropriate signal from the function generator, which was amplified by the amplifier. The cantilever was excited at first three modes of vibration, and the corresponding natural frequencies and mode shapes were recorded by the accelerometer by suitable positioning, data acquisition system and adjusting the vibration generator at the corresponding resonant frequencies. Similar procedure is adopted by all types of beam of different materials embedded with or without damage of different severities at different positions. The responses generated by the accelerometers are analyzed by PULSE Lab shop Software integrated with a personal computer. The snap shots of the various instruments used in the current experimental analysis are shown in Fig. 7.2(a) to Fig. 7.2(h). The PCMCIA card is used to connect the vibration analyzer with the PULSE Labshop Software.

1. Vibration Exciter

Type : 4808 [Permanent Magnetic Vibration Exciter]
Force rating : 112N sine peak (187 N with cooling)
Frequency Range : 5Hz to 10 kHz
1st Resonance Freq. : 10 kHz
Acceleration : 700 m/s2 (71 g)
Max. Displacement : 12.7 mm
Manufacturer : Bruel & kjaer

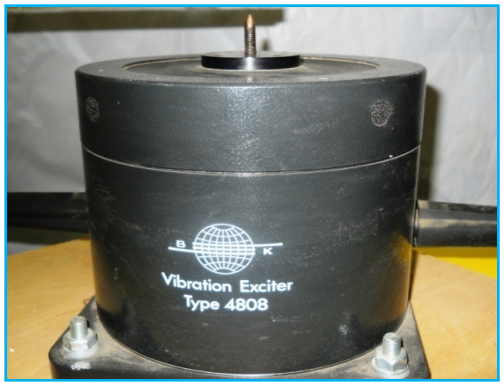

7.2 (a) Vibration Exciter

2. Accelerometer

Type : 4513-001
Make : Bruel & kjaer
Sensitivity : 10mv/g-500mv/g
Frequency Range : 1Hz-10KHz
Supply voltage : 24volts
Operating temperature Range : -50^0C to $+100^0$cconnectors
Manufacturer : Bruel & kjaer

7.2 (b) Accelerometer

3. Composite cantilever beam platform

Damaged (severity 4 mm at middle) cantilever beams made from composite with dimension 1000 mm x 50 mm x 8 mm is used in the set up shown. Apart from this fixed-fixed beam & cantilever of all three materials (Al, composite, steel) of damage severities 3 mm, 4 mm, 5mm at middle, one fourth and three fourth of total length of beam is engaged for experimentation.

7.2 (c) Composite cantilever platform

4. Vibration Analyzer

Type	:	3560L
Product Name	:	Pocket front end
Manufacturer	:	Bruel & kjaer
Frequency Range	:	7 Hz to 20 Khz
ADC Bits	:	16
Channels	:	2 Inputs, 2 Tachometer
Input Type	:	Direct/CCLD

7.2 (d) Vibration analyzer

5. Vibration Monitor

PULSE Lab Shop Software Version 12
Manufacturer : Bruel & kjaer

7.2 (e) Vibration Monitor

6. Function Generator

Model	:	FG200K
Frequency Range	:	0.2Hz to 200 KHz
Output Level	:	15Vp-p into 600 ohms
Rise/Fall Time	:	< 300 n Sec
Manufacturer	:	Aplab

7.2 (f) Function generator

7. Power Amplifier

Model	:	FG200K
Frequency Range	:	0.2Hz to 200 KHz
Output Level	:	15Vp-p into 600 ohms
Rise/Fall Time	:	< 300 n Sec
Manufacturer	:	Aplab

7.2 (g) Power amplifier

8. Power Supply: 220V power supply, 50Hz

7.3 Results and discussion of experimental analysis

This section presents the analysis of the results obtained from the developed experimental set up.

The damaged beam with different damage severities and damage positions have been tested to obtain the mode shape and natural frequency to validate the results from the various techniques mentioned above. Table 3.1 to Table 3.6 has been presented in chapter 3 compare the results from experimental and numerical analysis for damaged cantilever and fixed-fixed beam structures of Al, composite and steel and the results are found to be in close agreement. Nine sets of results for relative damage position and relative damage severities have been presented in Table 4.1 to Table 4.6 in chapter 4 to show the comparison between the experimental and finite element analysis. The results are found to be well in agreement. In chapter five, the results for relative damage position and relative damage severities from experimental analysis is compared with that of the fuzzy Gaussian, fuzzy triangular and fuzzy trapezoidal model in Table 5.3 and they are observed to be well in agreement. The results for relative damage position and relative damage severities from the neural model as discussed in chapter six are compared with that of the experimental set up and presented in Table 6.2 (a) to Table 6.2 (a). The results are found to be in close proximity.

Chapter 8
RESULTS AND DISCUSSION

8.1 Introduction

In the current chapter, investigation of the viability of the methods as mentioned in the thesis have been carried out, by systematically studying and presenting the performance of each methodology used for identification of damage in a cantilever and fixed-fixed beam structures of different materials such as Al, composite and steel. The vibration characteristics of the damaged beam members have been engaged to develop the damage diagnostic applications. The various techniques applied in the current research for characterization of damage in damaged structures are theoretical analysis (Chapter-3), finite element analysis (Chapter-4), Fuzzy Inference System (Chapter-5), Artificial neural network (Chapter-6), Experimental technique (Chapter-7).

8.2 Analysis of results

In the present investigation, for development of damage diagnosis methodologies in structural systems, five different techniques (Chapter 3 to chapter 7) have been employed as cited in the introduction section of the current chapter. Besides the five chapters, the thesis comprises of two other introductory chapters including the Literature review. This section depicts the analysis of the results from different chapters of the current research.

Chapter one the introduction section of the thesis presents the motivation factors to carry out the present research along with the aim and objective of the present diagnosis.

In chapter two various methodologies applied by researchers since last few decades for damage identification in engineering systems have been discussed. Applications of AI techniques for damage and fault diagnosis in different mechanical and electrical systems have also been discussed. This section in particular, provides the knowledge for finalizing the motivation of research.

The analytical model used to compute the vibration parameters of damaged and undamaged cantilever beam structure (Fig. 3.1) and detailed discussion of the theoretical model have been made in chapter three of the thesis. During the vibration analysis of the damaged cantilever and fixed-fixed beam structures of different materials such as Al, composite and steel, the first three relative natural frequencies and first three relative mode shape differences of the damaged and undamaged beam have been arbitrated. The experimental validation of the results from the theoretical model has been carried out in this chapter by using the developed experimental set up as shown in Fig. 3.5. A comparison of relative damage position and relative damage severities from the numerical and experimental analysis have been presented in Table 3.1 to Table 3.6, which shows the robustness of the analytical model developed for damage identification.

In chapter four finite element analysis has been conducted to measure the vibration responses (natural frequencies, mode shapes) of the damaged cantilever and fixed-fixed beam structures of Al, composite and steel. Different damaged beam elements have been considered to perform the finite element analysis to estimate the first three natural frequencies and first three mode shapes. A comparison of results for relative damage position and relative damage severities from FEA, numerical analysis and experimental analysis have been shown in Table 4.1 to Table 4.6 and they are found to be in close agreement.

Chapter five describes the steps used to design and develop fuzzy inference system to diagnose the damage parameters (position, severity) present in beam like structures in section 5.2. The fuzzy models have been designed with the help of triangular membership function (Fig.5.1 (a)), Gaussian membership function (Fig.5.1 (b)) and trapezoidal membership functions (Fig.5.1(c)). Detail architecture of the fuzzy inference system with the input and output parameters are shown in Fig. 5.2. The fuzzy models used in the current research for detection of damage position and their severity are fuzzy triangular (Fig. 5.3 (a)), fuzzy Gaussian (Fig. 5.3 (b)) and fuzzy trapezoidal (Fig. 5.3 (c)) models. The fuzzification mechanism using the triangular, Gaussian, triangular and trapezoidal membership functions with fuzzy linguistic terms in details are graphically presented in Fig. 5.4, Fig. 5.5 and Fig. 5.6 respectively. The fuzzy linguistic terms used for formulation of the fuzzy inference system is expressed in Table 5.1. Out of several hundred fuzzy rules used for fabrication of the fuzzy system for damage identification, twenty numbers are presented in Table 5.2. The

defuzzification process adopted to estimate the relative damage position and relative damage severity by effectuating the rule no 5 and rule no 15 from Table 5.2 for triangular, Gaussian and trapezoidal fuzzy model are shown in Fig. 5.7, Fig. 5.8 and Fig. 5.9 respectively. Center of gravity procedure has been followed to get the crisp value of the relative damage position and damage severity. The results for the damage attributes such as relative damage position and relative damage severity from the developed fuzzy models (triangular, Gaussian, triangular) are compared with that of the numerical, finite element and experimental analysis for validation in Table 5.3 (a) and Table 5.3 (l). From the analysis of results in Table 5.3 (a) to Table 5.3 (f), it is evident that the fuzzy Gaussian model provides the best results in comparison to other two fuzzy models, theoretical analysis and finite element analysis.

Chapter six analyses the development of an artificial neural network model trained with back propagation technique for damage diagnosis in beam structures. The working principles with the main features of the neuron model (Fig. 6.1) and the back propagation technique (Fig. 6.2) have been discussed in section 6.2.1. A schematic diagram representing the proposed neural network model with input and output parameters is shown in Fig. 6.3. The working model of the 5 layer neural network used in the current research for damage identification in beam members with the detail architecture has been exhibited in Fig. 6.4. Table 6.1 (a) to Table 6.1 (f) presents the test patterns required to train the neural model to estimate the relative damage position and relative damage severity. The results obtained from the neural model for diagnosing the damage characteristics are compared with the results obtained from the fuzzy models described in the above chapter, FEA and experimental analysis in Table 6.2 (a) and Table 6.2 (f). By analyzing the results provided in Table 6.2 (a, f), it can be concluded that the proposed neural network gives better results in comparison to the fuzzy techniques mentioned in the Table 6.2 (a, f).

The developed experimental set up comprises of the following instruments; 1- Vibration analyzer, 2- Accelerometer, 3- Composite cantilever platform, 4- Function Generator, 5- Power Amplifier, 6- Vibration Exciter, 7- Vibration monitor (embedded with PULSE Labshop software. Section 12.2 presents the procedures adopted to carry out the experiments to evaluate the natural frequencies and mode shapes of damaged and undamaged beam structures. Efforts have been made to reduce the effect of external parameter such as noise on the vibration signatures of the damaged beam during experimentation.

Chapter 9

CONCLUSIONS AND FUTURE WORK

In the current investigation, identification and assessment of damages present in structural beam members from the measured vibration responses has been emphasized. In the research, to design and develop a damage diagnostic tool a vibrating structural member with damage in the transverse direction has been studied. During the diagnosis procedure, analytical method, finite element method and experimental method have been embraced to realize the actual working condition. The measured natural frequencies and mode shapes at different modes of vibration, which are known as modal parameters, have been used to develop inverse methodologies based AI techniques such as fuzzy logic, neural network techniques for identification of relative damage position and relative damage severity.

From the analysis and discussion of the results from the various techniques cited in the above chapters, the following contributions and conclusions have been presented in section 14.1, 14.2 and section 14.3 respectively.

9.1 Contributions

It is a fact that, the damages present in structural systems introduces a local flexibility, which is a function of damage characteristics such as position and severity. The change in flexibility changes the dynamic responses like frequency response and amplitude of vibration. In previous works done by various researchers, damage diagnosis of structures has been studied to explore the effect of damage on the natural frequencies and mode shapes. In the current research, effort has been made to design artificial intelligent inverse models to detect the damage positions and their severities present in structural systems using the natural frequencies and mode shapes.

In the current research work, damage identification tool has been modeled using the stress intensity factors and strain energy release rate to estimate the deviations in the vibration

parameters due to the damage present in the damaged structures. Finite element analysis and experimental analysis have also been engaged on the damaged beam members of different materials with different boundary conditions to determine the impact of damages on the dynamic characteristics of the beams. Moreover, AI models have been composed for damage diagnosis using fuzzy inference system, artificial neural network.

9.2 Conclusions

The conclusions are drawn on the basis of results obtained from various analyses as discussed above.

- ✓ Theoretical and finite element analyses have been presented to identify characteristics (natural frequencies, mode shapes) of the structural response that is associated with the presence of transverse damage.
- ✓ During the analysis it is observed that, the alteration in frequency response due to the presence of damages is very less significant for small value of damage depth ratio. But the effect of damage severities is very prominent on the mode shapes. So, any change in frequency and mode shape allow characterizing the damage efficiently.
- ✓ Experimentations on the damage cantilever & fixed-fixed beams of Al, composite and steel with different configuration of damage positions and damage severities have been performed to compare the modal parameters obtained from the analytical and finite element model and the results are found to be in very good agreement.
- ✓ The vibration signatures from the first three modes of the cantilever & fixed-fixed beams of Al, composite and steel and the corresponding relative damage severities and damage positions have been used to design the fuzzy inference system for damage detection in structural beam members.
- ✓ The fuzzy system has six inputs and two outputs. The fuzzy models are based on fuzzy Gaussian, fuzzy triangular and fuzzy trapezoidal membership functions. From the analysis of results, it has been found that, the proposed fuzzy inverse technique estimates the relative damage positions and their severities more accurately than the

theoretical and finite element analysis. Experimental data have also been used to validate the results from the fuzzy models.

- ✓ From the analysis of the results of the three fuzzy models for relative damage severities and relative damage positions, it is observed that the fuzzy model with Gaussian membership function produces better results than the fuzzy model with triangular membership function, fuzzy model with trapezoidal membership function. Hence, the fuzzy Gaussian model was found to be most desirable to identify the damage in vibrating engineering systems.
- ✓ A multi layer artificial neural network model with six inputs and two outputs has been devised for damage diagnosis in beam structures. The training patterns for the proposed neural network model have been derived from theoretical, finite element and experimental analysis. The results estimated by the neural network for relative damage severities and relative damage positions are very closer to the experimental results, thereby justify the engagement of neural model in damage diagnosis beam structures.
- ✓ From the comparison of results (relative damage severities and relative damage positions) among the fuzzy models and neural model, it is clear that the results obtained from neural system are converging towards actual results in contrast to the fuzzy models.
- ✓ The developed damage diagnosis tool can be utilized for online condition monitoring of turbine shafts, various engineering structures such as bridges, cranes, towers, industries, mechanical structures, beam like structures, marine structures, engineering applications, etc.

9.3 Future work

- The artificial intelligent techniques can be used in hybrid form such as neuro-fuzzy, GA-fuzzy, neuro-fuzzy-GA etc. to diagnose faults in complex engineering structures.
- The composite material used can be varied with different orientations for test specimen. Moreover, structural beam members of non-uniform cross section can also be considered for analysis.

- Apart from the mega structures, micro leveled structures can also be subjected to damage diagnosis techniques, which subsequently assist to ensure the functioning of small robots.

REFERENCES:

1. E. Douka, G. Bamnios, A. Trochidis,. "A method for determining the location and depth of crack in a double cracked beam", *Applied acoustics*, 2004, Vol. 65, pp.997-1008.

2. Y. C. Huh, T.Y. Chung, S. J. Moon, H. G. Kil and J. K. Kim, "Damage detection in beams using vibratory power estimated from the measured accelerations", *Journal of Sound and Vibration*, 2007, Vol. 330 (15), pp.3645-3665.

3. H. Nahvi and M. Jabbari, "Crack detection in beams using experimental modal data and finite element mode", *International Journal of Mechanical Sciences*, 2005, Vol. 47, pp. 1477-1497.

4. A.K. Darpe, K. Gupta and A. Chawla, "Experimental investigations of the response of a cracked rotor to periodic axial excitation", *Journal of Sound and Vibration*, 2003, Vol 260, pp. 265–286.

5. H. Hein, L. Feklistova, "Computationally efficient delamination detection in composite beams using Haar wavelets", *Mechanical Systems and Signal Processing,* 2011, Vol. 25 (6), pp.2257-2270,.

6. T.Curry and E.G. Collins, "Robust Fault Detection and Isolation Using Robust ℓ1 Estimation", *Proceeding of the 2004 American Control Conference Boston*, Massachusetts, June 30 - July 2, 2004.

7. A.J. Hoffman and N.T. van der Merwe, "The application of neural networks to vibrational diagnostics for multiple fault conditions", *Computer Standards & Interfaces*, 2002, Vol. 24, pp.139–149,.

8. A. Salam, Y. Alsabbagh, O.M. Abuzeid and Mohammad H. Dado, "Simplified stress correction factor to study the dynamic behavior of a cracked beam", *Applied Mathematical Modelling*, 2007, Vol. 33, pp. 127–139.

9. J. Sanza, R. Pererab ,C. Huertab, "Fault diagnosis of rotating machinery based on auto-associative neural networks and wavelet transforms", *Journal of Sound and Vibration*, 2007, Vol. 302, pp.981–999.

10. S.M. Murigendrappa, S.K. Maiti and H.R. Srirangarajan, "Experimental and theoretical study on crack detection in pipes filled with fluid", *Journal of Sound and Vibration*, 2004, Vol. 270, pp.1013–1032.

11. S. Chinchalkar, "Determination of crack location in beams using natural frequencies", *Journal of Sound and Vibration*, 2001, Vol. 247, pp. 417-429.

12. S. Loutridis, E. Douka and L.J. Hadjileontiadis, "Forced vibration behaviour and crack detection of cracked beams using instantaneous frequency", *NDT&E International*, 2005, Vol. 38 (5), pp. 411–419.

13. H. Tada, P.C. Paris and G.R. Irwin, "The stress analysis of cracks hand book", Del Research Corp. Hellertown, Pennsylvania, 1973.

14. D. Ravi and K.M. Liew, "A study of the effect of micro crack on the vibration mode shape", *Engineering Structures*, 2000, Vol. 22, pp. 1097–1102.

15. G. M. Owolabi, A. S. J. Swamidas and R. Seshadri, "Crack detection in beams using changes in frequencies and amplitudes of frequency response functions", *Journal of Sound and Vibration*, 2003, Vol. 265, pp.1-22.

16. M. H. Dado, "A Comprehensive Crack Identification Algorithm for Beams Under Different End Conditions", *Applied Acoustics*, 1997, Vol. 51, pp. 381-398.

17. T.R. Babu, and A.S. Sekhar, "Detection of two cracks in a rotor-bearing system using amplitude deviation curve", *Journal of Sound and Vibration*, 2008, Vol. 314, pp.457-464.

18. G.D. Gounaris and C.A. PapadoPoulos, "Analytical and experimental crack identification of beam structures in air or in fluid", *Computers and Structures*, 1997, Vol. 65 (5), pp.633-639.

19. D.P. Patil and S.K. Maiti, "Detection of multiple cracks using frequency measurements", *Engineering Fracture Mechanics*, 2003, Vol. 70 (12), pp.1553-1572.

20. R.S. Prasad, SC Roy and KP Tyagi, "Effect of Crack Position along Vibrating Cantilever Beam on Crack Growth Rate", *International Journal of Engineering Science and Technology*, 2010, Vol. 2 (5), pp.837-839.

21. S. M. Al-said, "Crack detection in stepped beam carrying slowly moving mass", *Journal of sound and vibration*, 2008, Vol. 14, pp-1903-1920.

22. K.Wang, J.D.Inman and R.F.Charles, "Modeling and analysis of a cracked composite cantilever beam vibrating in coupled bending and torsion", *Journal of sound and vibration*, 2004, Vol. 284 (1-2), pp.23-49.

23. W. M. Ostachowicz, and M. Krawczuk, "Vibration analysis of a cracked beam", *Computers & Structures*, 1990, Vol. 36, pp. 245-250.

24. M. Krawczuk, M. Palacz, W. Ostachowicz, "The dynamic analysis of a cracked Timoshenko beam by spectral element method", Journal *of Sound and Vibration*; 2003, Vol.264 (5), pp 1139-1153.

25. P.N. Saavedra and L.A.Cuitino, "Crack detection and Vibration behavior of Cracked beams", *Computers and Structures*, 2001, Vol. 79 (16), pp.1451-1459.

26. M. Kisa, "Free vibration analysis of a cantilever composite beam with multiple cracks", *Composites of science and Technology*, 2004, Vol. 64 (9), pp 1391-1402.

27. T.G. Chondros, A.D. Dimarogonas, J. Yao, "Vibration of a beam with a breathing crack", *Journal of Sound and Vibration*, 2001,Vol. 239(1), pp 57-67.

28. G. L. Qian, S. N. Gu and J. S. Jiang, "The dynamic behaviour and crack detection of a beam with a crack"*, Journal of Sound and Vibration*, 1990, Vol. 138, pp. 233-243.

29. S. K Panigrahi, "Damage analyses of adhesively bonded single lap joints due to delaminated FRP composite adherends", *Applied Composite Materials*, 2009, Vol. 4, pp. 211-223.

30. A.S. Shekhar and B.S. Prabhu, "Crack detection and vibration characteristics of cracked shafts", *Journal of sound and vibration*, 1992, Vol. 157, pp. 375-381.

31. M. Chandrashekhar and R.Ganguli, "Damage assessment of structures with uncertainty by using mode- shape curvatures and fuzzy logic", *Journal of Sound and Vibration*, 2009, Vol. 26, pp. 939–957.

32. T. Boutros and M. Liang, "Mechanical fault detection using fuzzy index fusion", *International Journal of Machine Tools & Manufacture*, 2007, Vol. 47, pp. 1702–1714.

33. L. J. de Miguel and L. F. Blazquez, "Fuzzy logic-based decision-making for fault diagnosis in a DC motor", *Engineering Applications of Artificial Intelligence*, 2005 Vol. 18, pp.423–450.

34. D. R. Parhi**,** "Navigation of mobile robot using a fuzzy logic model", *Journal of Intelligent and Robotic Systems*, *Theory and Applications*, 2005, Vol. 42, pp. 253-273.

35. J. Fox, "Some observations on fuzzy diagnosis and medical computing", *International Journal of Bio-Medical Computing*, 1977, Vol. 8, pp.269–275.

36. A. K. Dash, D.R. Parhi, "Development of an inverse methodology for crack diagnosis using AI technique", *International Journal of Computational Materials Science and Surface Engineering (IJCMSSE)*, 2011, Vol. 4(2), pp.143-167.

37. P. Angelov, E. Lughofer, X. Zhou, "Evolving fuzzy classifiers using different model architectures", *Fuzzy Sets and Systems*, 2008, Vol. 159, pp.3160–3182.

38. H.J. Zimmermann, "Fuzzy programming and linear programming with several objective functions", *Fuzzy Sets and Systems*, 1978, Vol. 1, pp.45–55.

39. V. Sugumaran and K.I. Ramachandran, "Fault diagnosis of roller bearing using fuzzy classifier and histogram features with focus on automatic rule learning", *Expert Systems with Applications*, 2011, Vol. 38(5), pp.4901-4907.

40. Y. M. Kim, C.K. Kim and G. H. Hong, "Fuzzy set based crack diagnosis system for reinforced concrete structures", *Computers and Structures*, 2007, Vol. 85, pp.1828–1844.

41. D. K. Mohanta, P. K. Sadhu, R. Chakrabarti, "Fuzzy Markov Model for Determination of Fuzzy State Probabilities of Generating Units Including the Effect of Maintenance Scheduling", *IEEE Transactions on Power Systems*, Vol. 20, pp. 2117-2124, 2005.

42. D. R. Parhi**,** "Navigation of mobile robot using a fuzzy logic model", *Journal of Intelligent and Robotic Systems*, Theory *and Applications*, 2005, Vol. 42, pp. 253-273.

43. I. Eski, S. Erkaya, S. Savas, S. Yildirim, "Fault detection on robot manipulators using artificial neural networks", *Robotics and Computer-Integrated Manufacturing,* 2011, Vol. 27, pp. 115–123.

44. D.R.Parhi, A. K. Dash, "Application of neural network and finite element for condition monitoring of structures", *Proceedings of the Institution of Mechanical Engineers, Part C: Journal of Mechanical Engineering Science*, 2011, Vol. 225, pp. 1329-1339.

45. G. Paviglianiti, F. Pierri, F. Caccavale and M. Mattei, "Robust fault detection and isolation for proprioceptive sensors of robot manipulators", *Mechatronics*, 2010, Vol. 20, pp.162–170.

46. M. Mehrjoo, N. Khaji, H. Moharrami and A. Bahreininejad, "Damage detection of truss bridge joints using Artificial Neural Networks", *Expert Systems with Applications*, 2008, Vol. 35, pp. 1122–1131.

47. N. Saravanan , V.N.S. Kumar Siddabattuni and K.I. Ramachandran, "Fault diagnosis of spur bevel gear box using artificial neural network (ANN), and proximal support vector machine (PSVM)", *Applied Soft Computing*, 2010, Vol. 10, pp. 344–360,.

48. J.D. Wu and J.J .Chan, "Faulted gear identification of a rotating machinery based on wavelet transform and artificial neural network", *Expert Systems with Applications*, 2009, Vol. 36, pp. 8862–8875.

49. A.J. Oberholster and P.S. Heyns, "On-line fan blade damage detection using neural networks", *Mechanical Systems and Signal Processing*, 2006, Vol. 20, pp.78–93.

50. F.J.Agosto, D. Serrano, B. Shafiq and A. Cecchini, "Neural network based nondestructive evaluation of sandwich composites", *Composites: Part B*, 2008, Vol. 39, pp. 217–225.

51. V. N. Ghate, S.V. Dudul, "Optimal MLP neural network classifier for fault detection of three phase induction motor", *Expert Systems with Applications,* 2010, Vol. 37, pp.3468–3481.

52. H. Das, D.R. Parhi, "Application of neural network for fault diagnosis of cracked cantilever beam" *World Congress on Nature and Biologically Inspired Computing*, Coimbatore, 2009; article no-5393733, pp 1303-1308.

53. D.R. Parhi, S. Chaudhury, "Smart crack detection of a cracked cantilever beam using fuzzy logic technology with hybrid membership functions" *Journal of Engineering and Technology research*, 2011, Vol-3 (8), pp 270-278.

54. A.Gentile, A. Messina, "On the continuous wavelet transforms applied to discrete vibrational data for detecting open cracks in damaged beams", *International journal of solids and structures*, 2003, Vol-40 (2), pp 295-315.

55. D.Srinivasarao, K. M. Rao and G.V.Raju, "Crack identification on a beam by vibration measurement and wavelet analysis", *International Journal of Engineering Science and Technology*, 2010, Vol. 2, pp.907-912.

56. H. Kim, A. Tan, J. Mathew and B. Choi, "Bearing fault prognosis based on health state probability estimation", *Expert Systems with Applications*, 2012, Vol. 39 (5), pp. 5200–5213.

57. D.Y. Zheng and S.C. Fan, "Vibration and stability of cracked hollow sectional beam", *Journal of sound and vibration*, 2003, Vol. 267, pp.933-954.

58. S.T. Quek, Q. Wang, L.Zhang and K.K. Ang, "Sensitivity analysis of crack detection in beams by wavelet technique", *International Journal of Mechanical Sciences*, 2001, Vol. 43, pp. 2899-2910.

59. M. Cao and P. Qiao, "Novel Laplacian scheme and multi resolution modal curvatures for structural damage identification", *Mechanical Systems and Signal Processing*, 2009, Vol. 23, pp.1223–1242.

60. Karaagac c., Qzturk H., Sabuncu M.F., "Free vibration and lateral buckling of a cantilever slender beam with an edge crack", *Journal of Sound and Vibration*, 2009, Vol-326 (1-2), pp 235-250.

61. G. Rus and R. Gallego, “Hyper singular shape sensitivity boundary integral equation for crack identification under harmonic elastodynamic excitation”, *Computer Methods Appl. Mech. Engg*. , 2007, Vol. 196, pp.2596–2618.

62. M. I. Friswell, “Damage identification using inverse methods”, *Philosophical transactions of the royal society A: physical and engineering sciences*, 2007, Vol. 365, pp.393-410.

63. E. Fagerholt, C. Dørum, T. Børvik, H.I. Laukli and O.S. Hopperstad, “Experimental and numerical investigation of fracture in a cast aluminum alloy”, *International Journal of Solids and Structures*, 2010, Vol. 47(24), pp.3352–3365.

64. Y. K. An, H. Sohn, “Integrated impedance and guided wave based damage detection”, *Mechanical system and signal processing*, 2012, Vol. 28, pp. 50-62.

65. M.Fledman, “Hilbert transform in vibration analysis, Mechanical systems and signal processing”, 2011, Vol. 25(3), pp.735–802.

66. S. Haykin, “Neural Networks, A comprehensive foundation”, *Pearson Education*, 2006.

List of Publications:

1. D.K. Agarwalla, D.R. Parhi; “Effect of crack on modal parameters of a cantilever beam subjected to vibration”; Procedia Engineering; 2013, Vol. 51, pp. 665-669.

2. D.K. Agarwalla, D.R. Parhi;“Diagnosis of Modal Characteristics of Aircraft Wing Model subjected to Irregularities”; *International Journal of Engineering Science Invention*; 2013, pp. 6-10.

3. D.K. Agarwalla, D.R. Parhi; “Diagnosis of Damaged Al Cantilever Beam Subjected to Free Vibration by Numerical and Experimental Method”; *International Journal of Artificial Intelligence and Computational Research*; 2012, No.2, Vol. 4, pp. 71-77.

4. D.K. Agarwalla, D.R. Parhi; “Determination of Modified Natural Frequencies of Fractured Fixed-fixed beam by Numerical & Experimental Method”; *International Journal of Applied Artificial Intelligence in Engineering System*; 2012, No.2, Vol. 4, pp. 95-101.

5. S.K. Behera, D.K. Agarwalla, D.R. Parhi, Das H.C.; “Vibration Analysis of a Cracked Composite Beam Using Various Techniques - A Review”; *International Journal of Artificial Intelligence and Computational Research*; 2012, No.2, Vol. 4, pp. 95-101.

6. D.K. Agarwalla, D.R. Parhi, A.K. Baliarsingh; “Analysis of Vibrating Steel Structures Subjected to Various Damage Attributes”; *Advances in Tribology*; Hindawi Publishing house, 2013. [In press]

APPENDIX

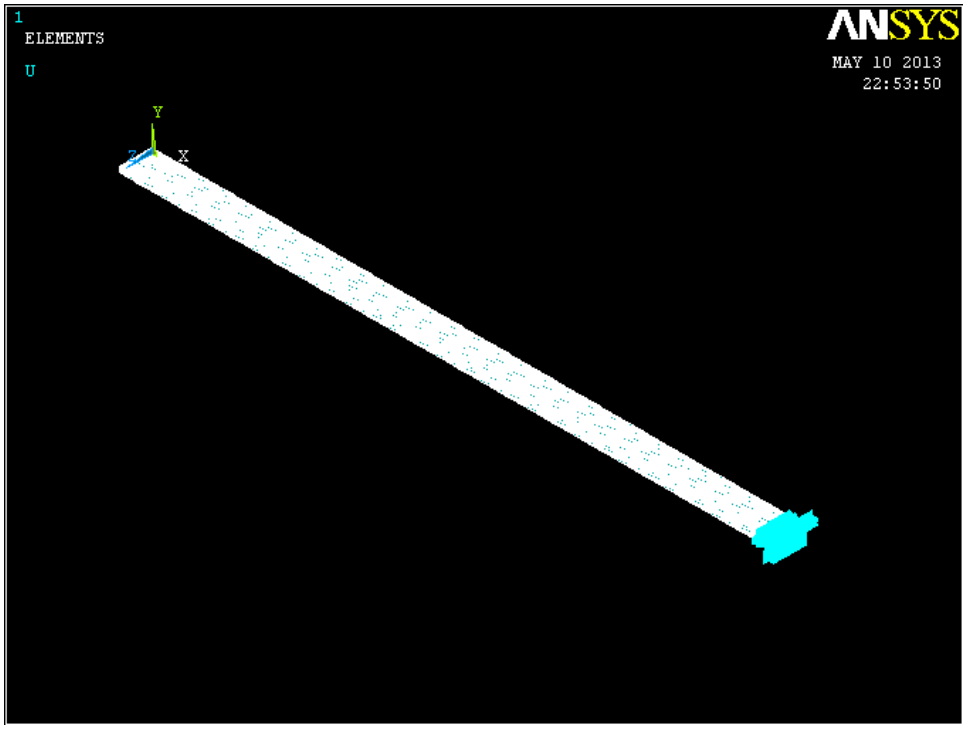

Fig. A. 1 Meshed composite cantilever beam model

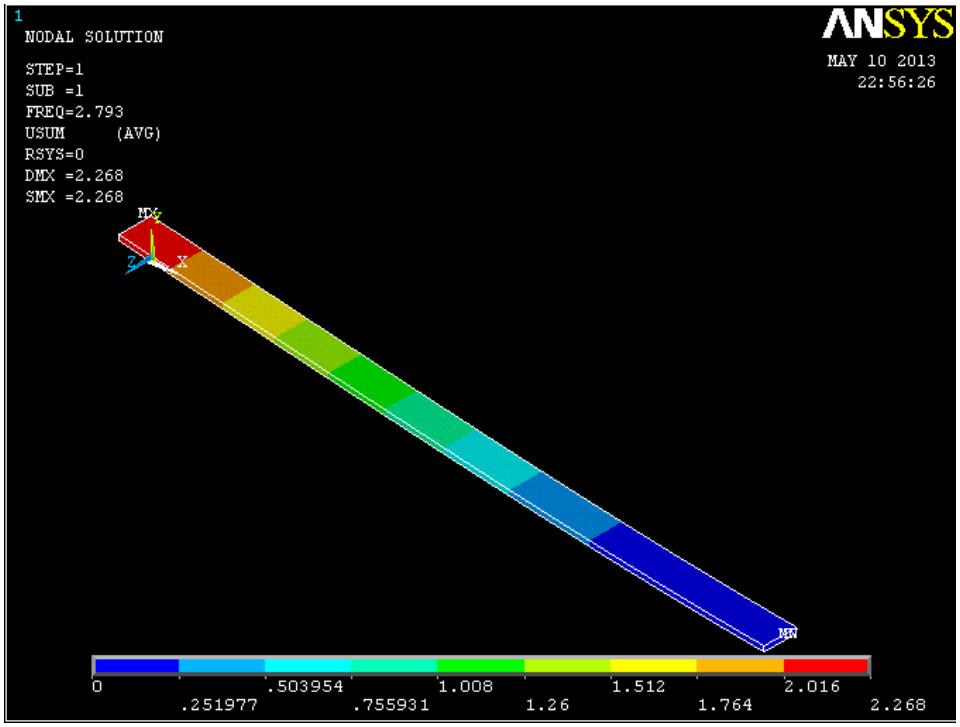

Fig. A. 2 Deformed shape for 1st mode of vibration of composite cantilever beam without damage

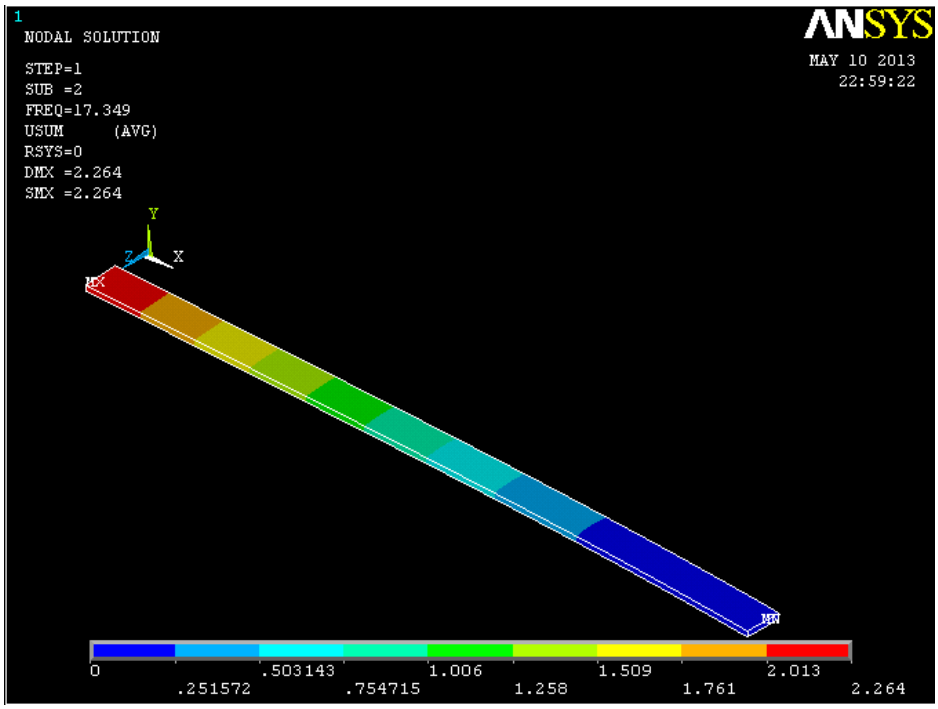

Fig. A. 3 Deformed shape for 2nd mode of vibration of composite cantilever beam without damage

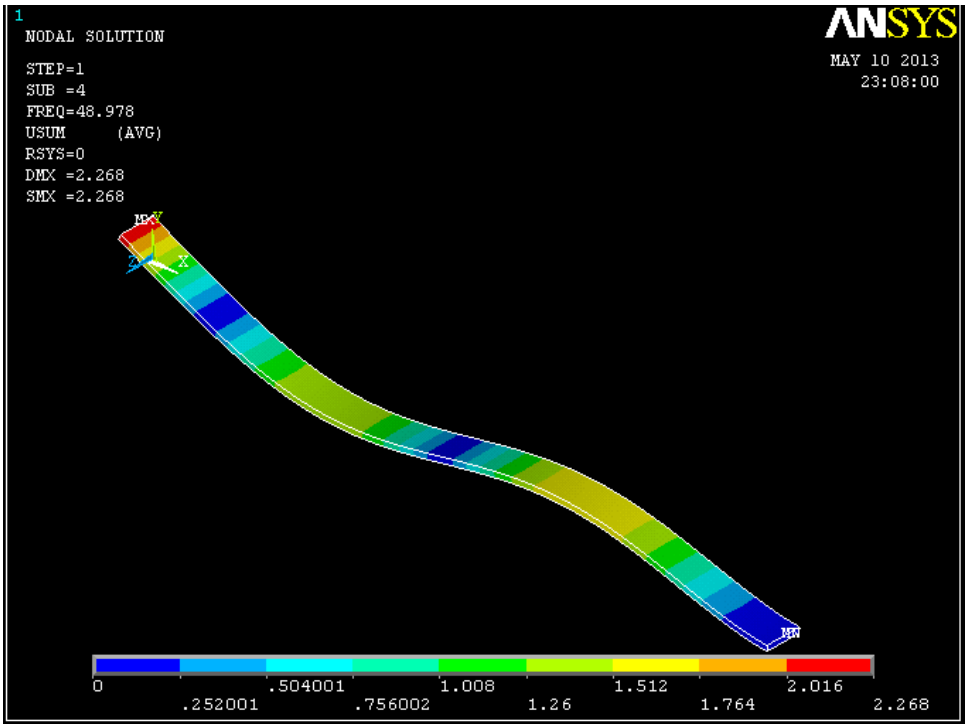

Fig. A. 4 Deformed shape for 3rd mode of vibration of composite cantilever beam without damage

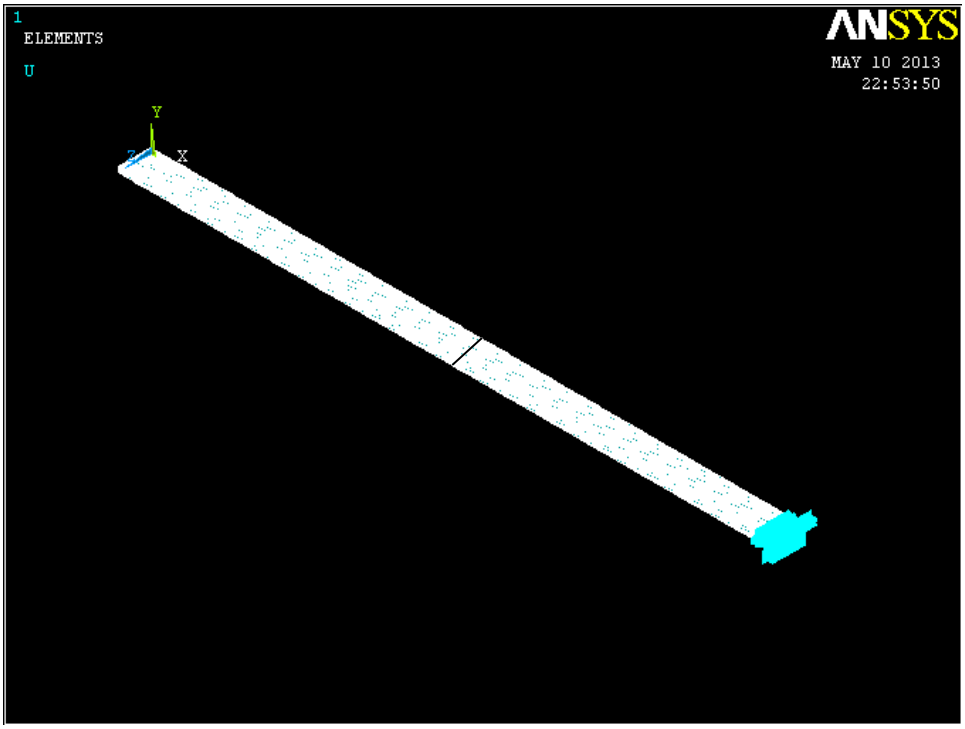

Fig. A. 5 Meshed composite cantilever beam model with damage 4mm

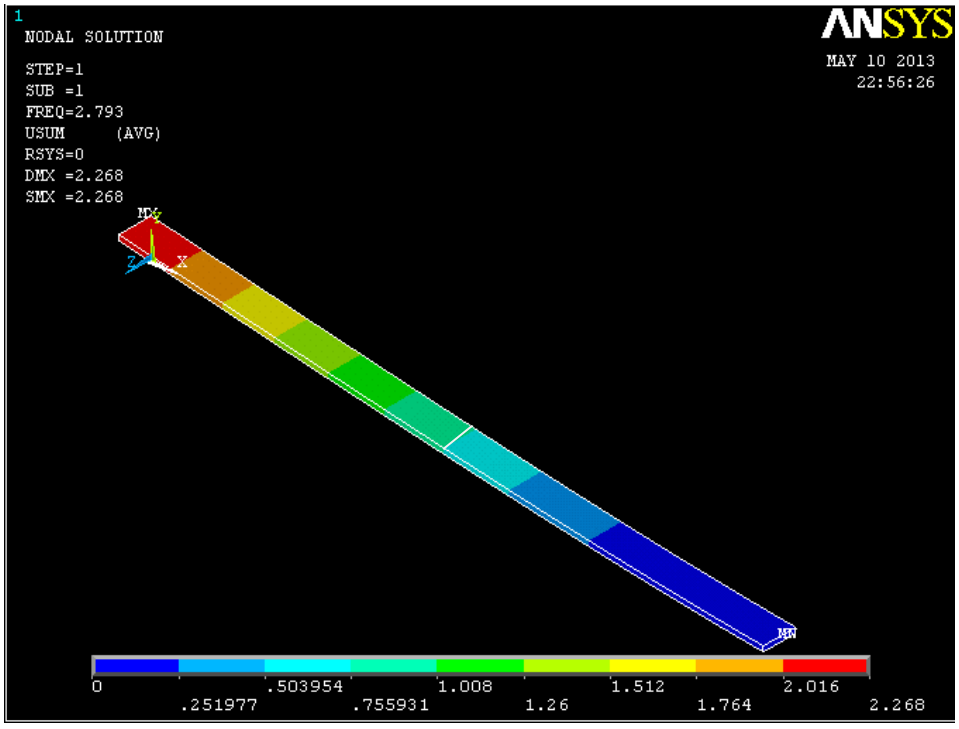

Fig. A. 6 Deformed shape for 1st mode of vibration of composite cantilever beam with damage 4mm

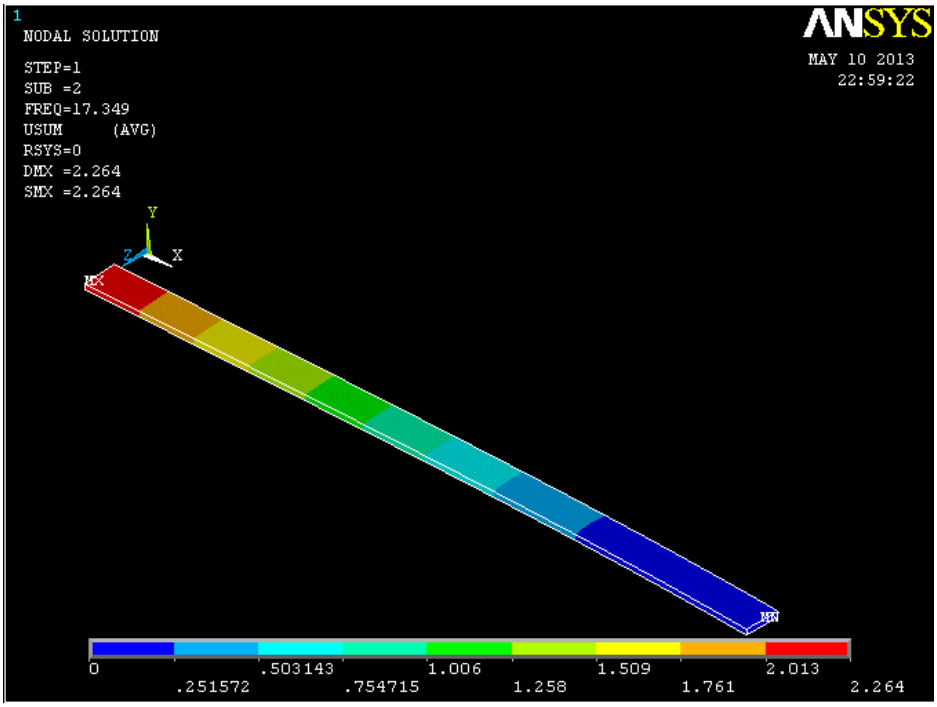

Fig. A. 7 Deformed shape for 2nd mode of vibration of composite cantilever beam with damage 4mm

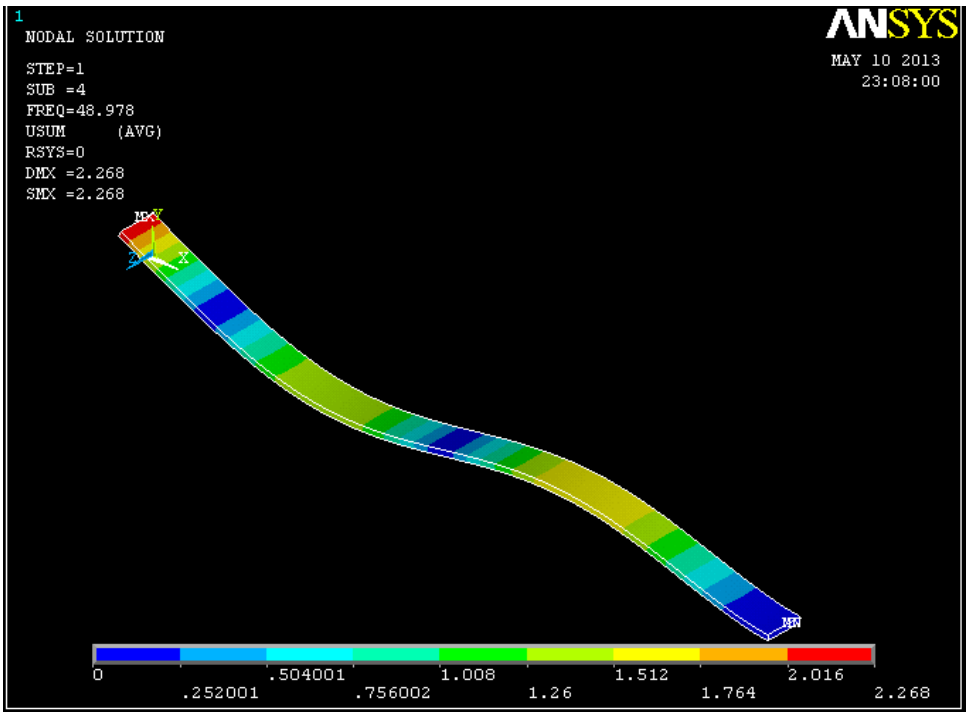

Fig. A. 8 Deformed shape for 3rd mode of vibration of composite cantilever beam with damage 4mm

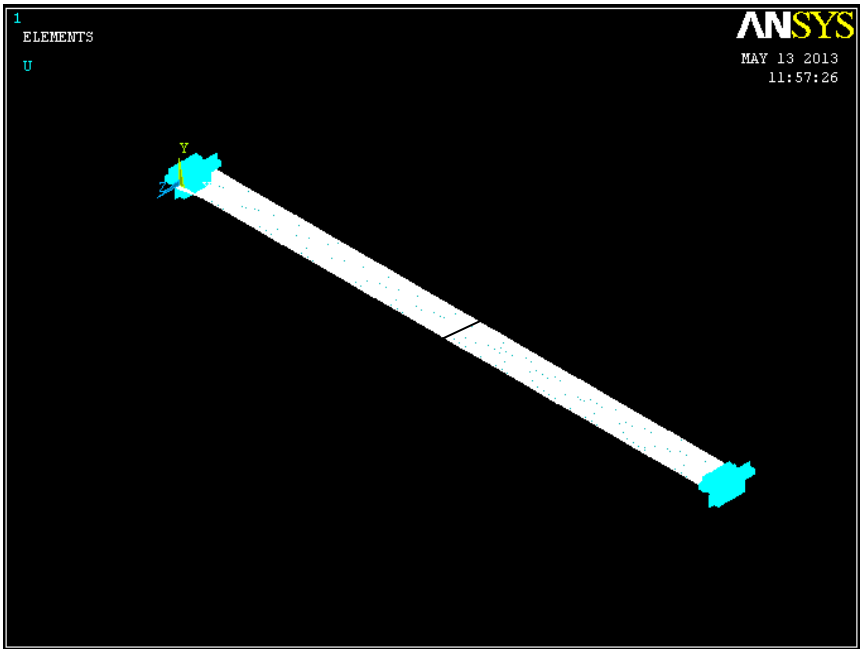

Fig. A. 9 Meshed composite fixed-fixed beam model with damage of 4 mm

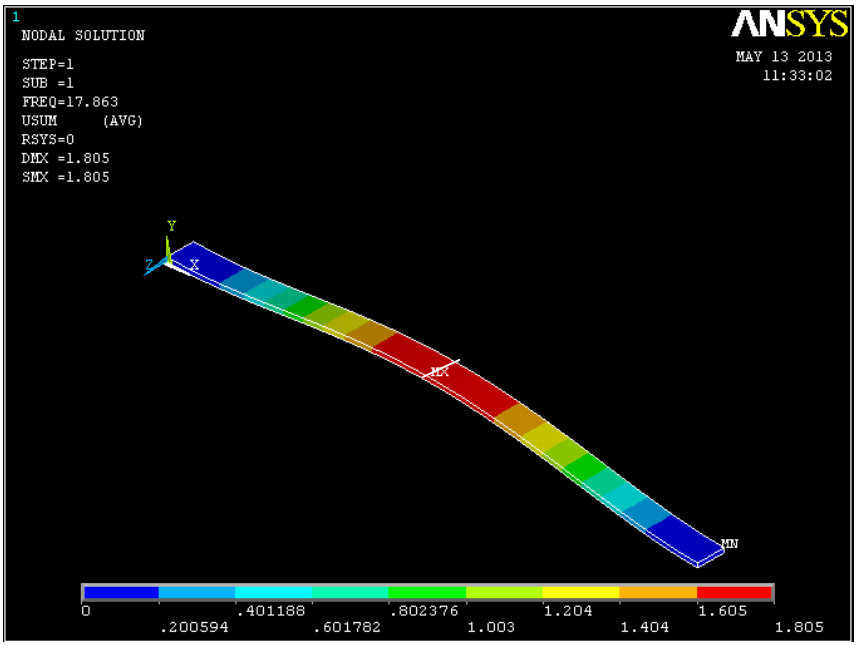

Fig. A. 10 Deformed shape for 1st mode of vibration of composite fixed-fixed beam with damage of 4 mm

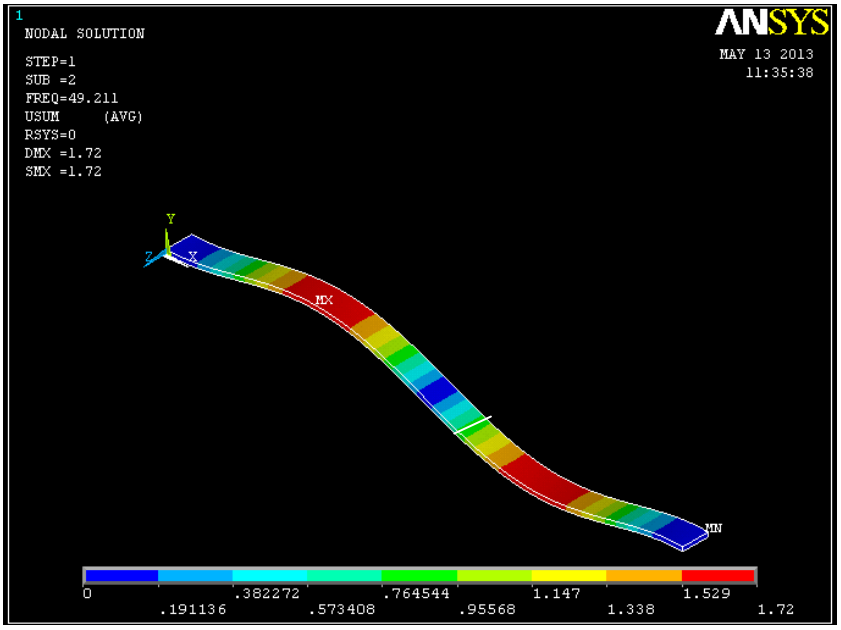

Fig. A. 11 Deformed shape for 2nd mode of vibration of composite fixed-fixed beam with damage of 4 mm

Fig. A. 12 Deformed shape for 3rd mode of vibration of composite fixed-fixed beam with damage of 4 mm